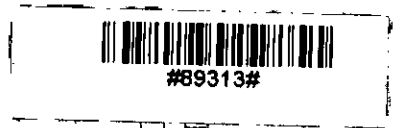# THREE-DIMENSIONAL SATURATED-UNSATURATED FLOW SIMULATION BY GALERKIN FINITE ELEMENT METHOD

A.B.M. FARUQUZZAMAN BHUIYAN

Department of Water Resources Engineering
Bangladesh University of Engineering and Technology,
Dhaka

October 1995

THREE-DIMENSIONAL SATURATED-UNSATURATED FLOW SIMULATION BY GALERKIN FINITE ELEMENT METHOD.
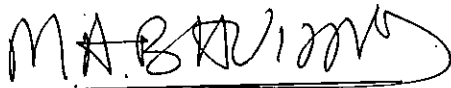
Submitted by

A. B. M. FARUQUZZAMAN BHUIYAN

In partial fulfilment of the requirements for the
degree of Master of Science in Engineering (Water Resources)

**Department of Water Resources Engineering
Bangladesh University of Engineering and Technology, Dhaka**

October 1995

CERTIFICATE

This is to certify that this thesis work **Three-Dimensional Saturated-Unsaturated Flow Simulation by Galerkin Finite Element Method** has been done by me. Neither of this thesis nor any part thereof has been submitted elsewhere for the award of any degree or diploma.

_____

(Dr. Muhammed Ali Bhuiyan)

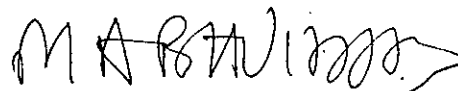Countersigned by the Supervisor

_____

(A.B.M. Faruquzzaman Bhuiyan)

Signature of the Candidate

BANGLADESH UNIVERSITY OF ENGINEERING AND TECHNOLOGY
DEPARTMENT OF WATER RESOURCES ENGINEERING
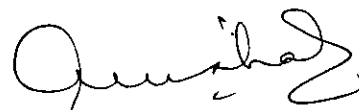
CERTIFICATE OF APPROVAL

We hereby recommend that the thesis presented by **A.B.M. FARUQUZZAMAN BHUIYAN** entitled **"THREE-DIMENSIONAL SATURATED-UNSATURATED FLOW SIMULATION BY GALERKIN FINITE ELEMENT METHOD"** be accepted as fulfilling this part of the requirements for the degree of Master of Science in Engineering (Water Resources).

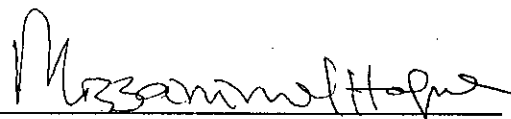Chairman of the committee

_____
Dr. Muhammed Ali Bhuiyan

Member

_____
Prof. Ainun Nishat

Member

(External)

_____
Prof. M. Mozzammel Hoque

Member

(Head of the Department)

_____
Prof. Md. Monowar Hossain

October 22, 1995

TABLE OF CONTENTS

ABSTRACT

A three-dimensional mathematical model has been developed using Galerkin finite element method for simulation of transient saturated-unsaturated groundwater flow in multi-aquifer system. The program deals with a variety of boundary conditions encountered in real hydrogeological situation consisting of simple constant or time dependent prescribed head (surface water bodies) or prescribed flux boundaries (pumping well, recharging well etc.), complicated system-dependent and atmosphere-controlled boundary including the near-surface activities i.e., precipitation, evaporation, root water extraction and surface ponding caused by excess precipitation and also boundary along the river side having variable seepage face conditions. The supporting programs developed are a mesh generator for three-dimensional domain discretization, and two other for checking, interpolating and arranging the input data like precipitation, evaporation, river water level which finally create input files for the main program. For parameterization of the unsaturated soil properties three characteristic functions are included in the main program which are optionally available.

To test the different features incorporated in the model, a number of published schematized problems have been simulated by the program. Six such problems are presented in detail in this thesis with simulated results and their comparisons with published results where available. Two problems show the model responses in purely unsaturated conditions. In the first problem, the program simulates the moisture content propagation under the specified constant pressure head at the top of a soil column. The results show increase of pressure head and moisture content in the column with a moving front. In the second problem the imposed flux at the top is varying linearly with time and the simulation results show how the pressure head profiles rapidly changes from their initial hydrostatic distribution. In the third problem a fully saturated steady state confined groundwater flow under pressure head difference between two ends with vertical flux at the top surface is simulated where the results are compared with the available analytical solution of the problem. The fourth problem deals with the near surface activities due to the heavy precipitation followed by subsequent ponding on the surface after a long dry spell with the evaporation, root water extraction occurring at the same time. The resulting groundwater rise

and fall due to recharge from infiltration are exhibited in a layered soil column. The fifth and sixth problems show the drainage and replenishment simulation with river bank situation. The fifth problem shows the drainage from a homogeneous soil due to sudden lowering of water level in the adjacent surface water body. Transient positions of the groundwater table and seepage face with the outflow volume through this face are simulated and compared with published results. The last problem is close to the real river bank situation where the soil domain consists of three layers of soil with different hydraulic characteristics and the adjacent river water level is changed to high flood condition followed by prolonged low level and a second flood thereafter. The program simulates the replenishment and drainage of the zone, the pressure head contours and the velocity vector profiles at different flood and low level conditions. The time and location of probable bank failure are also identified by these results.

To verify the model responses in simulating a complex real hydrogeological situation a strip area of Dhaka city along the bank of Burhiganga river is studied. The boundary conditions of the domain are derived from the river water level and piezometric level data. The simulated domain is composed of four layers: upper aquitard, upper aquifer, lower aquitard and lower or main aquifer. Model calibration and sensitivity analysis of the parameters have been performed under this study. The model is calibrated in trial-and-error approach with the help of observed piezometric level data. After having a set of calibrated parameters, sensitivities of the different parameters have been examined by perturbing a parameter at a time while keeping the other parameters constant. Simulated piezometric head profiles show the trend of rise and fall with the river water level at the nodes nearer the river but this phenomena diminishes rapidly away from the river at the remote nodes where continuous declining trend of piezometric levels are observed. Simulated water balance components identify the river effect as the most dominating recharge mechanism of the area which contributes around 60 percent of the total volume of abstraction. Urban recharge and storage reduction of the upper aquifer also contribute to the abstraction volume of the area.

ACKNOWLEDGEMENTS

LIST OF TABLES

LIST OF FIGURES

LIST OF SYMBOLS

Symbols	Meanings
A_{mn}	Matrix elements in the global matrix equation
A_t	Area related to transpiration
$a(\psi)$	Water stress response function
B_{mn}	Storage matrix elements in the global matrix equation
$b(x,y,z)$	Normalized water uptake distribution function
C	Soil moisture capacity
E_m	Vector elements in the global matrix equation related to sink term, S
e	Element
G_m	Vector elements in the global matrix equation related to vertical hydraulic conductivity
h	Total hydraulic potential
K	Soil water pressure head
K_{ij}	Hydraulic conductivity tensor
k_r	Relative permeability
K_s	Saturated hydraulic conductivity
K_{ij}^{A}	Dimensionless anisotropy tensor for hydraulic conductivity
N	Total number of nodes in the region
n,m	Node numbers
n_i	Unit normal vector in the direction i
O	Rate of inflow or outflow
Q_n	Boundary flux at node n in the global matrix equation
q_x, q_y, q_z	x-, y- and z-components of the nodal Darcian flux
S	Water extraction term in the governing flow equation
S_p	Potential water uptake rate by root

S_s	Storage coefficient
S_w	Degree of saturation
T_p	Potential transpiration rate
T_a	Actual transpiration rate
V	Volume of water in considered region
v_e	Volume of an element
W_m	Vector elements in the global matrix equation related to point source or sink
α	Empirical parameter in the van Genuchten equation
δ	Kronecker delta
Γ	Boundary segment
θ	Moisture content
θ_r	Residual water content
θ_s	Saturated moisture content
ξ	Elemental local basis function
ϕ	Global basis function
Ω	Flow region considered
ψ	Pressure head

CHAPTER ONE

INTRODUCTION
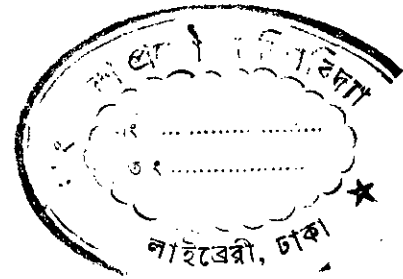
1.1 General

Mathematical modeling of flow and transport phenomena in porous media is an increasingly important tool in the management of water resources. Although most groundwater is located in the saturated zone, which is therefore the main focus of groundwater research, it is the unsaturated zone that controls the infiltration and evaporation phenomena which in turn determine the recharge of groundwater. The processes that occur there are physically and mathematically more complicated than those in the saturated zone due to the nonlinearity of the equations governing unsaturated flows. The heterogeneity of the soil together with complicated boundary conditions of temporal and spatial variability compound the matter even further. Atmospheric boundary condition associated with seepage faces, infiltration and evaporation are the main processes occurring there which make frequent switching between different types of boundary conditions. Although certain simple flow problems in the saturated and unsaturated zone can be solved analytically for homogeneous soils, such solutions of most of flow problems for heterogeneous soils are not available; numerical methods are necessary to approximate them.

Groundwater is the principal source of freshwater for drinking and sanitation purpose in Bangladesh. A major problem that Bangladesh faces is that of too much water in the wet seasons when the riverbank overflow and rainwater stagnation affects detrimentally the agricultural and other developments. On the contrary, the amount of available water in the dry seasons is too little for irrigation and other activities. Due to this fact, dry season irrigation is predominantly based on groundwater abstraction. The period of rapid groundwater exploitation for irrigation started in early seventies and continued by increasing the wells at a compound rate. The consequences of this are now apparent. In the area of overexploitation, lowering of groundwater level is occurring at a rate such that rainy season replenishment is not sufficient to cover up this declining trend which ultimately creating

1

adverse affect on the environment (MPO,1989). In case of densely populated urban areas like Dhaka city, a huge amount of water is required for drinking and sanitation purposes and this demand is exclusively (95% of total abstraction) fulfilled from the tubewell abstractions of groundwater from the underlying aquifers of Dhaka city. There are approximately two hundred deep-tubewells installed in the main aquifer. The situation in Dhaka city has become more critical due to unprecedented growth rate of the city both in terms of population and size. The high demand of water by this densely habitat city is reflected from the fact that the respective water supply authority (DWASA) has to increase the production of drinking water supply by more than six times since the early sixties but still the supply is far lagging behind the demand. As a result, beneath Dhaka city, water levels in the aquifers have fallen steadily over the last twenty five years in response of ever increasing abstraction. So the groundwater resource evaluation, prediction and management bear much attention at this time in Bangladesh where mathematical modeling as an useful , sophisticated and modern tool has been used by the engineers and planners to some extent.

Groundwater model used for different development scenarios serves to study the probable management policies. These models are the abstractions of the complex real world situation achieved by making a considerable number of simplifying assumptions about the geology, hydraulic properties and the water balance. It is obvious that an aquifer system, or a part of the system can be modelled in a great number of ways depending on the assumption we make in order to simplify the real physical system starting from basic mathematics involved in it. The conceptual simple water balance method which involves simple mathematics, the finite difference method and finite element methods are the most frequently used methods for this purpose. Finite element is the most sophisticated method now a days used because of it's some definite advantages. Starting from a couple of decades back, at present much numerical experimentation and researches are devoted to this method.

A real aquifer system is composed of irregular geometry and multiple layers with different geophysical and hydraulic characteristics (Fig. 1.1). The aquifer excitations are also different in different parts of the aquifer depending on the land use pattern and other human activities and the resulting aquifer responses are subjected to spatial and temporal variations depending on the boundary and atmospheric conditions. So to have a realistic
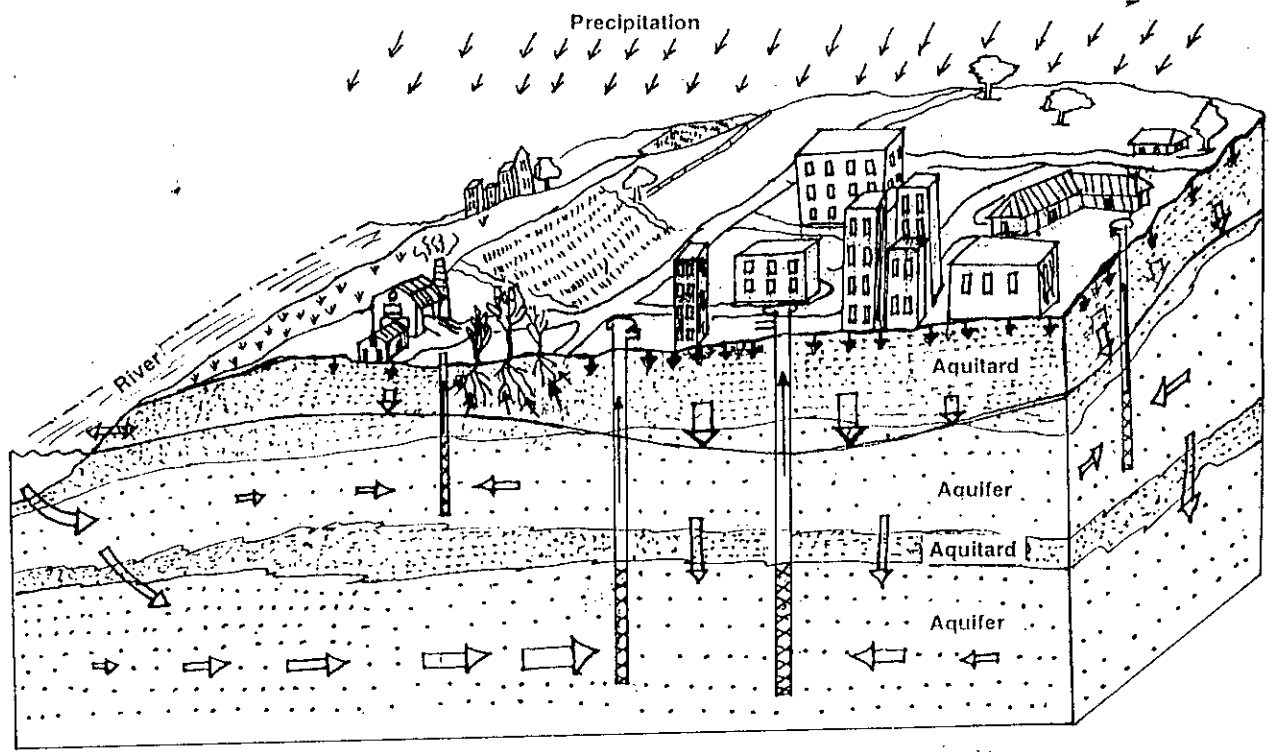
FIG. 1.1 : BASIC HYDROGEOLOGICAL SYSTEM

approach to simulate a natural catchment consisting of multi-aquifer system with heterogeneous material properties, three-dimensional approach will give rise to more understanding to it's intricacy. Three-dimensional modeling involves with high core storage and computational costs. But at present, with the rapid advancement of computer technology, the computational costs are reduced enormously and high speed computers with required memory and storage are readily available. It is only recently that much experimentation is going on with three-dimensional simulation of groundwater basins especially with finite element method.

In case of Bangladesh, the aquifers are further complicated with respect to physical structure and boundary conditions. In monsoon period there is heavy rainfall over the country upto a magnitude of 2200 mm per annum. This heavy rainfall associated with external cross-border flow of water through the rivers causes flooding of the lands and long term submergence of a considerable portion of the country. So aquifers are replenished directly from the precipitation-infiltration process, from the accumulated standing water over the submerged lands, the occurrence and distribution of which vary with time. On the other hand, the rivers which partially or fully penetrate the aquifers or overlying aquitards fed the aquifers naturally, or in induced way when heavy pumping near the rivers occur. The aquifers are also of compound nature with variable properties of soil creating multiple resistance layers partially confining the high yielding porous materials those serves as good storage. In case of urban areas, like densely populated Dhaka city, human activities in the area reduced the natural replenishment from the surface but contributed considerably in other way by return flow from the sanitary and industrial water supply.

Although till now, a large number of numerical models in finite element method have been developed which are discussed later as literature review, the number of models handling real problems are very few. The present work is devoted to develop a three-dimensional groundwater model that can handle a situation like Dhaka city. The saturated and unsaturated flows are treated simultaneously. To obtain proper global mass-balance that is sometimes, in case of variably saturated flow, poor in finite element method as reported by the literature, a mass-balance computational strategy is used which is developed by Celia et. al. (1990) for an one-dimensional problem. A number of published problems from the

4

literature have been solved in the course of development and testing of the different features of the model and finally a strip of Dhaka city along the bank of the river Burhiganga has been analyzed for the demonstration and application purposes of the present algorithm.

1.2 Objective and Scope of the Study

(a) To develop a three-dimensional groundwater flow model to simulate saturated-unsaturated flow of water in multiaquifer system of complex hydrogeological situation. To ensure proper global mass balance of the solution a mass conservative method of computation as proposed by Celia et al. (1990) will be implemented.

(b) To apply the proposed model in some published saturated-unsaturated problems and thereby examine it's numerical efficiency and accuracy.

(c) Finally, to apply the model to a real hydrogeological situation composed of multiple layers with natural or induced recharge simultaneously from river water, surface atmospheric activities and from other types of replenishment (e.g., urban return flow). A strip of Dhaka city along the bank of the river Burhiganga will be studied for this purpose.

5

1.3 Organization of the Present Thesis

This report is composed of seven chapters in total. Upto chapter five, related literature and theoretical aspects are discussed. Chapter Six presents the results of model testing and applications. The conclusions and recommendations with respect to the published example testing and Dhaka city strip modeling are included in Chapter Seven.

The review of literature on the methods of solving groundwater flow problems with special focus on the finite difference and finite element models are presented in Chapter Two. A brief recapitulation of the development of groundwater flow theories are also discussed in this chapter. Chapter Three deals with the core portion of the mathematical background of the model development which describes Galerkin finite element formulation with the adopted solution scheme and iteration strategy. In Chapter Four and Five implemented auxiliary features of the model are discussed in brief.

Chapter Six consists mainly of two parts ; one dealing with the results of simulation for model testing for different schematized problems and subsequent part describes Dhaka city strip modeling. The results obtained from each such application are discussed and accompanied with required graphs in the corresponding subsections in a sequential order.

CHAPTER TWO

REVIEW OF LITERATURE

2.1 Introduction

Groundwater or subsurface water, is a term used to denote all the waters found beneath the surface of the ground in the void spaces of the soil. Groundwater development dates from ancient time. Starting from the seventeenth century when a clear understanding of groundwater as a hydrologic cycle was developed, up to now, a large number of scientists and engineers devoted their research in this field. The literature is now composed of inter-disciplinary contributions from geologists, hydrologists, engineers, chemists, mathematicians and petroleum and agricultural scientists.

Practically all groundwater can be thought of as part of the hydrologic cycle which in simplest way is the earth's water circulatory system. Very small amount, however, may enter the cycle from other sources (e.g., magmatic water). The science of the occurrence, distribution and movement of water below the earth surface is called groundwater hydrology. Water bearing formations of the earth's crust act as conduits for transmission and as reservoirs for storage of water. Water enters these formations from the ground surface or from bodies of surface water is called recharge after which it travels slowly underneath varying distances until it returns to the surface by action of natural flow, vegetation or abstraction is called discharge phenomena. The storage capacity of groundwater aquifers with slow rates of flow combination provide large and extensive sources for water supply.

2.2 Development of Groundwater Theories

Groundwater exploitation preceded the establishment of the rudiments of groundwater science by many centuries. The source of groundwater remained unproven, if not

undisclosed, until the later part of the 17th century when some European scientists (e.g.,Pierre Perrault, 1674; Edone Mariotte, 1686) concluded from rainfall-runoff measurements that yearly precipitation volume was high enough with respect to river flow which can contribute to groundwater body and other surface water bodies and before that it was widely believed that earth is practically impermeable by rain water.

The 19th century saw the development of the basis for the quantitative description of groundwater motion. Hagen (1839) and Poiseuille (1840) derived, independently, the equations for viscous flow in capillary tubes and Darcy (1856), published his now famous empirical equation for flow of water through sand. Darcy's law, in a generalized form, remains today the fundamental flow rate equation in the analysis of groundwater motion. Thiem (1870) developed equations for flow toward wells and galleries. Forchheimer (1886) introduced the concepts of conformal mapping and the construction of flow nets, the method of images, and the theory of functions of the complex variable. He was the first to solve the problem of groundwater flow in a semi-infinite water-yielding formation bounded by a perennial stream and the problem of a well discharging from a water-yielding formation that is supplied by uniform recharge.

In the twentieth century, increased activity in all phases of groundwater hydrology has occurred. Boussinesq (1903-4) first addressed the problem of the falling water table and introduced the concept of specific yield to take into account the contribution of drainage from the unsaturated zone to the flux through the water table. Meinzer (1923) evaluated early studies on the framework of principles and methodologies for investigations of the occurrence and distribution of groundwater and provided the first manual for groundwater hydrologists. One of the most important milestones in the development of groundwater resource evaluation was Theis's (1935) introduction of an equation for the non-steady state flow to a well. As mentioned above Boussinesq equation, however, does not consider the physics of the water movement in the unsaturated soil. The problem of unsaturated flow was tackled mainly by Buckingham (1907), then by Green and Ampt (1911) and finally by Richards (1931) who was able to develop further the Buckingham's (1907) concept of soil water potential of unsaturated soils. At present, most of the studies of soil water movement is based on Richards (1931) equation.

Childs (1945) and Youngs (1957) described that both the soil water pressure head and the soil moisture content approach constant values during a prolonged vertical infiltration in long columns, in which therefore the hydraulic conductivity equals to the vertical downward flux. The effect has been used for the measurement of hydraulic conductivity of unsaturated porous materials (Childs and Collis-George, 1950). For upward movement caused by evaporation at the soil surface or by root water uptake, it was found that the water movement can be limited by the soil conditions, being dependent on the depth of the water table as well as the soil hydraulic properties (Gardner, 1958; Gardner and Fireman, 1958).

For non-steady conditions, the mechanisms of water flow and water retention in unsaturated soils interfere, which is reflected in diffusion formalism of the underlying mathematical theory. Childs and Collis-George (1950) defined the soil water diffusivity by rearranging the terms in Richards equation and suggested the diffusion-type Richards equation as suitable for possible solution of vertical infiltration from a ponded soil surface into a uniform porous material when the effect of gravity is negligible. Philip (1955), utilizing the results of Crank and Henry (1949), recognized that the flow equation with the earth gravity neglected becomes a nonlinear diffusion equation, the solution of which with the ponded infiltration boundary conditions can be obtained using a numerical iterative method.

In the case of unsaturated flow theory existing paradoxes and realities are discussed by Gray and Hassanizadeh (1991) and they gave unsaturated flow theory including interfacial phenomena and advance theory of multiphase flow in general. In recent decades, much attention has been paid to hill-slope hydrology, as attested by volumes edited by Kirkby (1978) and Abrahams (1986). In this communication Philip (1991) developed extensions to infiltration theory for horizontal land surfaces needed to embrace hill-slope conditions.

Two-and three-dimensional soil-water flow problems that arise, for example, when water is supplied from sources of finite areal dimensions on the surface, present a more difficult problem for analysis than the one-dimensional flow. In these cases analytical solutions to Richards' equation have been possible only for particular mathematical forms of the relationships between soil-water properties and are as good as those relationships which describe the properties of the given soil (e.g., Wooding, 1968; Philip, 1969). Waechter and

9

Philip (1985) recognized that an analogy exists between the quasi-steady absorption of water from cavities and the scattering of the plane acoustic waves around soft obstacles. Large series of analytical solutions has resulted from this recognition for absorption and infiltration from cavities of different shapes, as well as for water exclusion from empty subterranean holes (e.g. Philip, 1986; Philip, 1989; Philip et al., 1989).

2.3 Solution of Groundwater Flow Problems

Groundwater flow problems are initial and initial boundary value problems. In principle, three classes of methods exist for solving such problems. These are analytical methods, methods based on the use of physical models and analogs and numerical methods which are mathematical models.

For a number of problems involving linear or quasi linear equations and region of simple and regular geometry, it is possible to obtain exact solutions by analytical methods. Scale model like sand box model and analogs or electric analogs, membrane analogs were used for some special purposes. For most regional studies of practical interest of irregular shaped aquifer with nonhomogeneous or anisotropic materials and variable boundary none of the first two methods are suitable. Computer based numerical methods are, nowadays, the major tool for solving large scale groundwater forecasting problems as encountered in practice. In last few decades, parallel to the advance in computer technology, much effort has been devoted, in many parts of the world, to the development of the methodology and techniques for numerical solution of the mathematical formulation of the problem.

As per the conceptual basis of construction of models, groundwater model can be single cell model or multi-cell model. Single cell model is perhaps the simplest model which visualizes an entire basin as a single cell. The underlying assumption is that average conditions (e.g., an average water table elevation) suffice to describe the behavior of the aquifer cell. The single cell model comprises a horizontal area bounded by impervious boundary. In the case of multi-cell model the investigated aquifer is divided into a number of cells with the considerations of the basic ideas of single cell model. The major difference

lies in the assumption that the horizontal boundaries of each cells are pervious and flows occur across the boundaries (Bear, 1978).

2.3.1 Analytical Solutions

Although limited in application, analytical models are useful in aquifer test analysis ; evaluation of simple aquifer systems; design, calibration, or verification of numerical models; and understanding basic principles of groundwater flow and transport. Advances in analytical modeling virtually dominated groundwater literature through the 1950's. A large number of analytical models structured to solve partial differential equations governing the flow of groundwater to and from wells has been developed. Among others ., contributors for non-steady artesian aquifer are Theis (1935), Hantush (1959,1964) , Papadopulos (1965,1967), Boulton and Streltsova (1977 a,b), for leaky artesian aquifer with negligible aquitard storage and isotropic aquifers are Hantush (1959), Witherspoon (1967), for water table aquifers are Boulton (1963), Neuman (1975), Boulton and Streltsova (1976,78). A few analytical models involving finite single boundary and multiboundary aquifer systems have been developed (e.g., Stallman,1963; Vandenberg, 1977 etc.) . A brief review of the models developed up to 1979 are given by Walton (1979).

For unsaturated flow case, initially, most solutions were applied only to one-dimensional, horizontal or vertical systems. Highly significant is the early work of Philip (1955,1957) that provided much of the physical and mathematical groundwork for subsequent analysis by others. Numerous studies have followed for both one- and multi-dimensional problems (Parlange 1971; Warrick 1974; Babu 1976; Raats 1976; Lomen and Warrick 1976; Batu 1979; among many others).

Philip (1957a) has derived his series solution for one-dimensional vertical infiltration. Since the series does not converge for large time, it was rather the simplified semi-empirical two-term Philip's (1957b) infiltration equation which became popular. Philip (1960a, b,c) has shown that the nonlinear diffusion problem can be solved analytically if the diffusivity-moisture content relation belongs to a certain class of functions. Later, new quasi-analytical

techniques have been suggested by several authors for the solution of non-linear diffusion and vertical infiltration problems (e.g., Parlange, 1971a,b; Philip and Knight, 1974), with an increasing accent on infiltration from rain of constant or variable intensity, i.e., on the Neuman-type boundary condition (e.g., Smith and Parlange, 1978; Morel-Seytoux 1978,1982; White et al., 1979; Clothier et al., 1981; Broadbridge and White, 1988). Another quasi-analytical solution for infiltration on planer slopes was developed by Philip in 1991.

Other one-dimensional processes, like the water redistribution after infiltration (Youngs and Poulovassilis, 1976) and transient or quasi-steady column drainage (Swartzendruber, 1969; Raats and Gardner, 1974) received less theoretical attention, particularly because they are less apt to an analytic solution. The effect of hysteresis in the soil moisture content - matric head relation must be inevitably taken into account when treating the process of water redistribution after infiltration.

2.3.2 Numerical Methods

Regarding the techniques of solution there are currently five widely used numerical methods exist (Huyakorn and Pinder, 1983). These are finite difference methods, Galarkin or variational finite element methods, collocation methods, method of characteristics and boundary element methods. These methods are closely related. In several cases the finite difference, finite element, and collocation methods yield the same approximation. The method of characteristics is a variant of the finite difference method and is particularly suitable for solving hyperbolic equations. Finally, the boundary element method, a variant of the conventional finite element method, is especially useful in the solution of elliptic equations for which Green's functions exist. In the next three subsections the finite difference and finite element methods and corresponding models of groundwater problems are reviewed briefly. The status of three-dimensional groundwater flow modeling has presented in a separate subsection.

2.3.2.1 Finite Difference Method

Finite difference methods are conceptually straightforward. Finite difference method (Remson et al., 1971), with explicit, implicit or mixed difference schemes, belong to the most frequently used techniques in modeling groundwater flow. The fundamental idea here is to replace all derivatives by finite differences and thus reduce the original continuous boundary value problem to a discrete set of simultaneous algebraic equations. The advantage of the finite difference method is in its simplicity and efficiency in treating the time derivatives. On the other hand, the method is rather incapable to deal with complex geometries of flow regions. A slow convergence, a restriction to bilinear grids and difficulties in treating moving boundary conditions are other serious drawbacks of the method. In dealing with non-uniform soils of complex geometry and arbitrary anisotropy, the finite difference approach is often difficult to apply. The treatment of system-dependent atmospheric boundaries, such as seepage faces and evaporation surfaces, are difficult with this approach because the handling of prescribed flux boundary conditions lead to complex expressions and to non-symmetric matrices (Forsythe and Wasow, 1960).

Finite difference approximations have been used in a large number of studies solving one-dimensional (vertical), variably saturated flow problems (e.g., Day and Luthin, 1956; Whisler and Watson, 1968; Freeze, 1969; Brandt et al., 1971; Haverkamp et al., 1977; Dane and Mathis, 1981; Haverkamp and Vauclin, 1981). Fewer researchers have attempted finite differences to solve variably saturated flow problems in higher dimensions (e.g., Rubin, 1968; Cooley, 1971; Freeze, 1971a,b; Narasimhan et al., 1978 ; Healy et al., 1990 ; Kirkland et al., 1992). Most of the existing two-dimensional finite difference solutions to variably saturated flow problems have limitations. The finite difference models of Freeze (1971a,b) and Colley (1971) are not robust because they incur numerical instabilities and convergence difficulties. These problems arise primarily from inefficiencies of the line successive over-relaxation and alternating directional implicit schemes used in solving the two-dimensional, nonlinear equations. Kirkland et al. (1992) presented an efficient algorithm of a finite difference solution to two-dimensional, variably saturated flow problems. However, the objective of Kirkland et al. (1992) was to develop competitive numerical procedure to solve infiltration problems in dry soils. The fundamental flow equation solved

by Kirkland et al. (1992) (Richards' equation) does not account for the effects of specific storage and consequently it cannot be used to model accurately a wide variety of variably saturated flow problems, including many transient drainage and seepage-face phenomena in large domains. Clement et al.(1994) mentioned some of the limitations of the existing models and developed a physically based two-dimensional finite difference algorithm for variably saturated flow.

2.3.2.2 Finite Element Method

It is a powerful and extremely flexible method which can easily handle irregularly shaped flow regions composed of non-uniform soils with arbitrary anisotropy. The method was first applied to a problem involving saturated-unsaturated flow in porous media by Neuman (1973). With finite element methods the domain is divided into a number of grid elements. Each element is characterized by local coordinate functions . This permits the application of variational or weighted residual principles (Wang and Anderson, 1982). In this method, the objective is to transform the partial differential equation into an integral equation which includes derivatives of the first order only. Then the integration is performed numerically over elements into which the considered domain is divided. Huyakorn and Pinder (1983) reviewed and presented the application of finite element methods to groundwater problems.

Finite element method have been successfully used by several researchers to solve the flow in saturated, unsaturated and variably saturated cases. The classic papers by Javandel and Witherspoon (1968) and Zienkiewicz et al. (1966) appear to be first two publications describing the use of triangular finite element in porous media flow. Shortly thereafter Neuman and Witherspoon (1970, 1971) and Taylor and Brown (1967) demonstrated the application of this methodology to the analysis of free surface groundwater flow. Models for infiltration in unsaturated soil have been developed by several researchers. Abriola (1986) developed a finite element model for unsaturated flow using hierarchic basis functions. Hayhoe (1978) studied the relative efficiencies of finite difference and Galarkin techniques

for modeling soil-water transfer. Celia et al. (1990) developed a general mass-conservative numerical solution for the unsaturated flow equation ; a modified numerical approach with mixed form of the unsaturated flow equation was used. Gottardi et al. (1992) used moving finite element method for one-dimensional infiltration into homogeneous unsaturated soil and concluded that this method is faster than finite difference and finite element method for this specific case.

Finite element techniques to two-dimensional saturated-unsaturated flow problems were applied by several researchers . Among them are Neuman (1973), Neuman et al. (1974), Reeves and Duguid (1976), Bruch (1977), Frind et al. (1977), Yeh and Ward (1980). In all of these studies nonlinearities were treated using standard Picard solution algorithm. In order to deal with a wider range of field conditions, an improved Picard algorithm and a Newton-Raphson algorithm were used by Huyakorn et al. (1984). In this model the element matrices are evaluated in a simple and efficient manner using a technique referred to as the "influence coefficient" technique. All of the models stated in so far are developed by Galarkin finite element method. Cooley (1983) used somewhat different sub-domain finite element method in combination with Newton-Raphson and strongly implicit procedure. Allen and Murphy (1986) introduces a finite element collocation technique for solving variably saturated flow in two space dimensions. The scheme used a mass-conserving formulation of Richards' equation as the basis for the finite difference time stepping method. Panday et al. (1993) discussed recent advances in finite element modeling techniques for variably saturated flow problems.

2.3.2.4 Three-Dimensional Groundwater Flow Modeling

In the past twenty years or so, a number of three-dimensional groundwater flow models have been developed by using various numerical methods. Freeze (1971) was the first to present a three-dimensional finite difference model. Frind et al. (1978) closely examined the practical aspects of three-dimensional modeling of groundwater flow system and concluded it as a practical option. Reisenauer et al. (1982) used integrated finite difference method. Those models have some limitations which have been pointed out by

Huyakorn et al. (1986). Gupta et al. (1984) developed a model to simulate multi-aquifer system and applied to Long Island, New York. A different approach was used by Gambolati et al. (1986) in which they used a quasi three-dimensional approach by considering the transient leakage across the aquitards using the convolution approach originally derived by Herrera (1970). Recently Paniconi et al. (1993) developed catchment scale models and applied these to real situations. Yu et al. (1994) used Galerkin finite element method combined with the collocation method to handle the time derivative terms in the governing equation. He indicated a number of limitations to some existing models. For instance, Gupta and Tanji's model (1976), assumed that groundwater flow is steady, the model of Gupta et al. (1984) and Istok's model (1989) assumed that all sources and boundary conditions are time invariant. In all the above applications, the pressure based form of the variably saturated flow equations are used. Unfortunately numerical solutions of the pressure-based form of the closely related, but more restrictive, Richards equation are known to have poor mass-balance properties in saturated-unsaturated media (Celia et al., 1990; Kirkland, 1991; Clement et al., 1994).

2.4 Status of Groundwater Modeling in Bangladesh

The first groundwater model used in Bangladesh is in 1977 under BADC/IDA Tubewell Project. Afterward a variety of groundwater modeling studies have been carried out. Between 1977-1984, eight groundwater modeling exercises have been undertaken. The water balance study of the BWDB/UNDP (1984) project also modeled the groundwater component. According to MPO (1987), these models can be classified into three types; Single Cell models, Multiple Single Cell models and Multiple Cell Integrated Finite-difference models. A brief description about these models are summarized below.

2.4.1 BADC/IDA Tubewell Project (1977)

Under this project, the main model covered most of northwest region at north of Atrai basin and another sub-model covered the area between the rivers Atrai and Ganges. Both of the models were finite difference single layer model with aquifer system of semi-confined

or unconfined type. The objectives of the models were to forecast the development of DTW. But the quality of data base was not sufficient for accurate simulation. The calibration period for main model was November to June and that for the sub-model was September to May.

2.4.2 ADB Tubewell Project: North Bangladesh (1980)

The model was single layer finite difference type with unconfined aquifer system . The model area covered parts of Dinajpur and Rangpur districts. The objectives of the model were to forecast DTW development and refinement of BADC/IDA (1977) main model. The quality of data base was reasonable and the calibration period was dry season.

2.4.3 Rajshahi, Pabna Groundwater Model (1980)

The model was two layer finite difference type with the aquifer system consisting of confined aquifer overlain by a semi-confining layer. The objectives of the model were to forecast the development level of DTW. The calibration period was dry season. The quality of data base was reasonable for aquifer geometry but poor for other parameters. The simulation being based on sparse data, results were not published widely.

2.4.4 Development Plan for Waste Water Systems for the Dhaka Metropolitan Area (1980)

The model used was of single layer and of finite difference type. The aquifer system considered consist of semi-confined aquifer. The objective of the model was assessment of piezometric head declined under different future abstraction schemes for the period 1980-2010. The calibration period was from 1966 to 1978. But the quality of data base was poor.

2.4.5 ADB-II DTW Project (1982)

Under this project, a single cell model was developed for the northwest region to simulate aquifer responses in six typical areas of six major physiographic units. To test the effect of river level fluctuations on the aquifer; strip models were used. The simulated flow balance was thus consisted of vertical flow and lateral flow as in single cell model.

17

2.4.6 Southwest Rural Development Project (1984)

The model was single layer finite difference type with a semi-confined aquifer. The modeled area was southwest region of Bangladesh comprising the districts of greater Jessore, Kushtia and Faridpur. The objective of the model was to forecast STW/DTW development potential. The components of flow balance equation consisted of leakage, recharge, discharge, inflow/outflow across boundaries which were computed explicitly with no integrated interaction being taken care between aquifer and semi-confining layer. So this could affect the accuracy of simulation.

2.4.7 The Northwest Bangladesh Groundwater Model

The prime objective of the model was to obtain realistic estimates of STW development levels in Rajshahi division of Bangladesh. Two criteria were set to determine the optimum development level of STW. Firstly, the maximum depth to pumping level should be less than 7.5 m and secondly, the system should be adequately re-filled during wet season. So the complete hydrologic cycle was incorporated in the model simulation unlike for dry period. The model was finite difference type with internal boundaries primarily based on major physiographic units and internal rivers whereas the external boundaries were formed by rivers Ganges and Jamuna and geographical boundary with India. The aquifer system was simulated as a single aquifer of variable thickness overlain by a semi-confining layer.

2.4.8 Water Balance Studies (1983) BWDB/UNDP

For the northwest and northeast regions of Bangladesh, wet and dry deep percolation rates for 27 aquifer units were determined from this model simulation. But they did not represent actual field values. Considering a minimum and maximum recharge periods during monsoon to be 90 to 150 days, a minimum and maximum potential recharge quantity based on wet land deep percolation rate were calculated. As only 23 percent of the total land area was cultivated by T. Aman (wet land); the cumulative recharge assuming wet land was less

18

than the weighted average recharge considering both wet and dry land conditions. However, this recharge value could represent potential recharge where no rejection of recharge occurs due to aquifer full condition.

2.4.9 Model Used by MPO (1987 & 1991)

The setup of MPO in the study of groundwater availability and planning for development is basically equipped with a network of groundwater models. The output from one model acting as an input for another model and depending on the stage of formulation or implementation of the plan; different models of qualitatively different status are supposed to be used as needed. From 1983-1986, MPO within the National Water Plan (NWP) preparation schedule, model was applied in eight special study areas, each with an area of 100 square km, dispersed across Bangladesh. These areas were intensively monitored and data acquired to calibrate the models. In catchment recharge simulation, all catchment which had data were modeled as a multiple single cell model in which only the vertical components of flow were considered. In the second phase of the NWP, the existing models of first phase were adapted for national assessment and future incremental resource available for development. There are four models in the network. The models are Recharge Model, Depth Storage Model, Resource Potential Model and Multi Cell Model. The detailed description of the models have been given in the following sections.

2.4.9.1 Recharge Model

Recharge model calculates the maximum possible recharge (unobstructed by raised groundwater table), and limited only by the rate of deep percolation of the top or subsoil. The conceptual basis is similar to Karim's (1984) study in calculation of potential recharge with provision for lowering the water table through irrigation during dry season.

2.4.9.2 Depth/Storage Model

This model is used to compute the net available storage in the aquifer system available for groundwater abstraction. This is an adaptation of the model used during the first phase. The methodology has been slightly modified in second phase and a range of specific yield values rather than single value are used in the simulation. The specific yield value and water table decline are the two determining factors of net available storage.

2.4.9.3 Resource Potential Model

The model combines results obtained from the recharge model and the depth/storage model and compute groundwater resource development potential for different flood phases and for different modes of pumping.

2.4.9.4 Multi-Cell Model

This model is used for the detailed analysis of groundwater behaviour in the MPO special study areas, and can also be used in a single cell mode for individual upazilas. The main purpose of the model is to obtain a better definition of the parameters which most strongly affect the computation of potential recharge and the net available storage.

2.4.10 Groundwater Model for Dhaka WASA

Three groundwater models have been used in the past to assess the groundwater resource availability in the Dhaka city region. RMP/Montgomery developed a groundwater model for Dhaka WASA in 1980, Solomon and Chidley review this model in 1986 and lastly in 1989 Dhaka region groundwater and subsidence model was developed. These are discussed briefly below :

2.4.10.1 RMP/Montgomery (1980)

The model was used to assess the impact of additional groundwater abstraction on the aquifer system. It was based on finite difference method. The aquifer system was simulated as a single aquifer unit overlain by a semi-confining layer. The study area being surrounded by major rivers, it was expected to prevail a good interaction between rivers and aquifer system. But when the model was run in predictive mode to assess the impact of increased abstraction from 1980 to 2010, the results of the model showed poor relation between the rivers and the aquifer.

2.4.10.2 Solomon and Chidley's Review of the Parsons' Model (1986)

The limitations of the Parsons' Model, as described by Soloman and Chidley, were due to poor representation of boundary conditions and recharge mechanism. They used a USGS (United States Geological Survey) model to assess the groundwater resource considering the effect of rivers and the potential recharge values from MPO and the hydrogeological parameters from BWDB. But still the results were not satisfactory, that is, similar to those of previous models of Tames M. Montgomery and R.M. Parsons. They did not calibrate their USGS model against historical data before predictive run. However, they came to a conclusion that a detailed modeling of Dhaka area is necessary with special emphasis on extending the model boundaries to the major rivers and improved simulation of recharge mechanism.

2.4.10.3 Dhaka Region Groundwater and Subsidence Model (1991)

In 1989, the Dhaka region groundwater and subsidence model study was started with the purpose of assessing the impact of the proposed installation of 50 new and 10 replacement tubewells. The model was based on integrated finite difference method. A basic feature of the model is the resolution of three-dimensional groundwater flow into it's horizontal and vertical components.

The areal extent of the model is bounded by three major rivers, Jamuna, Ganges and Meghna in three sides and the remaining northern part is bounded partly by Old Brahmaputra and partly by northern edge of Gazipur and Manikganj districts. The groundwater resources model consists of two integrated units. The regional model evaluated the consequences of groundwater development on a regional basis. The Dhaka sub-model considered the Dhaka metropolitan area and immediate surroundings. This model is sufficiently refined to take into account the spatial variability of various parameters such as local relief, geology, physiography, and distribution of abstraction.

The model developed is a four layer model; lower aquifer (main aquifer of abstraction), lower aquitard, upper aquifer and upper aquitard. The two fundamental principles used are continuity of mass and Darcy's law. The flows are horizontal in aquifers and vertical in aquitards. Both steady and transient state of flows are encountered in the model. The geometry of aquifer system is defined by the elevations of top and bases of different layers.

CHAPTER THREE

METHODOLOGY

3.1 Introduction

The physical processes involved in groundwater flow can be described mathematically coupling Darcy's law of groundwater flow with the equation of continuity that describes the conservation of fluid mass during flow through a porous medium. With some assumption the resulting mathematical statement of the problem is a second order partial differential equation which is in generalized form called Richards' (1931) equation. In a slightly modified form it can be used for variably saturated flow. To solve this equation numerically a class of weighted residual finite element method, Galerkin method is used here. In the following sections the theoretical background of the equation of flow and formulation of the groundwater flow model has been described.

3.2 The Governing Flow Equation

Darcy's law in generalized form can be written as $q = -K \underline{\nabla} h$ where, h is the total hydraulic potential, K is the hydraulic conductivity tensor. If we denote saturated hydraulic conductivity tensor by K_{ij} and relative permeability with respect to water phase by k_r, then the equations can be written by Einstein's summation convention as :

$$q_i = -K_{ij} \, k_r \, \frac{\partial h}{\partial x_i} \qquad ; \qquad i,j \in x,y,z \qquad\qquad (3.1)$$

where q_i is the volumetric flux of water (LT^{-1}) in three axis directions each having a summation of three terms in right hand side.

For conservation of mass, from the continuity equation, the rate of mass inflow equals the rate of increase of mass in a control volume. In case of transient flow in saturated-unsaturated soil, considering a local sink, S ,this equation can be expressed as,

$$-\frac{\partial(\rho_w q_i)}{\partial x_i} = \frac{\partial(\rho_w S_w n)}{\partial t} + S \qquad (3.2)$$

where ρ_w is the density of water ; S_w is the degree of saturation ; n is the porosity; and S is the intensity of local sink. For incompressible fluid, density of water (ρ_w) is constant. In that case,

$$-\frac{\partial q_i}{\partial x_i} = \frac{\partial(S_w n)}{\partial t} + S \qquad (3.3)$$

Coupling Eq. 3.1 and Eq. 3.3, equation for layered, multi-dimensional flow through porous media is obtained. The final form can be written as,

$$\frac{\partial}{\partial x_i}(K_{ij} \ k_r \frac{\partial h}{\partial x_j}) = \frac{\partial}{\partial t}(S_w n) + S \qquad (3.4)$$

If we introduce pressure head (ψ) instead of total potential h such that h=ψ+z, the equation can be written in a modified form,

$$\frac{\partial}{\partial x_i}[K_{ij} \ k_r \frac{\partial \psi}{\partial x_j} + K_{iz} \ k_r] = \frac{\partial \theta}{\partial t} + \frac{\theta}{n} S_s \frac{\partial \psi}{\partial t} + S \qquad (3.5)$$

where K_{iz} is the saturated hydraulic conductivity for z direction ; θ is the volumetric moisture content; and S_s is the specific storage term for the media.

This mixed form of the equation consists of two state variables. One is moisture content, θ, which is normally used in unsaturated flow case and other is ψ, the pressure head, used in saturated flow case. In the unsaturated or variably saturated case, because of the nonlinear nature of the relations between relative permeability, water saturation, and pressure head, the governing equation is highly nonlinear.

3.3 Mathematical Formulation of the Solution Scheme

The basic approach of the finite element solution scheme is based on subdividing the flow region into finite segments called elements bounded and represented by a series of nodal points at which a solution is obtained. The solution depends on the solution in the surrounding nodal points and on an appropriate set of auxiliary conditions. Each elements of the domain is characterized by local coordinate functions (Neumann et. al., 1975). This permits the application of variational or weighted residual principles. In the following sections mathematical formulation of the groundwater flow problem in terms of the Galerkin finite element method is presented.

3.3.1 Discretization of the Flow Domain

Initially to avoid complicacy in the representation, the flow domain is subdivided into a network of simple brick elements. These brick elements once again subdivided into four noded tetrahedral elements as shown in the Figure 3.1. The four corners of each element are the nodal points and the global space coordinates (x,y,z) of a node n can be designated by x_i^n (i=1,2,3). Each element, e, in the domain is associated with a local coordinate function or basis function $\xi_n^e(x,y,z)$, which are used to express the variation of unknown variables within an element and also coordinate transformation from global (domain, x,y,z) to local (element) coordinates. These shape functions vary linearly inside the element, vanish outside the element and satisfy the requirement $\xi_n^e(x_i^m) = \delta_{mn}$; where δ_{mn} is the Kroneker delta having values of either 1; if m=n or zero , if m $\neq$ n. The tetrahedral element is associated with volumetric local coordinate system. These coordinate system has identical property to basis functions and the required integrations can be performed easily by some direct integration formulas (Zienkewisch, 1977). The nodes of the elements are counted in a specified manner to obtain homogeneity in the computation . The convention followed here is : observing from a node (node 4) , the other three nodes are numbered in anticlockwise direction as 1,2,3 .
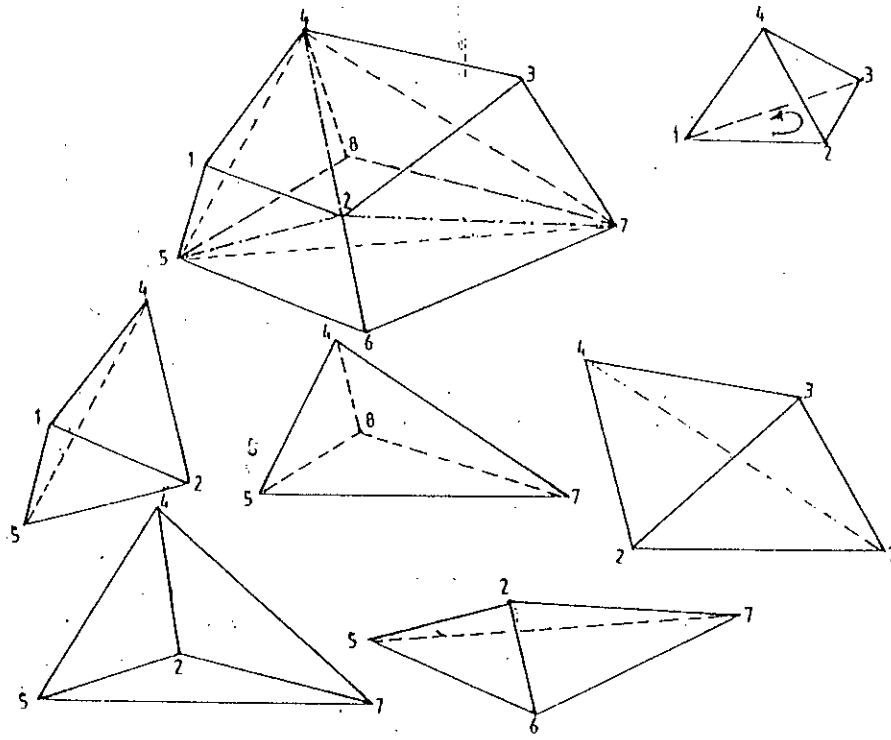
Fig. 3.1 : Discretization of a brick element into tetradedral
sub-elements with numbering convention

3.3.2 Galerkin Approximation

Introducing a general well function Q_k (x,y,z) , denoting soil water capacity by $C (= \frac{d\theta}{d\psi})$, the flow equation (3.5) can be generalized as :

$$\frac{\partial}{\partial x_{ij}} [KK_{ij}^{A} \frac{\partial \psi}{\partial x_j} + KK_{iz}^{A}] = C \frac{\partial \psi}{\partial t} + \frac{\theta}{n} S_s \frac{\partial \psi}{\partial t} + S + \sum_{k=1}^{r} (\delta(x - x_k) \delta(y - y_k) \delta(z - z_k)) Q_k$$

$$(3.6)$$

sink term S denotes the water extraction by root system (T^{-1} i.e., volume of water extractions per unit volume of soil per unit time) ; Q_k is the volumetric water flux at a point located at (x_k, y_k, z_k) [L^3/T] and r is the total no. of such locations ; K_{ij}^{A} is the anisotropy tensor for hydraulic conductivity.

According to Galerkin method, an approximate or trial solution $\hat{\psi}$ in terms of the pressure head ψ at any given time t is obtained in the form of a sum of a finite sequence.

To solve the above equation numerically a trial solution is selected as:

$$\psi(x, y, z, t) \approx \hat{\psi}(x, y, z, t) = \sum_{n=1}^{N} \psi_n(t) \phi_n(x, y, z) \tag{3.7}$$

N is the number of nodes ; ϕ_n is a set of independent shape functions which are specified beforehand. Substituting the trial solution of Eq.(3.7) in Eq.(3.6) will result in a residual, R.

Residual:

$$R(x, y, z, t) = L(\hat{\psi})$$

$$= \frac{\partial}{\partial x_i}[KK_{ij}^A \frac{\partial}{\partial x_j}(\sum_{n=1}^{N} \psi_n(t) \phi_n(x, y, z)) + KK_{iz}^A] - (C + \frac{\theta}{n} S_s) \frac{\partial}{\partial t}(\sum_{n=1}^{N} \psi_n(t) \phi_n(x, y, z)$$

$$- s(\psi, x, y, z) - \sum_{k=1}^{r}(\delta(x - x_k) \delta(y - y_k) \delta(z - z_k) Q_k) \tag{3.8}$$

This residual would be zero everywhere for all x,y,z and t, if the trial solution were the exact solution. In the method of weighted residuals, an attempt is made to force this residual to be zero, in an average sense over the entire domain, through the selection of the unknown values of ψ_n (n = 1,2,3,4....N). This is accomplished by forming a weighted integral of R over the entire solution domain and then setting this integral (weighted residual) to zero. In Galerkin method, the weighing functions are chosen to be identical to the basis functions, $\phi_m(x,y,z)$. Thus the values of ψ_n are determined such that these satisfy the initial and boundary conditions and also the orthogonality requirement of the expression R(x,y,z) to all of the functions $\phi_m(x,y,z)$ (m = 1,2,3,4...N). Thus the weighted residual equation becomes:

$$\int_{\Omega} R(x, y, z, t) \phi_m(x, y, z) d\Omega = 0 \quad ; \quad m \in 1, 2, 3, \ldots \ldots N \tag{3.9}$$

or,

$$\int_{\Omega} \frac{\partial}{\partial x_i}[KK_{ij}^A \frac{\partial}{\partial x_j}(\sum_{n=1}^{N} \psi_n(t) \phi_n(x, y, z) + KK_{iz}^A] \phi_m(x, y, z) d\Omega -$$

$$\int_{\Omega}(C + \frac{\theta}{n} S_s) \sum_{n=1}^{N} \frac{\partial \psi_n(t)}{\partial t} \phi_n(x, y, z) \phi_m(x, y, z) d\Omega - \int_{\Omega} S(\psi, x, y, z) \phi_m(x, y, z) d\Omega$$

$$- \int_{\Omega} \phi_m(x, y, z)(\sum_{k=1}^{r} \delta(x - x_k)(y - y_k)(z - z_k) Q_k) d\Omega = 0 \tag{3.10}$$

27

Now the first term of the above equation contains second order partial differential. This can be linearized by integral transformation with the help of divergence theorem which finally yields to Green's theorem. Then this can be written as :

$$\int_\Omega [\frac{\partial}{\partial x_i} [KK_{ij}^A \frac{\partial}{\partial x_j} (\sum_{n=1}^N \psi_n(t) \phi_n(x,y,z) + KK_{iz}^A] \phi_m(x,y,z) d\Omega$$

$$= \int_s \frac{\partial}{\partial x_i} [KK_{ij}^A \frac{\partial}{\partial x_j} (\sum_{n=1}^N \psi_n(t) \phi_n(x,y,z)) + KK_{iz}^A)] \phi_m(x,y,z) n_i ds$$

$$- \sum_{n=1}^N \psi_n \int_v KK_{ij}^A \frac{\partial \phi_m(x,y,z)}{\partial x_i} \frac{\partial \phi_n(x,y,z)}{\partial x_j} dv - \int_v KK_{iz}^A \frac{\partial \phi_m(x,y,z)}{\partial x_i} dv$$

$$= - \int_s q_i n_i \phi_m(x,y,z) ds - \sum_{n=1}^N \psi_n \int_v KK_{ij}^A \frac{\partial \phi_m(x,y,z)}{\partial x_i} \frac{\partial \phi_n(x,y,z)}{\partial x_j} dv$$

$$- \int_v KK_{iz}^A \frac{\partial \phi_m(x,y,z)}{\partial x_i} dv \tag{3.11}$$

where n_i is the unit normal vector to the surface S. Subscript v and s indicates volume and surface integrations respectively. Substituting Eq. (3.11) into Eq. (3.10), the final equation is,

$$- \int_s q_i n_i \phi_m(x,y,z) ds - \sum_{n=1}^N \psi_n \int_v KK_{ij}^A \frac{\partial \phi_m(x,y,z)}{\partial x_i} \frac{\partial \phi_n(x,y,z)}{\partial x_j} dv - \int_v KK_{iz}^A \frac{\partial \phi_m}{\partial x_i} dv$$

$$- \sum_{n=1}^N \int_v (C + \frac{\theta}{n} S_s) \frac{\partial \psi_n}{\partial t} \phi_m(x,y,z) \phi_n(x,y,z) dv - \int_v S \phi_m(x,y,z) dv$$

$$- \int_v \phi_m(x,y,z) (\sum_{k=1}^r \delta(x-x_k) \delta(y-y_k) \delta(z-z_k) Q_k) dv = 0$$

or,

$$\sum_{n=1}^N \psi_n \int_v KK_{ij}^A \frac{\partial \phi_m(x,y,z)}{\partial x_i} \frac{\partial \phi_n(x,y,z)}{\partial x_j} dv + \sum_{n=1}^N \int_v (C + \frac{\theta}{n} S_s) \frac{\partial \psi_n}{\partial t} \phi_m(x,y,z) \phi_n(x,y,z) dv$$

$$+ \int_s q_i n_i \phi_m(x,y,z) ds + \int_v KK_{iz}^A \frac{\partial \phi_m(x,y,z)}{\partial x_i} dv + \int_v S \phi_m(x,y,z) dv$$

$$+ \int_v \phi_m(x,y,z) (\sum_{k=1}^r \delta(x-x_k) \delta(y-y_k) \delta(z-z_k) Qu bk) dv = 0 \tag{3.12}$$

28

In matrix notation the above equation can be written as:

$$[A_{mn}]\{\psi_n\} + [B_{mn}]\{\frac{\partial \psi_n}{\partial t}\} - \{Q_m\} + \{G_m\} + \{E_m\} + \{W_m\} = 0 \quad ; \quad m, n = 1, 2, 3 \ldots N \quad (3.13)$$

Thus the finite element spatial discretization yields a system of ordinary differential equations. The equations are nonlinear in variably saturated flow conditions because the matrix elements A_{mn} and B_{mn} are function of the nodal unknowns ψ_n. The values of the matrix elements in the integral form are given by :

$$A_{mn} = \int_v KK_{ij}^A \frac{\partial \phi_m(x,y,z)}{\partial x_i} \frac{\partial \phi_n(x,y,z)}{\partial x_j} dv \qquad (3.14a)$$

$$B_{mn} = \int_v (C + \frac{\theta}{n} S_s) \phi_m(x,y,z) \phi_n(x,y,z) dv \qquad (3.14b)$$

$$G_m = \int_v kk_{iz}^A \frac{\partial \phi_m(x,y,z)}{\partial x_i} dv \qquad (3.14c)$$

$$E_m = \int_v S \phi_m(x,y,z) dv \qquad (3.14d)$$

$$Q_m = - \int_s q_i n_i ds \qquad (3.14e)$$

$$W_m = \int \phi_m(x,y,z) (\sum_{k=1}^r \delta(x-x_k) \delta(y-y_k) \delta(z-z_k) Q_k) dv \qquad (3.14f)$$

The above integrations are performed in a piecewise manner on an element basis. The use of element basis functions and local coordinate system facilitate this procedure. Thus element matrices are formed. Summing the contributions from each element matrix associated with a node, the global matrix for the entire domain is formed.

3.3.3 Time Discretization

To solve the ordinary differential equation (3.13), a proper time discretization is necessary. In saturated flow when the specific storage is zero the time derivative disappears. At this condition the governing equation becomes elliptic type and in other cases this is parabolic type. Change in boundary conditions of the saturated flow has an instantaneous effect on the entire saturated region. The solution is no longer a continuous function of time. Pressure head of current time level is independent of the pressure head of previous time level. For these reasons and to get a correct specification of the time dependent part a fully implicit difference scheme has been adopted here.

To ensure good mass conservation of computation especially in the unsaturated zone the mixed form of the governing flow equation is best suited. This mass conservative formulation have been introduced by Celia et al. (1990) and used by other researchers in finite element and finite difference methods successfully. To achieve this, time dependent storage term (in the equation 3.6) can be written as :

$$(\frac{\partial \theta}{\partial t} + \frac{\theta}{n} S_s \frac{\partial \psi}{\partial t})$$

Subsequently the computation of storage matrix $[B_{mn}]$ will be changed. So equation (3.13) can be written as (subscript m,n are omitted here) :

$$[A] \{\psi\} + [B_1] \{\frac{\partial \theta}{\partial t}\} + [B_2] \{\frac{\partial \psi}{\partial t}\} + \{ G \} + \{ E \} + \{ Q \} + \{ W \} = 0 \qquad (3.15)$$

where,

$$B_{1mn} = \int_v \phi_m(x,y,z) \phi_n(x,y,z) \ dv \qquad (3.15a)$$

$$B_{2mn} = \int_v \frac{\theta}{n} S_s \ \phi_m(x,y,z) \phi_n(x,y,z) \ dv \qquad (3.15b)$$

30

The time derivatives are approximated by backward Euler finite difference scheme. For the pressure head time derivative term,

$$\frac{\partial \psi}{\partial t} = \frac{\psi_{t+1}^{i+1} - \psi_t}{\Delta t} \tag{3.16}$$

where subscript t and superscript i indicate the previous time level and Picard iteration level respectively ; Δt is the time step ; $i+1$ and $t+1$ indicating the current levels, $\Delta t = t_{i+1} - t_i$ For the moisture content derivative term

$$\frac{\partial \theta}{\partial t} = \frac{\theta_{t+1}^{i+1} - \theta_t}{\Delta t} \tag{3.17}$$

To obtain compatibility of the two forms (θ and ψ) of the dependent variable together with mass conservation Celia et al. (1990) expanded θ_{t+1}^{i+1} in a truncated Taylor series with respect to the pressure head (ψ) perturbation arising from Picard iteration, about the expansion point (θ_{t+1}^{i}, ψ_{t+1}^{i}) . This is as follows :

$$\theta_{t+1}^{i+1} = \theta_{t+1}^{i} + \frac{d\theta}{d\psi}\Big|_{t+1}^{i} (\psi_{t+1}^{i+1} - \psi_{t+1}^{i}) + 0(\delta^2)$$

where δ is the difference of ψ between two successive iteration level. Neglecting higher order terms this can be written as :

$$\theta_{t+1}^{i+1} = \theta_{t+1}^{i} + C_{t+1}^{i} (\psi_{t+1}^{i+1} - \psi_{t+1}^{i})$$

$$\therefore \theta_{t+1}^{i+1} - \theta_{t+1}^{i} = C_{t+1}^{i} (\psi_{t+1}^{i+1} - \psi_{t+1}^{i}) \tag{3.18}$$

with the help of the Eq. (3.18) , the discretization of the moisture content can be divided into two parts as,

$$\frac{\partial \theta}{\partial t} = \frac{\theta_{t+1}^{i+1} - \theta_t}{\Delta t} = \frac{\theta_{t+1}^{i+1} - \theta_{t+1}^{i}}{\Delta t} + \frac{\theta_{t+1}^{i} - \theta_t}{\Delta t} = C_{t+1}^{i} \frac{\psi_{t+1}^{i+1} - \psi_{t+1}^{i}}{\Delta t} + \frac{\theta_{t+1}^{i} - \theta_t}{\Delta t} \tag{3.19}$$

The first term of the right hand side includes the pressure head difference between two

31

successive Picard iterations at the current time level. So this is an estimate of error between two successive iterations, which should be vanished with the contribution of water capacity at the end of the iteration process when the numerical solution converges. This particular feature guarantees relatively small mass balance error in the solution.

Now, in general, the space derivative terms can be written as a linear combination of two time levels as:

$$[A]\{\psi\} = \alpha[A]\{\psi\}_t + (1-\alpha)[A]\{\psi\}_{t+1} \qquad (3.20)$$

where, α is a time weighing factor.

So, from Eq. (3.13)

$$[A]^{t+\alpha}(\alpha\{\psi\}_{t+1} + (1-\alpha)\{\psi\}_t) + [B]^{t+\alpha}\frac{\{\psi\}_{t+1}-\{\psi\}_t}{\Delta t} + \{F\}^{t+\alpha} = 0$$

where F stands for the summation of all the terms in Eq. (3.13) or Eq. (3.15) excluding first two terms. By rearranging,

$$(\alpha[A]^{t+\alpha} + \frac{[B]^{t+\alpha}}{\Delta t})\{\psi\}_{t+1} = (\frac{[B]^{t+\alpha}}{\Delta t} - (1-\alpha)[A]^{t+\alpha}\{\psi\}_t - (\alpha\{F\}^{t+1} + (1-\alpha)\{F\}^t) \qquad (3.21)$$

In the above equation, α, the time weighing factor, may have values from 0 to 1.

if $\alpha = 0$, fully explicit scheme,

  $\alpha = 1$, fully implicit scheme,

  $\alpha = 1/2$, Crank Nikolson scheme.

To evaluate coefficient matrices A_{mn}, B_{mn}, pressure head values used from the relation

  $\psi^{t+\alpha} = \alpha\psi^{t+1} + (1-\alpha)\psi^t$

From equation (3.15), incorporating Eq. (3.19)

$$[A]^i_{t+1}(\alpha\{\psi^{i+1}_{t+1}\} + (1-\alpha)\{\psi_t\}) + [B_1]^i_{t+1}C^i_{t+1}\frac{\psi^{i+1}_{t+1}-\psi^i_{t+1}}{\Delta t} + [B_1]^i_{t+1}\frac{\theta^i_{t+1}-\theta_t}{\Delta t}$$

$$+[B_2]^i_{t+1}\frac{\psi^{i+1}_{t+1}-\psi_t}{\Delta t} = -\{G^i_{t+1} - \{E\}_{t+1} + \{Q\}_{t+1} - \{W\}_{t+1}$$

$$\left(\alpha[A] + \frac{[B_1]\, C^i_{t+1}}{\Delta t} + \frac{[B_2]}{\Delta t} \right) \{\psi\}^{i+1}_{t+1} = \frac{[B_1]\, C^i_{t+1}}{\Delta t} \{\psi\}^i_{t+1} + \left(\frac{[B_2]}{\Delta t} - (1-\alpha)[A] \right)$$

$$\{\psi\}_t - \frac{[B_1]}{\Delta t} \left(\{\theta\}^i_{t+1} - \{\theta\}_t \right) - \{G\} - \{E\} + \{Q\} - \{W\} \qquad (3.22)$$

The coefficient matrices are function of the dependent variable ψ, so this equation is nonlinear. At the start of a new time level this is linearized by evaluating the coefficient matrices using pressure head values obtained by linear interpolation of ψ over the time step. For fully implicit scheme, $\alpha = 1$, then,

$$\left([A] + \frac{[B_1]\, C^i_{t+1}}{\Delta t} + \frac{[B_2]}{\Delta t} \right) \{\psi\}^{i+1}_{t+1}$$

$$= \frac{[B_1]\, C^i_{t+1}}{\Delta t} \{\psi\}^i_{t+1} + \frac{[B_2]}{\Delta t} \{\psi\}_t - \frac{[B_1]}{\Delta t} \left(\{\theta\}^i_{t+1} - \{\theta\}_t \right) - \{G\} - \{E\} + \{Q\} - \{W\} \qquad (3.23)$$

As stated earlier, the coefficient matrices are determined element wise and then these are assembled to find out the global matrices. For elemental computation, local coordinate systems and local basis functions $\xi^e_i (x,y,z)$ are used. Now the aquifer properties may be considered constant over an element or to vary over each individual element in a designated fashion. In the later case, the concept of functional coefficients are used to approximate the aquifer property distribution over each element. In the same manner as was used for the head distribution, the aquifer property distribution is approximated using the shape functions. Thus the aquifer properties are approximated as a linear combination of the property values at the nodes. These relationships can be written for hydraulic conductivity, K, moisture content, θ, the soil water capacity, C, root water extraction rate, S as follows :

$$K(x,y,z) = \sum_{i=1}^{4} K(x_i, y_i, z_i)\, \xi^e_i(x,y,z)$$

$$\theta(x,y,z) = \sum_{i=1}^{4} \theta(x_i, y_i, z_i)\, \xi^e_i(x,y,z)$$

$$\qquad (3.24)$$

$$C(x,y,z) = \sum_{i=1}^{4} C(x_i, y_i, z_i)\, \xi^e_i(x,y,z)$$

$$S(x,y,z) = \sum_{i=1}^{4} S(x_i, y_i, z_i)\, \xi^e_i(x,y,z)$$

where $(x,y,z) \in \Omega_e$ and i stands for the corners of the element e. Then the integrations of Eq. (3.14) can be written for the final Eq. (3.23) as:

$$A_{mn} = \sum_e K_l K_{ij}^A \int_{v_e} \xi_l^e(x,y,z) \frac{\partial \xi_{m}^e(x,y,z)}{\partial x_i} \frac{\partial \xi_n^e(x,y,z)}{\partial x_j} \, dv$$

$$= \sum_e \frac{\bar{K}}{36 v_e} [\, K_{xx}^A B_m B_n + K_{yy}^A C_m C_n + K_{zz}^A D_m D_n + K_{xy}^A (B_m C_n + C_n B_n) + K_{xz}^A (B_m D_n + D_m B_n \qquad (3.25a)$$

$$+ K_{yz}^A (C_m D_n + D_m C_n) \,]$$

$$= \sum_e \frac{\bar{K}}{36 v_e} [\, K_{xx}^A B_m B_n + K_{yy}^A C_m C_n + K_{zz}^A D_n D_n)$$

Here, the last expression is for the case when the principal direction of anisotropy coincides with the coordinate axes (then $K_{ij} = 0$ for $i \neq j$) ; $\bar{K}$ is the average Hydraulic conductivity in the element ($\bar{K} = \sum_{l=1}^{4} K_l / 4$) ; 1 (=1,2,3,4) indicates the four corners of a tetrahedra element ; v_e is the volume of the element, the coefficients B_m, C_m, D_m are the coefficients associated with element basis functions.

In computing matrices $[B_1]$ and $[B_2]$, there are two alternatives. One is consistent formulation, i.e., evaluating the element coefficients as it is . Other is lumped formulation by lumping the total mass of an element equally at the nodes of the element . Experiences from the researchers indicate that, in the consistent formulation of the mass matrix, calculated pressure head, ψ, tends to exhibit oscillation around it's limit. A more stable solution is obtained with the lumped mass matrix (Huyakorn, 1983). In this case, storage matrices are diagonal.

Now, from Eqs. (3.15a,b),

$$B_{1mn} = \sum_e \int_{v_e} \xi_n^e \xi_m^e \, dv$$

$$= \delta_{mn} \sum_e \int_{v_e} \xi_n^e \, dv = \sum_e \frac{v_e}{4} \delta_{mn} \qquad ; \delta \text{ is the Kroneker delta} \qquad (3.25b)$$

$$= \sum_e \frac{v_e}{4} \qquad ; \text{ if } m = n$$

$$= 0 \qquad ; \text{ if } m \neq n$$

$$B_{2mn} = \sum_e \int_{v_e} \frac{\theta}{n} S_s \xi_n^e \xi_m^e \, dv$$

$$= (\frac{\theta}{n} S_s)^e \delta_{mn} \sum_e \int_{v_e} \xi_n^e \, dv \qquad ; \delta \text{ is the Kroneker delta} \qquad (3.25c)$$

$$= \sum_e (\frac{\theta}{n} S_s)^e \frac{v_e}{4} \qquad ; \text{ if } m = n$$

$$= 0 \qquad ; \text{ if } m \neq n$$

$$G_m = \sum_e \int_{v_e} K_I K_{iz}^A \frac{\partial \xi_m^e}{\partial x_i} \, dv = \sum_e \frac{\bar{K}}{6} [K_{xz}^A B_m + K_{yz}^A C_m + K_{zz}^A D_m] \qquad (3.25d)$$

$$E_m = \sum_e \int_{v_e} S(x,y,z) \xi_m^e(x,y,z) \, dv = \sum_e \frac{v_e}{20} (S_m + 4\bar{S}) \qquad (3.25e)$$

$$Q_m = - \sum_e \int_{\Gamma^e} q_i n_i \, d\Gamma = -q_m \frac{\Delta_e}{3} \qquad (3.25f)$$

$$W_m = \int_v \phi_n(x,y,z) (\sum_{k=1}^r \delta(x-x_k) \delta(y-y_k) \delta(z-z_k) Q_k) \, dv = Q_{wm} \qquad (3.25g)$$

In the above equations, S_m is the sink term associated with node m ; $\bar{S}$ is the average over the element ; Q_{wm} is the recharge (+ve) or discharge (-ve) of wells at node m ; Δ_e is the area of the triangular face exposed in the boundary ; and q_m [LT^{-1}] is the flux across the boundary node m (positive when directed outward of the system).

35

3.4 Computational Strategy

3.4.1 Iteration Process

After applying Galerkin approximation, the system of time dependent integro-differential equations are nonlinear because the matrix elements, A_{ij} and B_{ij}, are functions of the nodal unknowns, ψ_j . So the first estimate of solution must be improved by an iterative process leading to a convergent solution. Picard iteration method, and Newton - Raphson method are the two methods to treat this nonlinearity. Although Newton-Raphson method is second order convergent and Picard method is first order (i.e., error decreases linearly with the error at the previous iteration in Picard method and in Newton Raphson method the error in present iteration is approximately proportional to the square of the previous iteration's error), Newton - Raphson method, unlike Picard method, requires continuity of the gradient of hydraulic diffusivity ($\frac{dD}{d\theta}$) , for convergence (Huyakorn, 1983).

In the present case, Picard iteration method is used. At each iteration, the coefficients are determined using the solution of previous iteration and the new equations are again solved. Updating of matrix elements is performed by recomputing values of relative permeability, moisture content and overall storage coefficient of the mass accumulation terms. Iterations are performed until the successive change of pressure head values is within a prescribed head tolerance in all the nodes of the domain. At each time step, the first estimate (at zero iteration) of the unknown ψ value is obtained by extrapolation from the ψ values at the previous two time levels. To save a considerable amount of computer time, it is possible to reduce the computation region for a certain class of problems (e.g., for infiltration in relatively dry soil). This is done by a check after the first iteration (Staufer, 1984). Subsequent iterations are limited to those parts of the flow region which exhibited changes in the nodal value of the pressure head during the first iteration that exceeded a prescribed small tolerance. These parts include all elements surrounding nodes for which changes in the pressure head were recorded.

36

3.4.2 Time Control

For transient problem, computation is started from initial time (t=0) . After that computation is proceeded by time marching through the accretion of time steps with the old time. This is the time level of numerical scheme. Also we have some time dependent input (such as river water level, rainfall precipitation) which should be read in specified time levels. And finally the required output is sought in certain time levels. So during the computation there are three time levels such that first one is reforming as computation proceeded while the second and third time levels are predetermined by the user to input data and store output. These are discussed below :

Time Control in Numerical Scheme

Owing to severe nonlinierities encountered in problems of flow in variably saturated soils, the iterative procedure in the scheme may not converge unless time step (Δt) is unusually small, although this condition will be improved when a larger part of the flow region becomes saturated and thereby Δt can be increased. So a automatic time-stepping control is incorporated in the program as suggested by Huyakorn et al. (1983). This is done by:

a) Initial time step Δt and maximum allowable time step Δt_{max} is selected .

b) Maximum number of iteration per time step is selected (say, 10 iterations). This is used as a criteria for reducing or increasing the time step value.

c) If it takes more than the prescribed number of iteration (10) to obtain convergence, the time step would be reduced to 1/2 or 1/3 and the solution reinitiated from the old time level. The time-step reduction is continued until satisfactory convergence is attained.

d) If convergence is reached within a smaller number of iterations (say, ≤ 5), then increase the time step by multiplying a factor (1.1 to 1.5). This procedure is

37

continued until Δt is less than or equal to the preselected Δt_{max} .

e) If the number of iterations is in between the two as stated above (i.e.,$10 \geq$ iteration$>$5), then set time step to the same value as the current time step.

Time Control of Time Dependent Input

The input data for time dependent input variables such as river water level, rainfall, evaporation are generally found in hourly, daily or monthly basis. The time marching in the numerical scheme should coincide with the input time level to feed the data in proper time. So when solution time is approaching to the input time level, then an adjustment in the time stepping is made depending on the existing time step and the difference between the time level in the numerical scheme and the next time level of the input data.

Time Control for Output

During the data preparation of the program, a number of time levels is specified to store the output of simulated unknowns such as pressure head, moisture content, inflow/outflow through boundary, flux etc. Here also, an adjustment of the time stepping is required to coincide with the desired print levels.

3.4.3 Computation of Soil Hydraulic Properties

At every iteration level, for the unsaturated zone moisture contents (θ), hydraulic conductivities (K) and specific water capacities (C) are required for a set of pressure head (ψ) of the nodes for each soil type of the flow domain. These are calculated from the characteristics equations or hydraulic functions (e.g., van Genuchten and Nielsen, 1985) for a specified set of hydraulic parameters. In the program, at the beginning of numerical solution a table of these are produced at prescribed pressure heads, ψ_i , within a specified interval (ψ_1,ψ_2) such that the ratio between two consecutive entries of ψ in the table is

38

constant. During iteration the values of $\theta(\psi)$, $K(\psi)$, $C(\psi)$ are calculated by linear interpolation between the entries in the table. For large computation, this interpolation technique is much faster computationally than directly from the hydraulic functions.

3.4.4 Water Balance Computation

One measure of a numerical simulator is its ability to conserve global mass over the domain of interest. Adequate conservation of global mass is a necessary but not sufficient condition for acceptability of a numerical simulator. To measure the ability of the program to conserve mass, mass balance error (absolute and relative) are computed at designated time of the simulation period. Absolute mass balance errors are computed as the difference between the change in moisture storage in the catchment soil and the net boundary influx (amount of water entering or leaving the catchment at the boundaries).

Mathematically , Absolute mass balance error,

$$AMB(t) = V_t - V_o + \int_o^t T_a A_t \, dt - \int_o^t \sum_{n_L} Q_n dt \qquad (3.26)$$

where V_t and V_o are the actual volumes of water in the domain at time t and zero respectively; T_a is the actual transpiration rate ; A_t is the area of the soil surface associated with transpiration process. The first two terms (V_t - V_o) give the moisture change in the domain between time zero and t. The third term represents the volumetric sink term , i.e., cumulative root water uptake, and the fourth term gives the cumulative flux through nodes, n_L, located along the boundary of flow domain or at internal source and sink nodes.

The actual volume of water, V is calculated from

$$V = \sum_e \frac{v^e}{4} \left(\sum_{i=1}^{4} \theta_i \right) \qquad (3.27)$$

The first summation indicates the summation over all elements (e) with volume v_e of each element of the domain and the second indicates summation of moisture content (θ) of four corner nodes of an element. Normalized or relative mass balance errors are obtained by

39

dividing the absolute mass balance errors by the net influx. For three dimensional flow computation and catchment scale simulation a very small value to approximately 8% relative mass balance error has been reported by Paniconi et.al. (1993).

3.4.5 Computation of Nodal Fluxes

After computation of pressure head at the nodes, the components of the Darcian flux are calculated at selected print levels. The expressions for the three components of nodal fluxes (q_x, q_y, q_z) can be obtained from the Darcy's equation (3.1) by replacing ψ with it's approximate value in terms of basis function and performing the differentiations. For a node, the contribution from each of the elements associated with that node are considered. From Eq. (3.1),

$$q_i = -K(K_{ij}^A \frac{\partial \psi}{\partial x_j} + K_{iz}^A) = -K(K_{ij} \frac{\partial}{\partial x_j}(\sum_{k=1}^{4} \psi_k \xi_k^e(x, y, z)) + K_{iz}^A) \quad ; \quad i, j \in x, y, \quad (3.28)$$

where k = 1,2,3,4 , four nodes of an element.
After performing the differentiation and summing over elements,

$$q_i = -\frac{1}{N_e} \sum_{e_n} [\frac{K_n}{6 v_e} (\sum_{k=1}^{4} \psi_k \gamma_k^i) + K_{iz}^A] \quad ; \quad i \in x, y, z \quad (3.29)$$

where,

$$\gamma_k^i = K_{ix}^A B_k + K_{iy}^A C_k + K_{iz}^A D_k \quad ; \quad k=1, 2, 3, 4$$

and v_e is the volume of the element, N_e is the number of elements associated with node n.

CHAPTER FOUR

PARAMETERS OF THE MODEL

4.1 General

The success of a numerical model depends on the real hydrogeological characterization of the simulated system. In case of saturated-unsaturated flow in excess of saturated hydraulic conductivity and storage coefficient, the equation includes two hydraulic characteristics of the porous medium. These are the retention curve, $\theta(\psi)$ and the hydraulic conductivity function, $K(\psi)$ related to negative pressure head. The equation also contains a sink term, (S) and a root water extraction term. The parameters related with these are explained briefly in the following articles.

4.2 Characteristic Curves of Unsaturated Hydraulic Parameters

In order to solve the governing flow equations as described earlier, one must specify the constitutive relations between the dependent variable and nonlinear terms (moisture content, moisture capacity, and conductivity). These characteristic relations can be input to a numerical model as data in tabular form or more commonly, as empirical expressions fitted to observed data. There is no need for a separate expressions relating moisture capacity and pressure head, as this relation will follow by differentiating the moisture content-pressure head function. It is also common practice to use a conductivity-pressure head relationship which is derived from the moisture content-pressure head function, using some physically based approach such as the distribution of pore sizes. In this way the number of fitting parameters in the constitutive relations is kept to a minimum, and the need for unsaturated conductivity measurements is obviated, allowing the relations to be fitted using only measurements of moisture contents, saturated hydraulic conductivity, and pressure head,

which are more easily available and more reliable.

A number of equations can be found in the literature for approximating these functions. The present work makes use of a set of closed form equations resembling those of van Genuchten (1980), which are later modified by Vogel and Cislerova (1988). In the course of the development and testing of the present numerical code, two other formats of these functions are also included and these are optionally available in the program to use if necessary. One of these, is given by van Genuchten and Nielson (1985) and other is used by Huyakorn et al.(1986). An explanation of these equations are as follows.

4.2.1 Vogel and Cislerova's Modification (1988) over van Genuchten's Equation

van Genuchten (1980), used the statistical pore-size distribution model of Mualem (1976) to obtain a predictive equation for the unsaturated hydraulic conductivity function. The original van Genuchten equation for the retention curve is :

$$\begin{aligned} S_e &= [\,1+|\alpha\psi|^n\,]^{-m} & for \quad \psi<0 \\ S_e &= 1 & for \quad \psi\geq0 \end{aligned} \qquad (4.1)$$

where S_e (dimensionless) is the degree of saturation; ψ is the pressure head of dimension [L]; α an empirical parameter [L^{-1}]; n and m (=1-1/n) are dimensionless empirical exponents. The degree of saturation can be written as :

$$S_e = \frac{\theta-\theta_r}{\theta_s-\theta_r} \qquad (4.1a)$$

where θ [dimensionless] is the volumetric moisture content; θ_s is the saturated volumetric moisture content; and θ_r is the residual (immobile) volumetric moisture content.

By combining Eq. (4.1) with the Mualem's (1976) theory and assigning m=1-1/n , van Genuchten (1980) arrived at a hydraulic conductivity function :

$$K(\psi) = K_s K_r(\psi) \qquad\qquad for \qquad \psi < 0$$
$$K(\psi) = K_s \qquad\qquad\qquad for \qquad \psi \geq 0 \qquad\qquad (4.2)$$

where K is the unsaturated hydraulic conductivity [LT^{-1}]; K_s is the saturated hydraulic conductivity; and K_r (dimensionless) is the relative hydraulic conductivity, which equals to

$$K_r = S_e^{1/2}[\, 1-(1-S_e^{1/m})^m]^2 \qquad\qquad (4.2a)$$

Vogel and Cislerova (1988) suggested some improvements to the van Genuchten formulae, allowing for the non-zero air entry value as well as for an abrupt transition from the mobile state of the soil moisture to the immobile one during desaturation. Their formula for the retention curve is :

$$
\begin{aligned}
\theta(\psi) &= \theta_a + \frac{(\theta_m - \theta_a)}{(1+|\alpha\psi|^n)^m} & ; & \quad \psi_r < \psi < \psi_s \\
&= \theta_s & ; & \quad 0 \geq \psi \geq \psi_s \\
&= \theta_r & ; & \quad \psi \leq \psi_r
\end{aligned}
\qquad (4.3)
$$

where θ_m and θ_a are imaginary upper and lower limits, respectively, of the volumetric moisture content. ψ_s is the air-entry pressure head value; and ψ_r is the highest value of the pressure head for which the soil moisture is still immobile. A provision was also made by Vogel and Cislerova (1988) for the possibility of matching the hydraulic conductivity function to a measured non-saturated value of hydraulic conductivity K_k at some moisture content θ_k for which also the value of pressure head ψ_k is known ($\theta_k < \theta_s$, $K_k < K_s$). The resulting hydraulic conductivity function is :

$$
\begin{aligned}
K(\psi) &= K_s K_r(\psi) & ; & \quad \psi \leq \psi_k \\
&= K_k + \frac{(\psi - \psi_k)(K_s - K_k)}{\psi_s - \psi_k} & ; & \quad \psi_k < \psi < \psi_s \\
&= K_s & ; & \quad \psi \geq \psi_s
\end{aligned}
\qquad (4.4)
$$
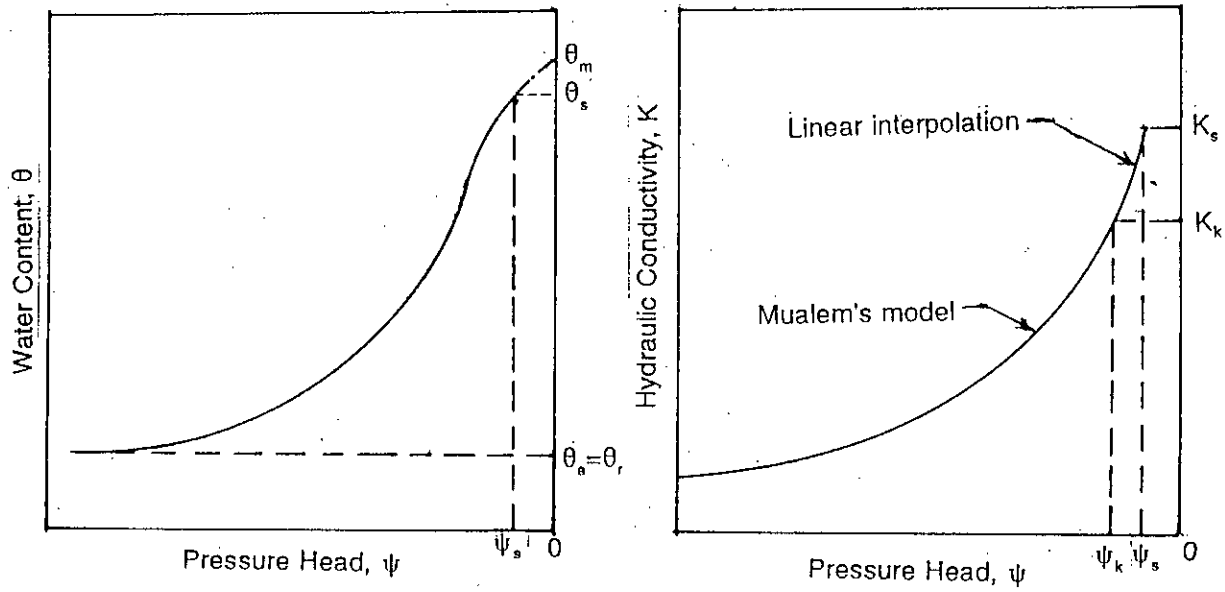
Fig. 4.1 : Schematics of the soil-water retention (a) and hydraulic conductivity (b)
functions as given by Eqs. 4.3 and 4.4 respectively

where

$$K_r = \frac{K_k}{K_s} \left[\frac{S_e}{S_{ek}} \right]^{\frac{1}{2}} \left[\frac{F(\theta_r) - F(\theta)}{F(\theta_r) - F(\theta_k)} \right]^2 \tag{4.5a}$$

$$F(\theta) = \left[1 - \left(\frac{\theta - \theta_a}{\theta_m - \theta_a} \right)^{\frac{1}{m}} \right]^m \tag{4.5b}$$

$$m = 1 - \frac{1}{n} , \qquad n > 1 \tag{4.5c}$$

$$S_e = \frac{\theta - \theta_r}{\theta_s - \theta_r} \tag{4.5d}$$

$$S_{ck} = \frac{\theta_k - \theta_r}{\theta_s - \theta_r} \tag{4.5e}$$

So, when this model of hydraulic characteristic functions of soil are used, the fitting

parameters that should be identified are :

$$\boxed{\theta_r \quad \theta_a \quad \theta_s \quad \theta_m \quad \theta_k \quad K_s \quad K_k \quad n \quad \alpha}$$

4.2.2 van Genuchten and Nielson (1985)

van Genuchten and Nielson (1985) gave retention curve and hydraulic conductivity function as follows:

$$\theta(\psi) = \theta_r + (\theta_s - \theta_r)[1+\beta]^{-m} \quad for \quad \psi \leq 0$$
$$\theta(\psi) = \theta_s \qquad\qquad\qquad for \quad \psi \geq 0$$

(4.6a)

$$K_r(\psi) = (1+\beta)^{-\frac{5m}{2}}[(1+\beta)^m - \beta^m]^2 \quad for \quad \psi \leq 0$$
$$K_r(\psi) = 1 \qquad\qquad\qquad for \quad \psi \geq 0 n$$

(4.6b)

where θ_r is the residual moisture content; θ_s is the saturated moisture content; ψ_s is the capillary or air entry pressure head value; $\beta = (\psi/\psi_s)^n$; and n can be interpreted as pore size distribution index such that, m = 1-1/n.

The parameters related to soil-moisture characterization are :

$$\boxed{\theta_r \quad \theta_s \quad \psi_s \quad n}$$

4.2.3 Constitutive Relations Used by Huyakorn et al. (1986)

To represent the soil moisture characteristics, the relations used are fitted curves of analytical expressions which are expressed as :

$$S_e = \frac{A}{A+(\,|\psi-\psi_a|\,)^B} \qquad \psi < \psi_a$$

$$S_e = 1 \qquad \psi \geq \psi_a$$

$$K_r = S_e^{\,n}$$

$$S_e = \frac{S_w - S_{wr}}{1 - S_{wr}}$$

$$(4.7)$$

where, S_e is the degree of saturation; A, B, n are fitting parameters; S_w is the water saturation, i.e., ratio of moisture content to porosity; S_{wr} is the residual water saturation; and ψ_a is the air entry pressure head value.

The parameters related here are :

A	B	n	Ψ_a	S_{wr}

4.3 Water Extraction by Roots

In the field, the living plant root system is dynamic (dying roots are constantly replaced by new ones), geometry is time dependent, water permeability varies with position along the root and with time . Root water uptake is most effective in young root material, but the length of young roots is not directly related to total root length (Feddes et al., 1988). In addition, experimental evaluation of root properties is hardly practical, and often impossible. Thus instead of considering water flow to and in single roots, a more suitable approach is the macroscopic one, in which a sink term S (volume of water per volume of soil per unit of time, T^{-1}) representing water extraction by a macroscopically homogeneous element of the root system, is added to the continuity equation for water.

46

The rate of water uptake by plant roots depends on the atmospheric conditions (expressed as the potential rate of transpiration) as well as on conditions prevailing in the underground, and of course on the state and properties of the root system itself. The rate of water extraction, S, is usually believed to depend in a linear way upon the difference in the water potentials between the bulk soil (not in the vicinity of the roots) and at some reference point in the plants (e.g., at the base of the stem ; Hillel, 1980, p.181). An alternative formulation , which is more suitable for computations but less explanatory from physical point of view, makes extraction rate, S , dependent directly upon the vertical depth below soil surface and upon transpiration rate, without feedback (e.g., Molz and Remson, 1970; Nima and Hanks, 1973a, b; Feddes et al., 1974). Feddes (1981), Molz (1981) and Campbell (1985) gave an overview of possible S- functions.

Feddes et al. (1978) described S semi-empirically as :

$$S(\psi) = a(\psi) S_p \qquad (4.8)$$

where the water stress response function a(ψ) is a prescribed dimensionless function (Fig.4.2) of the soil water pressure head ψ ($0 < a < 1$) and S_p is the potential water uptake rate [T^{-1}]. Fig. 4.2 gives a schematic plot of the stress response function as used by Feddes et al. (1978) . In this case, water uptake is assumed to be zero close to soil saturation (i.e., when the soil is wetter than some arbitrary anaerobiosis point, which in terms of pressure head is ψ_1) . For the soil drier than the wilting point pressure head ($\psi < \psi_4$), water uptake is also assumed to be zero. Optimal water uptake is considered between pressure heads ψ_2 and ψ_3 , whereas, for pressure head between ψ_3 and ψ_4 a linear variation and between ψ_1 and ψ_2 a linear or hyperbolic variation is assumed. The value of ψ_3 is dependent on the demand of the atmosphere and thus varies with potential transpiration rate. S_p is equal to the water uptake rate during periods of no water stress when $a(\psi) = 1$.
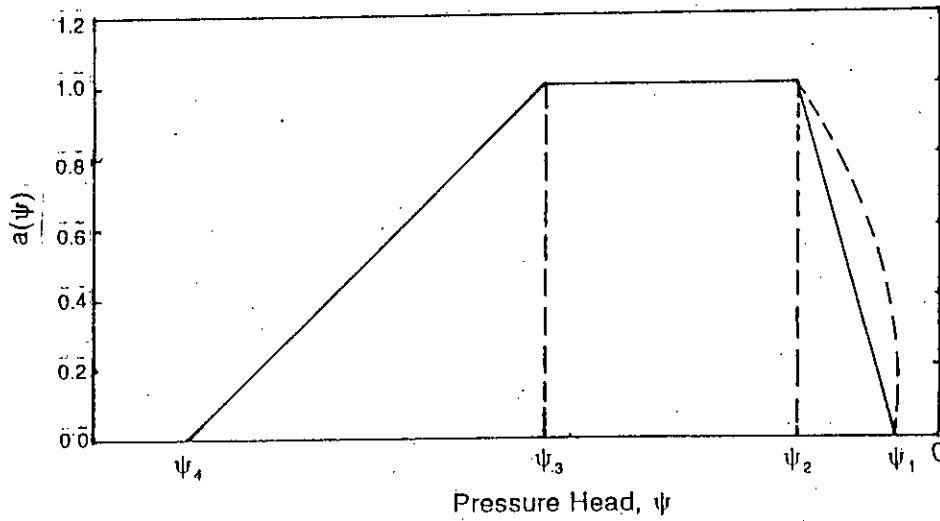
Fig. 4.2 : Schematic of the plant water response function, a(ψ), as used by Feddes et al., 1978

When the potential water uptake rate is equally distributed over a root domain , S_p becomes

$$S_p = \frac{1}{L_x L_y L_z} A_t T_p \qquad (4.9)$$

where T_p is the potential transpiration rate [LT^{-1}]; L_x, L_y, L_z are the dimensions of the root zone in three axis directions; and A_t is the area of the soil surface associated with the transpiration process. It can be noticed here that S_p reduces to T_p/L_z when $A_t = L_x L_y$.

The above equation may be generalized by introducing a nonuniform distribution of the potential water uptake rate over a root zone of arbitrary shape [Vogel, 1987] :

$$S_p = b(x,y,z) A_t T_p \qquad (4.10)$$

where $b(x,y,z)$ is the normalized water uptake distribution function [L^{-3}]. This function

describes the spatial variation of the potential extraction term S_p over the root zone, and is obtained from $b'(x, y, z)$ as follows :

$$b(x, y, z) = \frac{b'(x, y, z)}{\int_{\Omega_r} b'(x, y, z) \, d\Omega} \qquad (4.11)$$

where Ω_r is the region occupied by the root zone and $b'(x, y, z)$ is an arbitrarily prescribed distribution function. Normalizing the uptake distribution ensures that $b(x, y, z)$ integrates to unity over the flow domain belonging to the transpiration-associated area A_t, i.e.,

$$\int_{\Omega_r} b(x, y, z) \, d\Omega = 1 \qquad (4.12)$$

From Eqs. (4.10) and (4.12) it follows that S_p is related to T_p by the expression :

$$\frac{1}{A_t} \int_{\Omega_r} S_p \, d\Omega = T_p \qquad (4.13)$$

The actual water uptake distribution is obtained by substituting Eq. (4.10) into Eq. (4.8) as follows :

$$S(\psi, x, y, z) = a(\psi, x, y, z) b(x, y, z) A_t T_p \qquad (4.14)$$

whereas the actual transpiration rate , T_a, is obtained by integrating Eq. (4.14) as follows:

$$T_a = \frac{1}{A_t} \int_{\Omega_r} S \, d\Omega = T_p \int_{\Omega_r} a(\psi, x, y, z) b(x, y, z) \, d\Omega \qquad (4.15)$$

CHAPTER FIVE

TREATMENT OF AUXILIARY CONDITIONS

5.1 Introduction

The governing differential equation of flow through porous medium, describes a class of phenomena and does not represent any specific case. From infinite number of possible solutions, to find out the specific one, it is necessary to provide supplementary information that is not contained in the equation. Except the definition of the geometry of the flow domain, the most important informations are initial and boundary condition of the flow. Boundary and initial conditions are motivated by the physical reality of the flow. Hence, they are first determined or assumed, on the basis of the available information and past experience in the field and then expressed in mathematical forms. Different boundary conditions lead to different solutions, hence the importance of correctly determining the conditions which exist along the real boundaries.

5.2 Initial Conditions

Initial conditions include the specification of pressure head ψ or moisture content, θ at all points within the domain Ω at some initial time, usually denoted as t = 0. This can be written schematically as specifying

$$\psi = f(x, y, z, 0) \quad ; \qquad all \quad (x, y, z) \in \Omega \qquad (5.1)$$

where f is a known function. For three-dimensional case, setting of initial condition is complicated to some extent. Generally it is not possible to collect data for all the nodes from field. One can generate the initial heads based on knowledge of the initial water table distribution or initial soil saturation deficits at some selected locations in the field. For the

location of water table or piezometric level, at all nodes, some interpolation (bilinear, or weighted) are required. Alternatively, the initial head distribution can be obtained by solving a steady state problem, for example. A water table depth or soil moisture deficit can be converted into a vertical pressure head distribution using a hydrostatic assumption. In the present case, a separate program has been developed for three-dimensional mesh generation which includes an option for initial condition setting. A set of known piezometric level is used and the program transfer this known values of piezometric level to the pressure head of the nodal points of the domain by interpolation.

5.3 Boundary Conditions

The boundary conditions define the situation at the boundaries of the flow domain during the whole time period considered. Three basic types of boundary conditions are usually distinguished (e.g., Dennemeyer, 1968). These are Dirichlet type or prescribed head, Neumann type or prescribed flux and mixed type. Boundary conditions may be system independent i.e., when the condition in a given node is determined apriori (including its temporal variability, if such is the case). These may also be system dependent which change either its numerical value or its structure and type or both depending upon the instantaneous state of the flow domain or of its part. In the present case all of these kind of boundary conditions with their numerical implementation are used.

5.3.1 Dirichlet Boundary Condition

A certain value of a scaler quantity (here pressure head, ψ), is prescribed at every time instant in each nodal point of the boundary,

$$\psi(x,y,z,t) = f(x,y,z,t) \qquad for \quad (x,y,z) \, \epsilon \, \Gamma_D \qquad (5.2)$$

where Γ_D is a Dirichlet type boundary segment, and f is a known function of x,y,z, and t. Generally all boundary nodal points on the river bottom and on the permanently submerged

sides can be provided with a Dirichlet boundary condition. However, in the regions that can be variably under water or above water, a combined system-dependent Dirichlet/Neumann condition is to be defined.

Finite element equations corresponding to Dirichlet nodes where the pressure head is prescribed can be eliminated from the global matrix equation. An alternative and numerically simpler approach is to replace the Dirichlet finite element equations by dummy expression of the form (Neuman et al., 1974).

$$\delta_{nm}\psi_m = h_n \qquad (5.3)$$

where δ_{nm} is the Kronecker delta and h_n is the prescribed value of the pressure head at node n. The values of h_n in all other equations are set equal to ψ_n and the appropriate entries containing ψ_n in the left-hand side matrix are incorporated into the known vector on the right-hand side of the global matrix equation. When done properly, this rearrangement will preserve symmetry in the matrix equation. After solving for all pressure heads, the value of the flux Q_n can be calculated explicitly and accurately from the original finite element equation associated with node n (e.g., Lynch, 1984).

5.3.2 Neuman Boundary Condition

A certain value of a vector quantity such as the Darcian flux $\vec{q}$ is prescribed at every time instant in each nodal point of the boundary or in other words, the flux normal to the boundary surface is prescribed for all points. This can be expressed as

$$\vec{q} \cdot \vec{n} = q_i n_i = f(x, y, z, t) \qquad for \quad (x, y, z) \; \epsilon \; \Gamma_N \qquad (5.4)$$

where Γ_N indicates Neuman-type boundary segment, f is a known function of x, y, z and t ; n_i ($i \; \epsilon \; x, y, z$) are the three components of the outward unit vector normal to the boundary Γ_N , q_i ($i \; \epsilon \; x, y, z$) are the three components of Darcian flux in three axis directions at the point (x, y, z) . A special case of this type of boundary is the impervious

52

(no flow) boundary, where the flux normal to the boundary vanishes everywhere i.e., the function $f(x, y, z, t)$ is identically equal to zero. This type of condition is the most natural boundary condition of the finite-element method. In the present algorithm, the nodes with the no-flow condition are treated as internal nodes without sinks or sources. The values of the fluxes Q_n at nodal points along prescribed flux boundaries are computed according to equation (3.25 e). Internal nodes which act as Neumann type sources or sinks (such as pumping or recharging well) have values of Q_n equal to the imposed fluid injection or extraction rate.

5.3.3 Mixed Type Boundary condition

A relation is prescribed between a scaler quantity and a vector quantity at every time instant in each node of the boundary. If the pressure head ψ and the Darcian flux q are these quantities, then an equation is to be fulfilled which may be typically of the form

$$F (\psi, \nabla\psi, \vec{q}) = 0 \qquad for \quad (x, y, z) \in \Gamma_M \qquad (5.5)$$

where Γ_M is the mixed-type boundary segment and F is a scaler function of one scaler and two vector arguments ; it must be, of course, different from the Darcy's law which is of the same form. A simpler case is so-called free-drainage boundary condition where the gradient of hydraulic head is assumed unity at the bottom of a soil profile, so that the Darcian flux is equal to the instantaneous hydraulic conductivity in the node which, in turn, is a function of the nodal pressure head or moisture content. Simunek et al. (1992, p.14-15) speak in this context about the Cauchy boundary condition.

A characteristic example of mixed type of boundary is the bottom-flux (deep-drainage) boundary condition as defined by a semi-empirical equation suggested by Hopmans and Stricker (1988) :

$$q(\psi) = -A_{q\psi}\exp (B_{q\psi} |\psi-RGL|) \qquad (5.6)$$

where $A_{q\psi}$ and $B_{q\psi}$ are empirical parameter, RGL represents the reference position of the groundwater level which should be set equal to or higher than the z-coordinate of the soil surface. The discharge rate $Q(n)$ assigned to a node n is determined by multiplying $q(\psi)$ with the boundary area related to that node. This type of boundary condition has been used in two example problems in the next chapter.

5.3.4 System-dependent Boundary Conditions

In the simulation of a real situation, this type of boundary conditions play an important role in the overall process. These also arise complicacy in the solution algorithm. The faces of the boundary which are directly contact with the atmosphere and the influences of rainfall and evaporation are dominant, is one of such kind of boundary which may be called atmospheric boundary. Other one is the seepage face boundary, through which water moves out of the system in atmospheric pressure (e.g., in a river bank when water level of river is lower than groundwater table). System-dependent boundary conditions of these types and their implementation in the program are described below.

5.3.4.1 Atmospheric Boundary Condition

The potential fluid flux across the soil-air interfaces is controlled exclusively by atmospheric conditions. However, the actual flux depends also on the prevailing soil moisture and pressure head conditions. Soil surface boundary conditions may change from prescribed-flux to prescribed-head type conditions (and vice-versa). In the absence of surface ponding, the numerical solution of Eq. (3.5) is made possible by limiting the Darcian flux $\vec{q}$ and the pressure head ψ by the following two conditions (Neumann et al., 1974):

$$-I_s^* \prec q_x n_x + q_y n_y + q_z n_z \prec E_s^* \tag{5.7}$$

and

$$\psi_A \prec \psi \prec \psi_s \tag{5.8}$$

54

where E_s^* [LT^{-1}] is the maximum potential rate of evaporation and I_s^* [LT^{-1}] is the maximum infiltration rate under the current atmospheric condition, q_x, q_y, q_z, are components of the vector of Darcian flux at the soil surface, n_x, n_y, n_z are components of the unit vector of outer normal to the soil surface, and ψ_A and ψ_s are, respectively, minimum and maximum pressure head allowed under the prevailing soil properties. The value for ψ_A is determined from the equilibrium conditions between soil water and atmospheric water vapor, whereas ψ_s is usually set equal to zero. When one of the end points of (5.7) is reached, a prescribed head boundary condition (equal to the end value reached) will be used. Methods of calculating E_s^* and ψ_A on the basis of atmospheric data have been discussed by Feddes et al. (1974).

Formulae of these kind are, however, not included in the present case , where it is assumed that the potential evaporation, as well as potential infiltration ($=$ precipitation) is provided as the input data. It is in fact only the second of conditions (5.7) - (5.8) which is used. If the soil surface is very wet or very dry, the Dirichlet boundary condition with either $\psi = \psi_s$ or $\psi = \psi_A$ is maintained and the flux is computed by the finite element algorithm. As soon as this flux becomes algebraically either smaller or larger, respectively, than the potential flux suggested by the atmospheric input data, a reverse switch takes place to the Neumann boundary condition with the flux dictated by the atmosphere. Surface fluxes during this computation are positive out of and negative into the soil.

The above described mechanism of switching between the Dirichlet condition is maintained. However, at the instant when new atmospheric data enter the computation, the program calculates the difference between precipitation, evaporation and surface Darcian flux ($=$ infiltration) for the previous time step of the atmospheric input data. The calculation is done for the soil surface as a whole, i.e., a sum of infiltration over all" atmospheric" nodes is determined. The difference mentioned is algebraically added to the depth of water on the soil surface at the beginning of the previous time step (zero depth is assumed at the beginning of calculation). If a zero or negative new depth results (at the end of the previous time step), the boundary condition corresponding to the eqns. (5.7) and (5.8) is set for the whole following time step at the atmospheric boundary. If a positive new depth results from the

water balance at the soil surface during the previous time step, a constant pressure head Dirichlet boundary condition is set for the following time step at all "atmospheric" boundary nodes (it is assumed that if a water surplus occurs on a part of the soil surface, it will be immediately redistributed over the whole (horizontal) soil surface). No water from the soil surface is assumed to be discharged through surface runoff.

5.3.4.2 Seepage Face Boundary Condition

A seepage face through which water seeps out from the saturated portion of a porous medium is a system-dependent boundary condition. The extent of the seepage face varies with time in a manner that can never be predicted a priori. However, the boundary conditions cannot be completely specified to solve the problem unless the length of the seepage face is known. Hence, the seepage face must be determined using an iterative process. The pressure head along the seepage face is taken to be uniformly zero (because the atmospheric pressure head is also considered zero).

If the extent of the seepage face is known at a time level, the position of the seepage face for the next time level is determined by solving the governing equation at the subsequent iterations and modifying the seepage face to reflect information arising from the solution. The location of the seepage face is guessed during the first iteration, and this intermediate problem is solved with other type of boundary conditions. If the location of the seepage face is correct, then the solution gives a net outward flux in all the nodes along the seepage face, where ψ is zero. Values of ψ at all the boundary nodes above the seepage face where flux is set to zero are negative. If the height of the seepage face is overestimated, some of the boundary nodes where ψ is assumed to be zero have nonzero fluxes directed inward. On the other hand, if the seepage-face height is underestimated, boundary nodes above the seepage face, where flux is set to zero, have positive values for ψ. In either case, the fundamental physics of the variably saturated flow problem are violated for incorrect specification of the seepage face height. Using these principles, Neumann's iterative search procedure, as modified by Colley (1983), is determined the seepage face length.

When external water level (river water level) of the seepage face is time dependent, then the above described mechanism is allowed to operate between the time steps of the input data of river water level. As soon as new water stage enters, the vertical coordinates of all nodes on the potential variable seepage face are compared with it. Those lying below or at the new river water level are described as Dirichlet boundary condition of constant pressure head corresponding to the vertical distance of the node below the water level. The nodes lying above the river water level are considered for seepage face. The initial condition at these nodes at the start of iteration are set depending on the condition of previous time level (of river water level input data). These nodes of the seepage face are given a no flow boundary condition (i.e. unsaturated nodes in the seepage face), if they lie also above the previous time river water level. In other case, these nodes are given zero pressure-head Dirichlet boundary condition (i.e. saturated seepage face nodes with $\psi=0$), if they lie below or at the previous time water level.

APPLICATION OF THE MODEL

CHAPTER SIX

APPLICATION OF THE MODEL

6.1 Introduction

Based on the methodology as described in the earlier chapters, in combination with the computational strategy and techniques, the algorithm developed (SUFEM3D) to solve variably saturated flow problems, is capable of handling a wide variety of problems including multi-aquifer system of real situation with nonhomogeneous material properties and any combination of boundary conditions as described in Chapter Five. During the development and modifications of the different features of the model a number of familiar published problems have been used to verify the algorithm. In this chapter a few of these problems are presented for demonstration purpose. Because of the scarcity of three-dimensional ideal problems with simple analytical or semi-analytical solutions, these are actually one- and two-dimensional problems but in the present case these are solved three-dimensionally. To test a specific case (e.g., flow from surface in contact with the atmosphere, horizontal flow in confined aquifer etc.), these schematic types of problems are also suitable to verify the results manually and conceptually. Four types of such testing problems were selected ; first type check the model behavior solely in unsaturated flow, second type verify the saturated case, third type deals with variably saturated flow which concentrate upon the surface treatment of the atmospheric activities (precipitation, evaporation and surface ponding) and the fourth type tested the iterative algorithm for seepage face including constant or variable river water level. After having required performance of all the cases, a real situation in the Dhaka city is simulated to analyze the model behavior. In the subsequent sections these applications and results are discussed.

6.1.1 Soil-moisture Infiltration in a Soil Column (Dirichlet Boundary Condition)

This example is used to test, in initial stage, the behavior of the numerical scheme in purely unsaturated soil moisture transfer. This exhibits how a soil moisture front propagates with time. This problem has been used by Celia et al. (1990) and by EL-Kadi et al. (1993) in one-dimensional case and it has a semi-analytical solution by Philip (1957).

The soil column is 100 cm long with soil properties defined by the functions of Eq. (4.1). The parameters are given in Table 6.1. Initial condition of the soil profile is such that $\Psi_i = -1000$ cm everywhere except the upper boundary surface which is set at $\Psi_{z=100\,cm} = -175$ cm. It indicates that the soil at the surface is relatively of higher moisture content. So moisture will infiltrate downward with a sharp front due to the vertical potential head gradient.

For numerical solution, the column is discretized into 50 brick elements ; each element is eqi-dimensional with 2 cm thickness in z direction and 1 cm in both of other two x and y axes. This finite element discretization with the sequences of node numbering and element numbering are shown in Fig. 6.1. It is also possible to select finer nodal spacing at the upper portion of the column and coarser at the bottom to take care of the initial high pressure head gradient at the top portion and thereby reduce the total number of elements which will yield to results of almost same precision. But due to the smaller size of the problem, this is not done here. With the parameters as shown in Table 6.1 , the program is run setting the time step value (Δt) equals 3.5 minutes. Total time required to run this problem is approximately 1 minute in a 486DX2 66 MHz IBM PC.
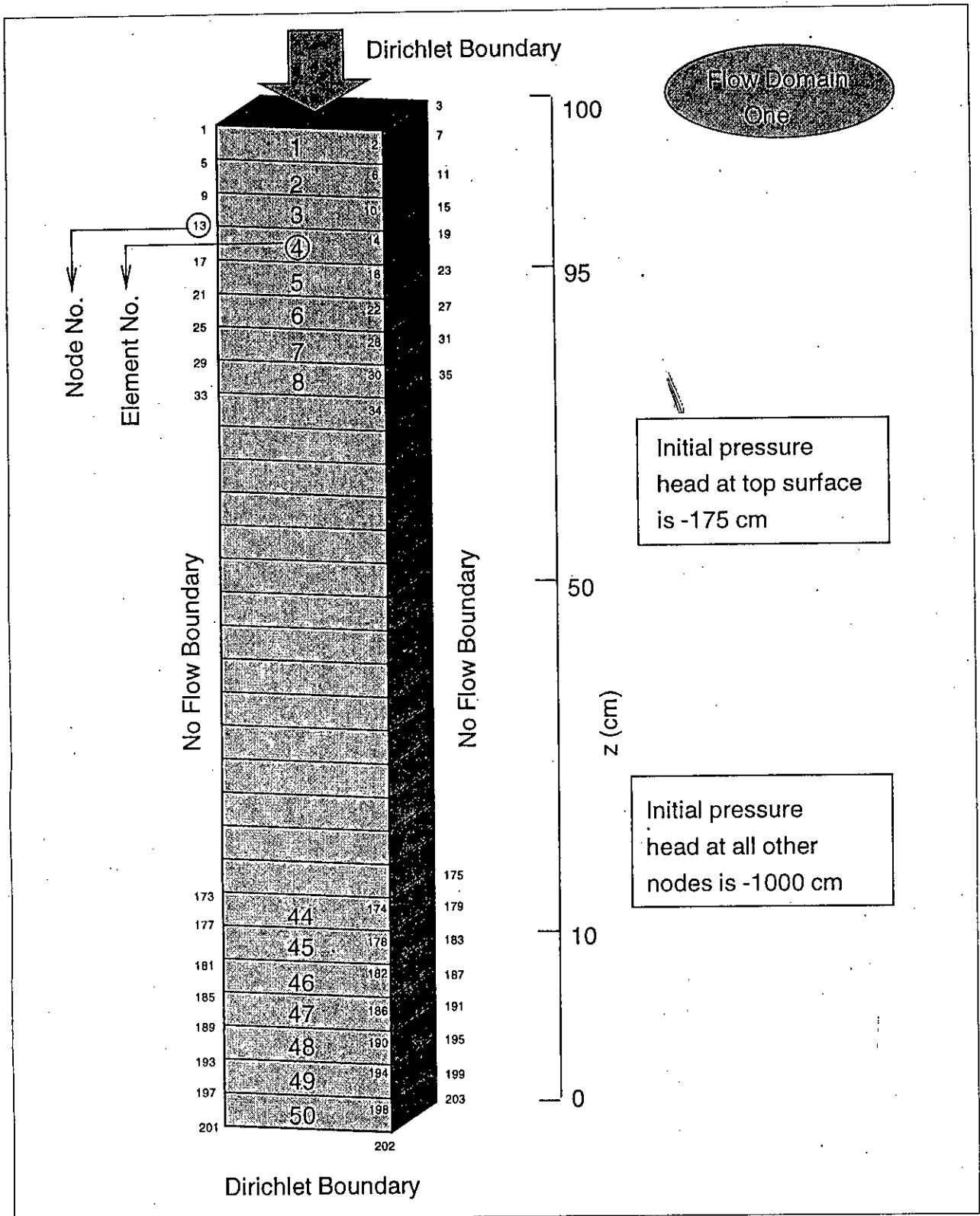
Fig. 6.1 : Flow domain discretization and initial and boundary conditions for one dimensional vertical flow (Example 6.1.1)
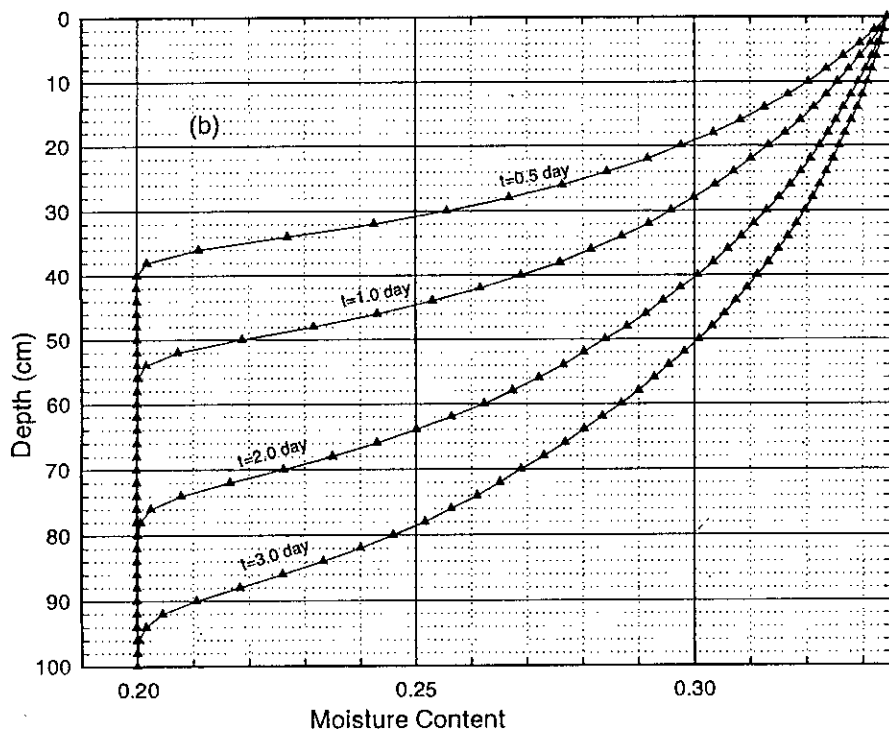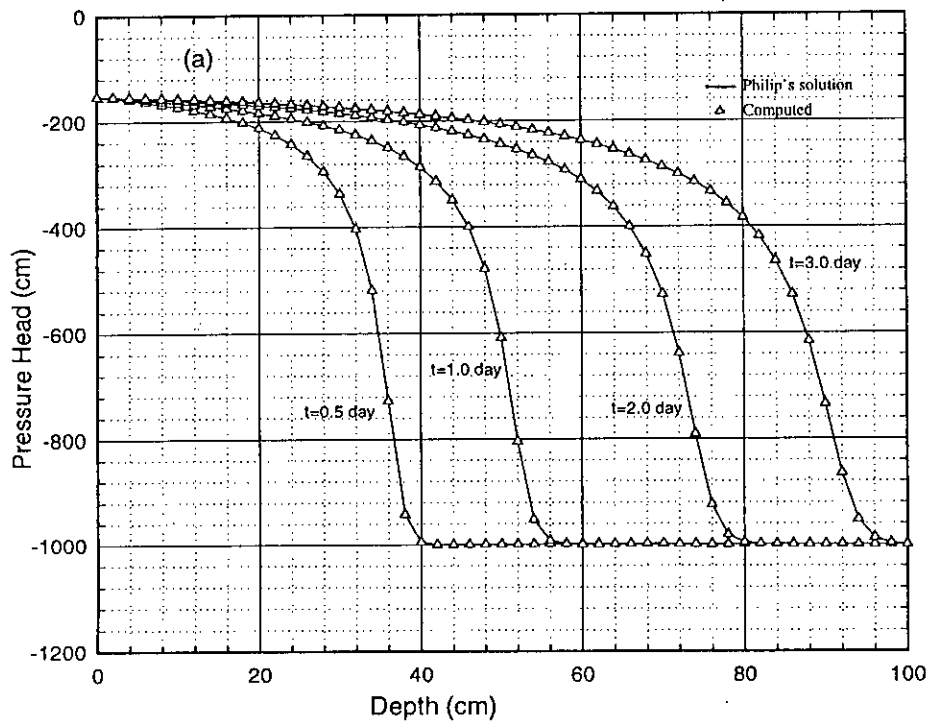
Fig. 6.2 (a) Simulated pressure head profiles compared with Philip's solution

(b) Simulated moisture content profiles
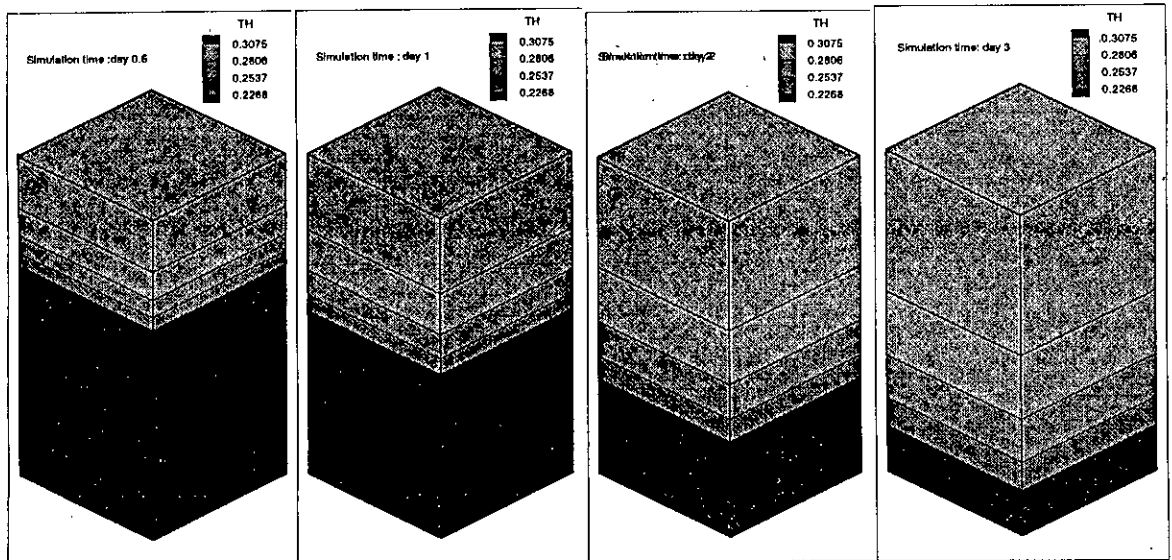
(a) Moisture content contour shade plot at different simulation time showing vertical propagation of moisture content front
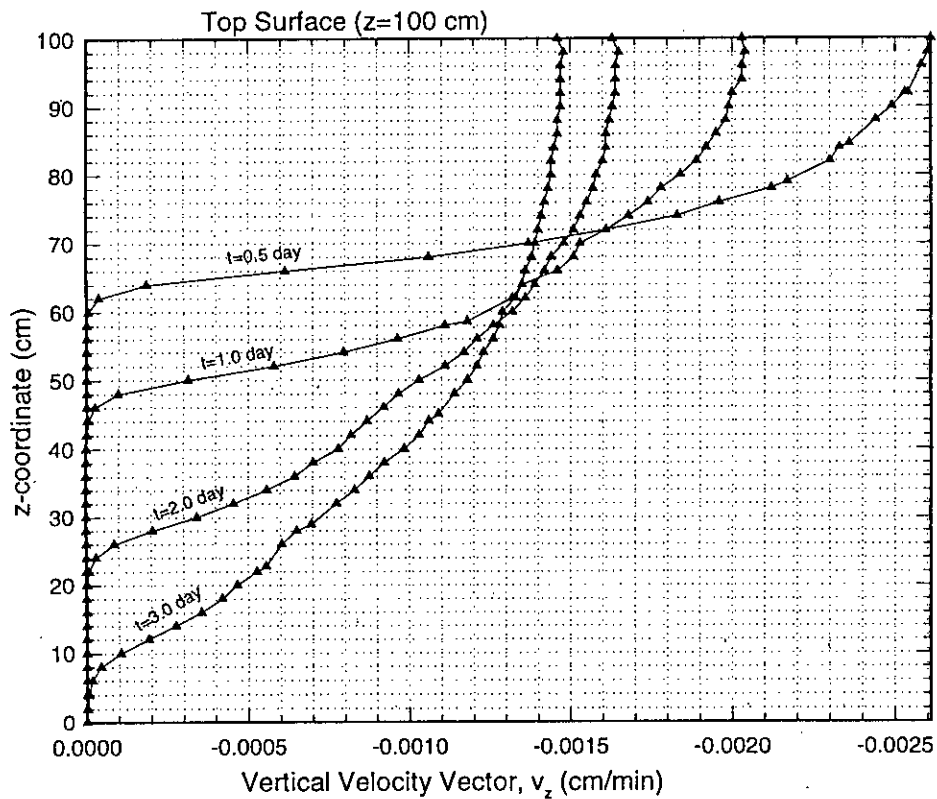
Fig. 6.3 : (a) Moisture content shade plot at different simulation time

(b) Vertical velocity vector plot

Table 6.1: Parameters for Example 6.1.1

Parameters	Values
Soil Characteristic Functions :	
van Genuchten,1980 (Eq. 4.1)	
θ_r	0.17
θ_s	0.47
α, cm^{-1}	0.010
n	2.00
K_s (cm/s)	8.7 X 10^{-4}
Time Information :	
Time Increment (Δt)	3.5 min
Maximum Iteration	10
Tolerance	0.0001 cm

The results for this example are shown in Figs. 6.2 and 6.3. Fig. 6.2(a) shows the pressure head distribution at 0.5, 1, 2, 3 days, respectively. The simulated values shown are averaged for every z level and gives an excellent agreement with the semi-analytical solution (Philip, 1957). It is noticeable that no major overshooting or undershooting in fluctuations has occurred near the front as was reported by Celia et al. (1990). This may be due to the averaging effect of the three-dimensional algorithm in discretization of the domain internally into smaller tetrahedral elements and also averaging the output pressure head values. As the upper boundary is maintained at a constant pressure head value of -175 cm, there is an induced flux through the upper nodes inwards the soil column. From Fig. 6.3(b) it is observed that, at the early stage of simulation (t=0.5 day), the flux is high at a value of 0.0026 cm/min downwards at the top surface and then reduces rapidly with depth. Due to this vertical flux , moisture content front moves downwards which is shown in Fig. 6.2(b) and 6.3(a). After 3 days, the moisture travels near the bottom and increases pressure head in the column (Fig. 6.2(a)) and decreasing the inward flow rate through the upper surface (Fig. 6.3(b)).

From the pressure head curves of Fig. 6.2(a), a rapid assessment of pressure gradient (change of pressure with respect to the space dimension, here z) can be done. For each time

(e.g., 0.5 day), near the surface the gradients of the curves is less than the middle portion of the curves but due to the nature of the unsaturated hydraulic conductivity functions in unsaturated zone, K_{unsat} is very small at middle due to higher suction heads than those values at the surface. So vertical flux is large at the surface and reduces rapidly through the depth as the soil suction increases. At the end of time 0.5 day, this relatively high flux, diminishes at a depth of approximately 40 cm. As the time passes, the pressure head profiles flattened with respect to the previous time profiles showing less gradient (e.g., comparing for time 0.5 and 3 day in Fig. 6.2(a)). Consequently the vertical flux values reduces (Fig. 6.3(b)) but in the meantime moisture has distributed to greater depth. After 3 days moisture has moved to a depth of approximately 96 cm. It is interesting to note that a number of slight wiggles are visible in the velocity vector plots of Fig. 6.3(b). These wiggles start at depths of 16, 28, 48 and 70 cm on t=0.5, 1, 2 and 3 days plots, respectively. As shown in Fig. 6.2(a), corresponding locations of these depths are at the verges of the pressure head fronts although no significant fluctuation are visible in these profiles.

6.1.2 Infiltration in Soil Column (Neuman Boundary Condition)

This problem is of same nature of the previous example but in this case at the surface nodes a time varying specified flux is imposed. Paniconi et al. (1991) used this to test different types of schemes in one dimension. This is set here to test the infiltration and redistribution simulation into a soil column initially at hydrostatic equilibrium under Neuman boundary condition with increasing flux at the surface as opposed to the previous problem where Dirichlet boundary was postulated. The parameters are given in Table 6.2. Total length of column is 10 m which is divided into 100 brick elements and the total no of nodes are 404. The sequence of node numbering and element numbering are same as the Example 6.1.1.

Imposed time varying Darcy flux q which increases linearly with time is shown in Fig. 6.4(a). The base nodes of the column are maintained at a fixed pressure head value of $\Psi = 0$, acting as a water table, allowing drainage of moisture through it .
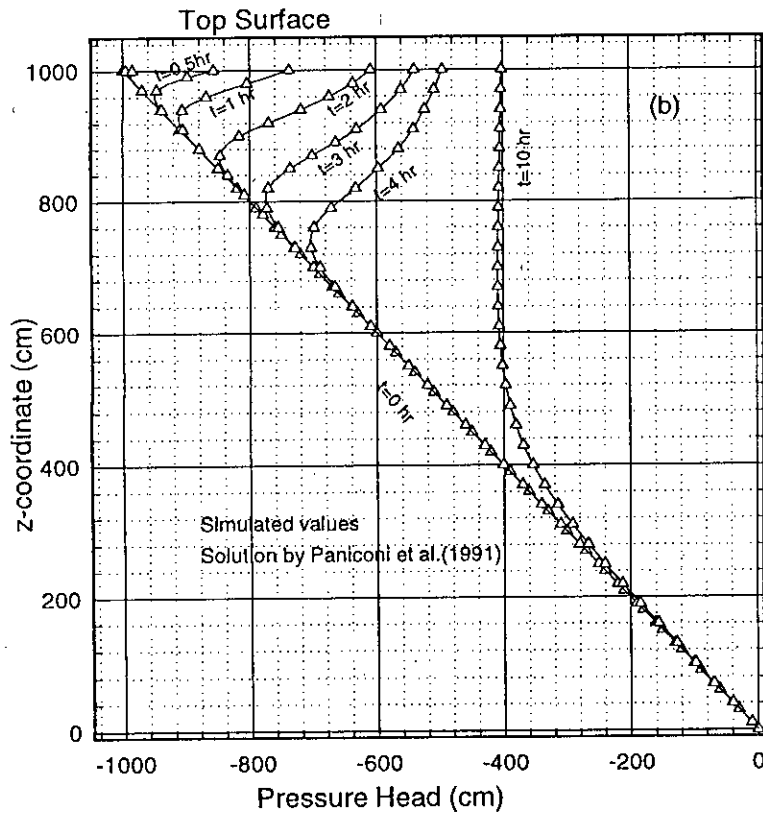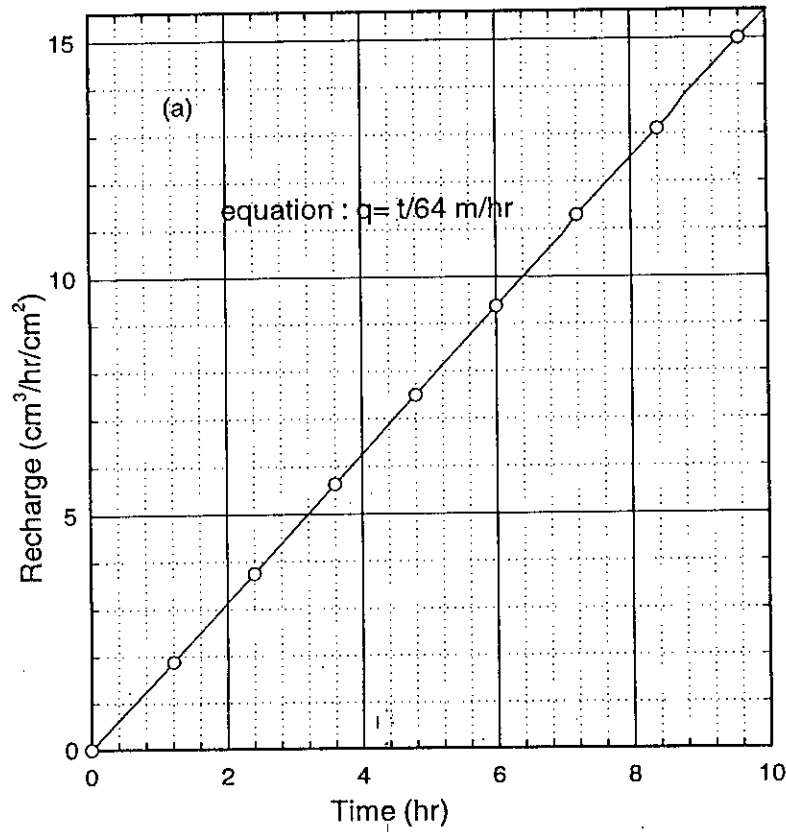
Fig. 6.4 : (a) Boundary influx for example 6.2.1 (b) Simulated pressure head profiles
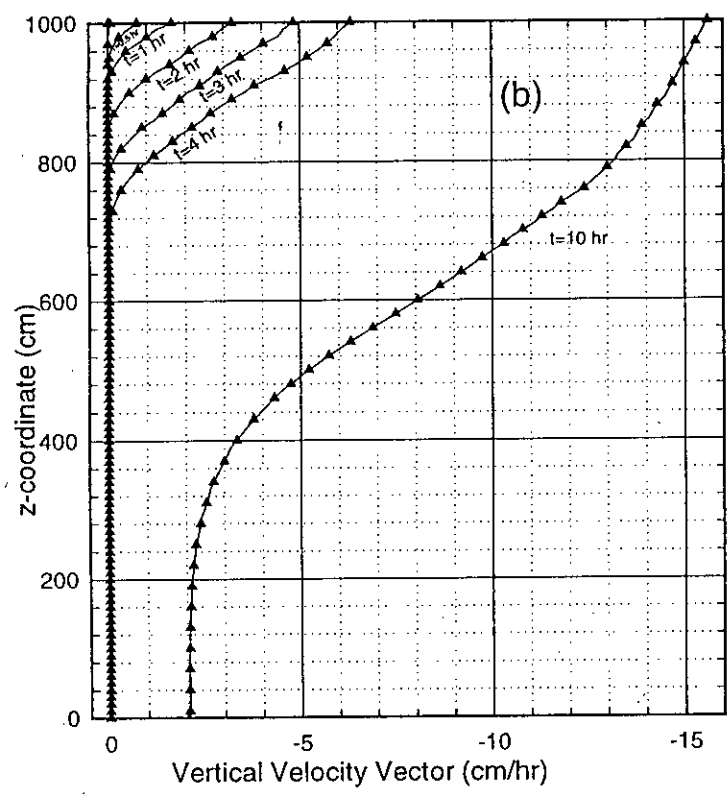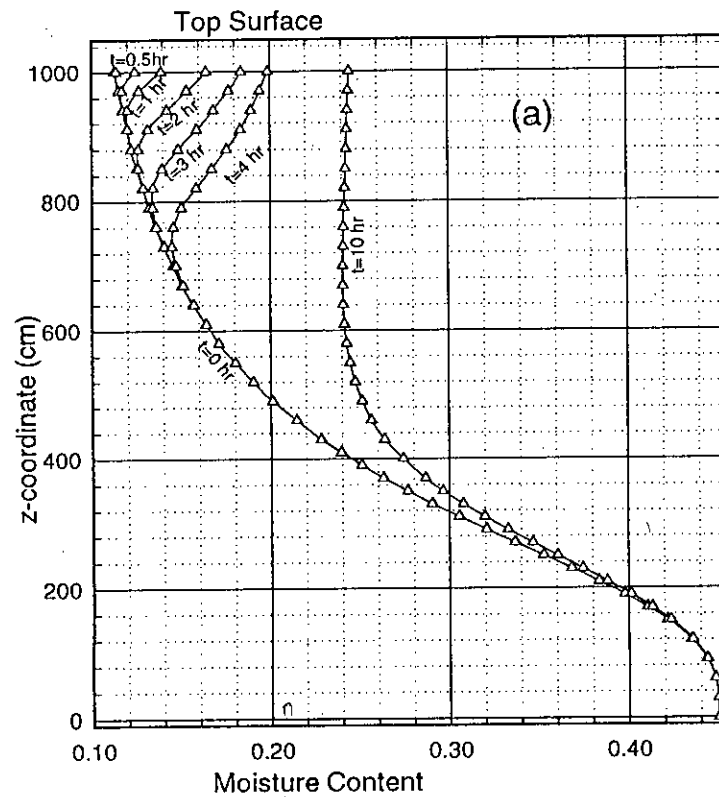
Fig. 6.5 : (a) Simulated moisture content profiles

(b) Vertical velocity vector along the depth of soil column

Table 6.2 : Parameters for Example 6.1.2

Soil Characteristic Functions : van Genuchten and Nielson, 1985 (Eqs. 4.6)					
Parameter	θ_r	θ_s	Ψ_s	n	K_s (m/h)
Value	0.08	0.45	-3	3	5.0

Snapshots in time of pressure head, moisture content, and flow velocity behavior are shown in Figs. 6.4 (b) and 6.5(a,b). In Fig. 6.4 (b), pressure head profiles indicate how pressure head is changing from the initial distribution of hydrostatic pressure. As water is entering the soil the initial moisture content curve (Fig. 6.5(a)) is shifted rightward indicating increase of moisture content from the surface. Due to non-entrance of moisture at certain depths, earlier time pressure head profiles (say, less than 4 hr profiles) of Fig. 6.4(b) merges rapidly to the hydrostatic pressure, while pressure head profile of t=10 hr. remains almost constant upto a considerable depth. These natures of the profiles are controlled by the unsaturated soil properties of the column and with the increase of pressure head the high value of saturated hydraulic conductivity (Table 6.2) is reflected. Fig 6.5(b) indicates how the downward velocity vectors change in response to the continuous change of pressure head gradient with time and depth. Due to the homogeneous nature of the soil and linearly increasing imposed flux at the top with a rate lower than the saturated hydraulic conductivity, no ponding on the surface occur and the vertical velocity vector profiles becomes almost parallel from the surface upto the high gradient moisture front.

6.2 Saturated One-dimensional Flow with Known Surface Flux

The purpose of this simple problem setting is to know the behavior of the code in saturated case. Here a one-dimensional (horizontal) steady groundwater flow through a confined aquifer is considered. An analytical solution of this problem exists, so the results can be easily verified with the computed values.
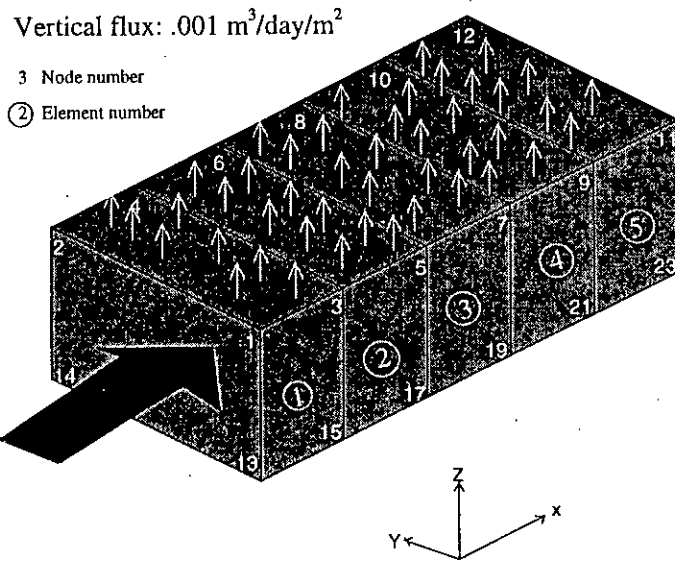
(a) Fully saturated flow domain showing elements and nodes
with sequential numbering scheme
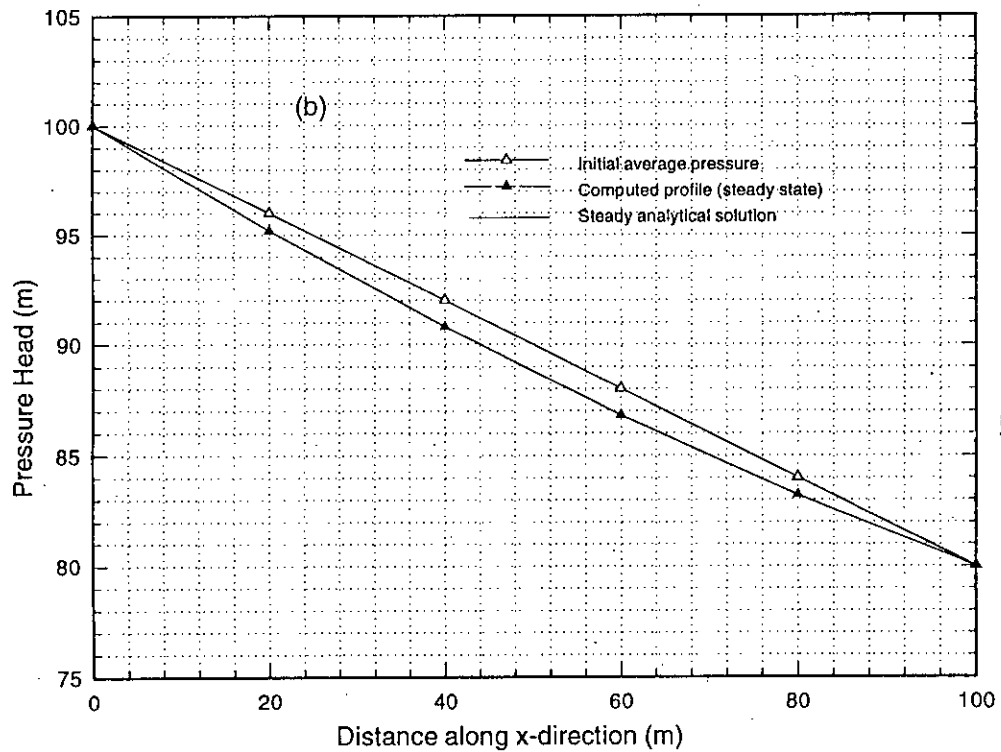
Fig. 6.6 : (a) Flow domain with Finite element discretization and boundaries
(b) Comparision of pressure head in stady state condition

The flow domain under consideration is shown in Fig. 6.6a . Length, L of the zone is 100 m in x-direction and to solve it three-dimensionally, unit length is considered in other two directions (y- and z- directions). The hydraulic head at the upstream end (x=0) of the aquifer is h_1 =100 m, and at the downstream end (x=L) is h_2 = 80 m, both being constant. Through the top surface of the aquifer exists an average outflow flux (evaporation) w = -0.001 $(m^3/d/m^2)$. The hydraulic conductivity, K_x = 1 m/d. Analytical solution of this problem is

$$h(x) = h_1 - \frac{h_1 - h_2}{L}x - \frac{wx}{2K_x}(L-x) \qquad (6.1)$$

To solve this problem by the developed three-dimensional program, the flow domain is divided into 5 brick elements consisting of 24 nodes as shown in Fig. 6.6(a). The initial condition is set with the linear variation of hydraulic head between upstream and downstream known values. The four nodes at x = 0 (i.e., number 1,2,13,14) and at x=L (i.e., 11,12,23,24) are set at Dirichlet boundary condition. The top surface nodes (i.e. nodes 3-10) are set Neuman boundary condition with specified flux. Then the program is run at steady state mode by setting the terms associated with right hand side of Eq. 3.15 to zero. The solution is obtained after three iterations. Because of upward flow, the computed hydraulic heads along any vertical line vary. So to compare these results with the one-dimensional solution, the average of these values are taken and the values agrees closely with those from the analytical solution. The results are shown in Fig. 6.6(b). The program output also shows that to maintain this steady state condition, an inward flow at the upstream side equals to .8 m^3/d and at the downstream side an outward flow 0.2 m^3/d should be maintained.

69

6.3 Problems Associated with Flow under Variable Atmospheric Influences

This example simulates one-dimensional water movement in a soil column in order to illustrate the effect of ponding that can occur on the soil surface in a multilayered soil profile. Hypothetical 60 days atmospheric data are created to provoke the effect. A 300 cm long vertical column with three-layered soil is considered which is shown in Fig. 6.7(a).

Soil hydraulic properties are assumed homogeneous and isotropic within each layer, according to Table 6.3(a) . The retention curves and hydraulic conductivity curves for all three layers are shown in Fig. 6.8(a) and 6.8(b). The soil surface boundary is exposed, after a short period of drought, to high precipitations for several days (with a peak of 100 mm in one day) to create surface ponding. This is followed by a longer dry spell. In the second half of the simulation period, after the ponding has disappeared, another similar group of rain for several days is imposed, to repeat the effect, followed by another dry spell till the end of simulation. The course of weather can be seen from Fig. 6.8(c). Constant rates of potential evaporation (2 mm/day) and transpiration (5 mm/day) were assumed during the whole simulation period. The surface fluxes (infiltration and evaporation), as well as the transpiration rate, were assumed uniformly distributed during 24 hours of each day. The bottom boundary condition is consisted of a prescribed drainage flux-groundwater level relationship, q(h), as given by Eq. 5.6. The groundwater level is initially set at 150 cm below the soil surface. The initial moisture content and pressure head profiles are assumed in equilibrium with the initial groundwater level.

The finite element mesh is constructed by dividing the flow region into 39 brick elements with 160 nodal points. The sequence of nodal and element numbering is shown in Fig. 6.7(b). In this example , three types of boundaries are defined. The bottom boundary face is identified as a variable flux boundary of mixed type, where q depends on h. The atmospheric surface can have either constant head Dirichlet boundary condition when surface ponding occurred or the atmospheric boundary condition in the absence of ponding .The sides of the column are set to Neuman no-flow boundary condition and behaved in the program like internal nodes. Basic parameters of numerical simulation are summarized in the following Tables 6.3(a) and 6.3(b).
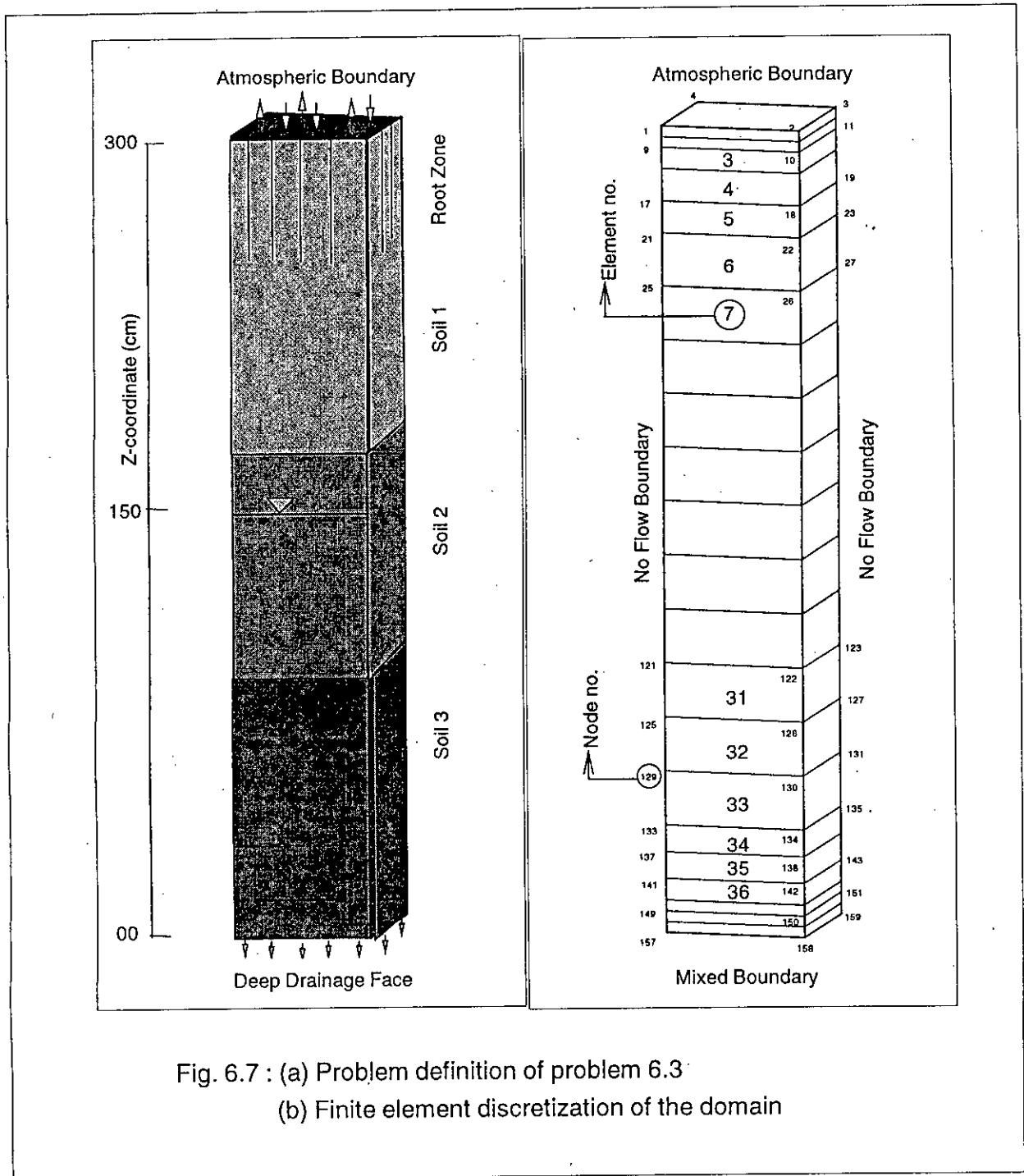
Fig. 6.7 : (a) Problem definition of problem 6.3
(b) Finite element discretization of the domain
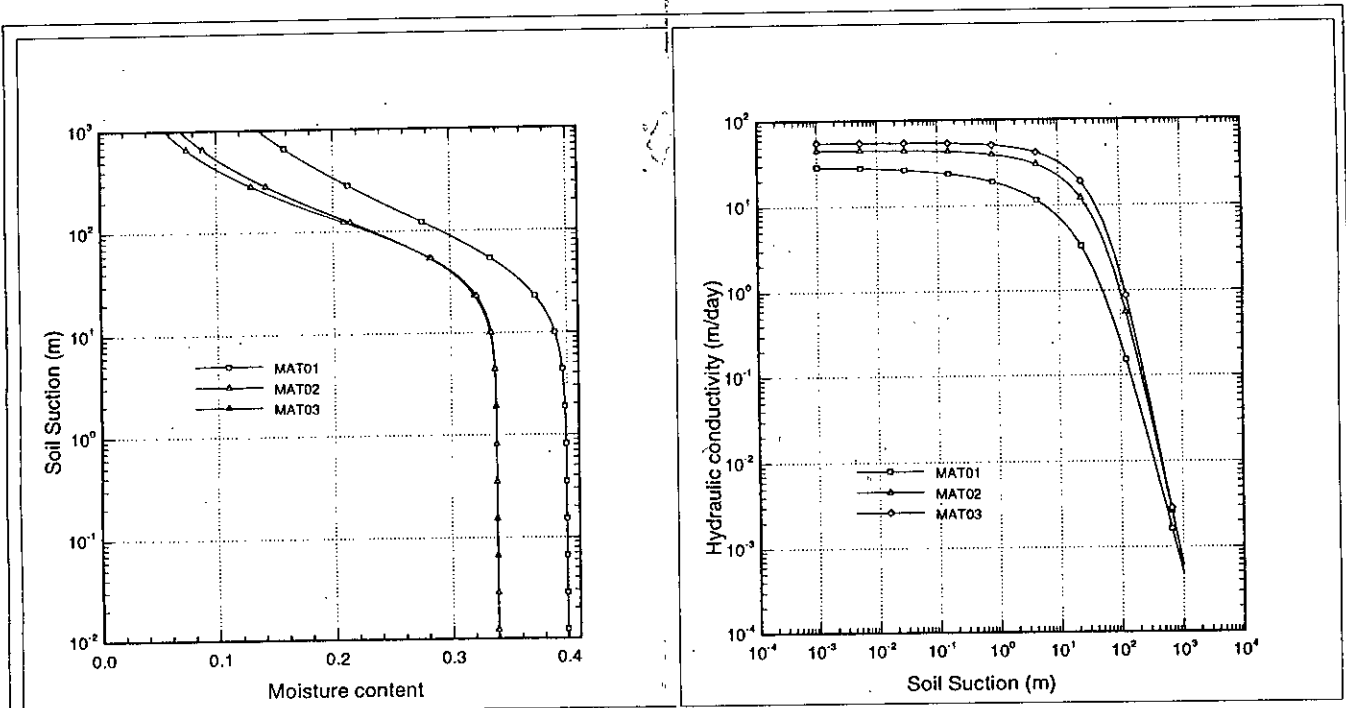
(a) Moisture content vs. pressure head

(b) Unsaturated Hydraulic conductivity vs. pressure head

(c)
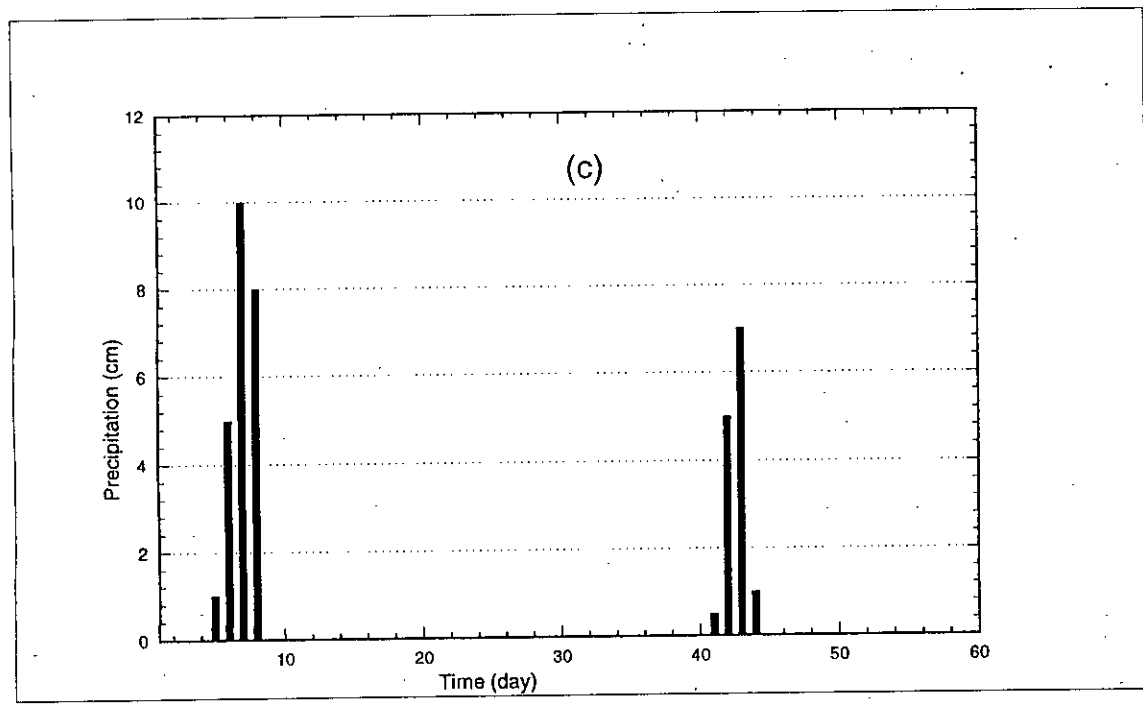
Fig. 6.8 : (a) & (b) Soil moisture characteristic curves for problem 6.3
(c) Precipitation events in the simulated 60 days period

Table 6.3(a): Input Hydraulic Parameters for Example 6.3

Soil Characteristic Functions : Vogel and Cislerova, 1988 (Eqs. 4.3 to 4.5)

Parameters	1st layer Depth (205-300 cm)	2nd layer Depth (105-205 cm)	3rd layer Depth (0-105 cm)
$\theta_s = \theta_m = \theta_k$	399	0.339	0.339
$\theta_r = \theta_a$	0.0001	0.0002	0.0001
$K_S = K_k$ (m/day)	0.2975	0.4534	0.5534
α (m^{-1})	1.740	1.390	1.300
n	1.3757	1.6024	1.7024

Table 6.3(b) : Numerical Simulation Information

Time Information	
Initial time increment: Δt	0.02 day
Minimum time increment:	1e-10 day
Maximum time increment	0.50 day
Other Information	
Maximum number of iteration: MaxIt	20
Absolute pressure head tolerance: Tol	0.01 cm

Discussion of the Simulated Results :

Time course of simulated mean pressure heads at the soil surface and in the root zone, cumulative flux (evaporation - precipitation) across the atmospheric boundary and cumulative transpiration flux are shown in Figs. 6.9(a), 6.9(b) and 6.9(c) respectively. Simulated profiles of volumetric moisture content and pressure head are shown in Figs. 6.10 and 6.11, respectively. The discussion of the results of simulation, in relation to those obtained with atmospheric boundary condition, is followed hereafter.

Fig. 6.9(c) shows that the mean pressure heads, both on the soil surface and in the root zone, are decreasing during the first several days of simulation, as the soil profile is dried and drained simultaneously (there was no precipitation during the first four days), evaporation takes place from the soil surface and water is extracted from the root zone by transpiration equal to the potential one (two lines coincide, in Fig.6.9(b)). Beginning from the 5th day, rainfall has reversed the situation and ponding finally occurred during the 8th day. After that date, the average pressure heads are positive with variable atmospheric boundary condition (Fig. 6.9(c)). The average pressure head in the root zone is larger than the average surface pressure head because the root zone is mostly saturated and lay under the temporary water table. Infiltration takes place under positive hydraulic head (with Dirichlet boundary condition) until all water on the soil surface has been depleted by both infiltration and evaporation. This takes place on the 30th day. Infiltration is rapid as long as there is some unsaturated space in the soil profile (Fig. 6.9(a) and (c), where -ve, i.e., inward cumulative flux is increasing rapidly) . After total saturation, which occurred during the 8th day, water is only drained from the soil profile by some (unspecified) natural or artificial drainage system according to Eq. 5.6 ; the infiltration can not therefore be higher than the drainage flux at the bottom of the profile.

In Fig. 6.9(a) the dashed line (actual cumulative flux) departs from the solid line (potential cumulative surface flux) beginning from the 8th day. It is still decreasing (infiltration continues) but its slope is much less then that corresponding to potential infiltration. After the 30th day, evaporation from the soil surface takes place again, and the

74
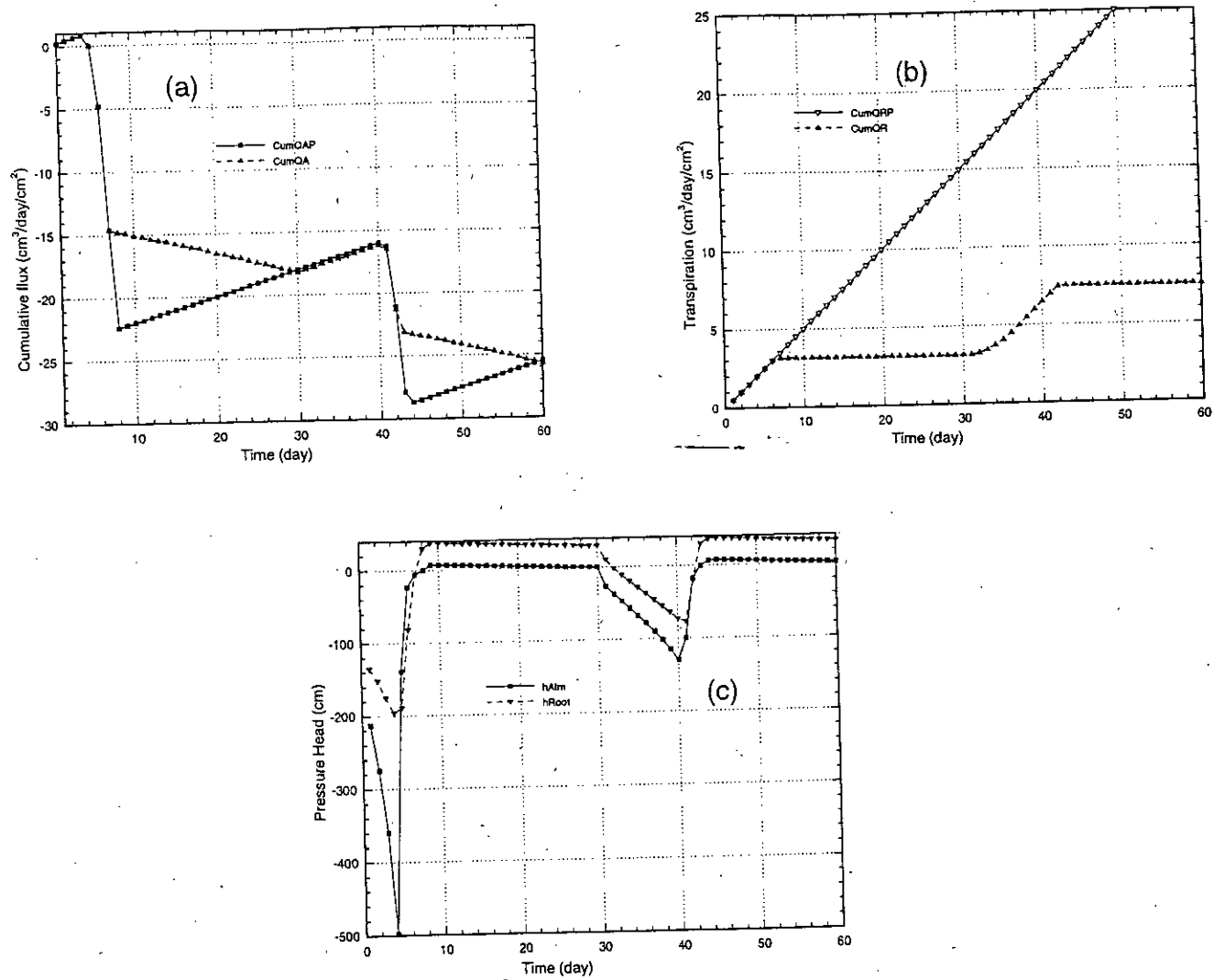
Fig. 6.9 : (a) Simulated cumulative flux through top surface

(b) Cumulative transpiration

(c) Mean pressure head at the top surface
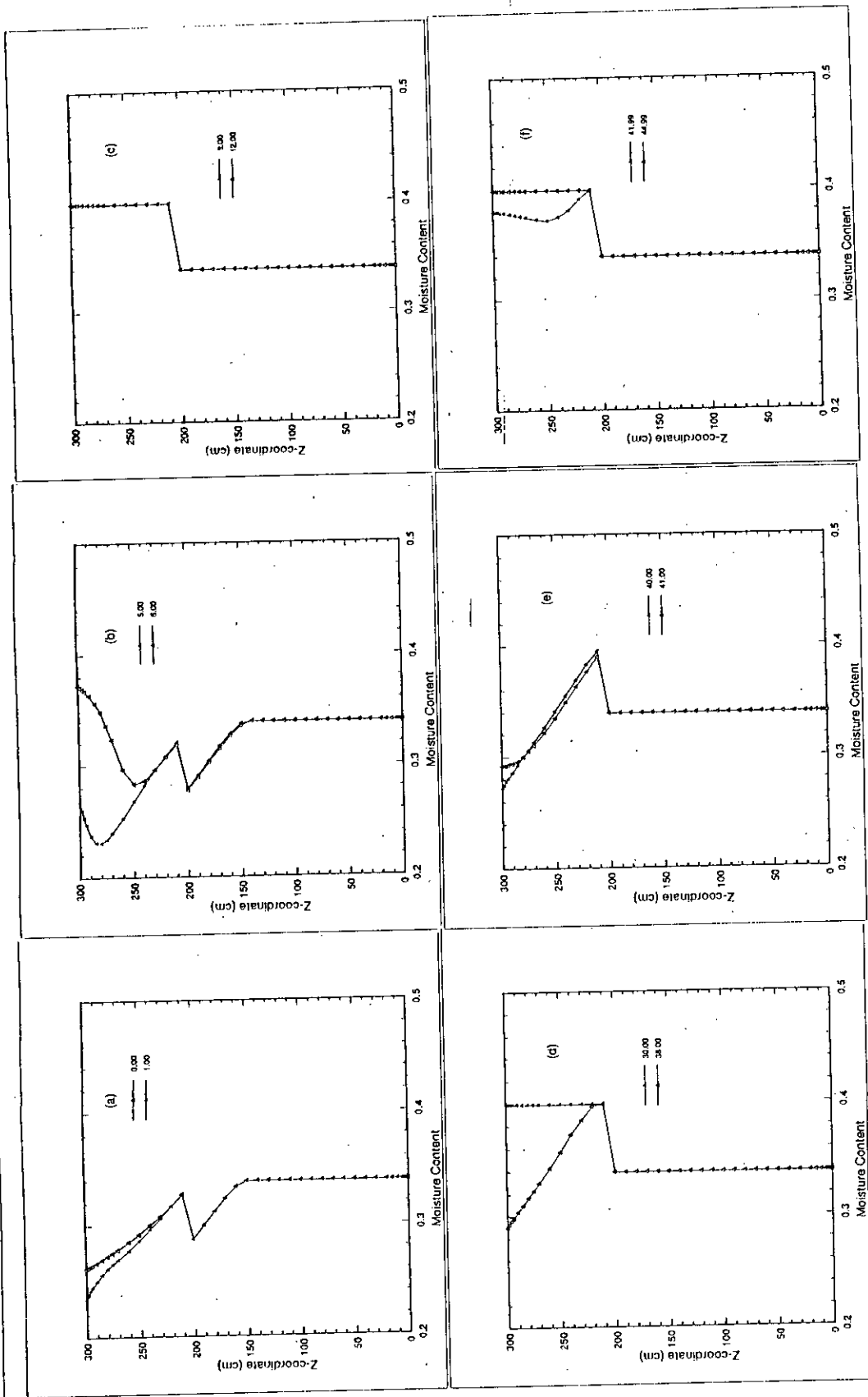
Fig.6.10: (a) to (f) Simulated moisture content profiles along depth at different days
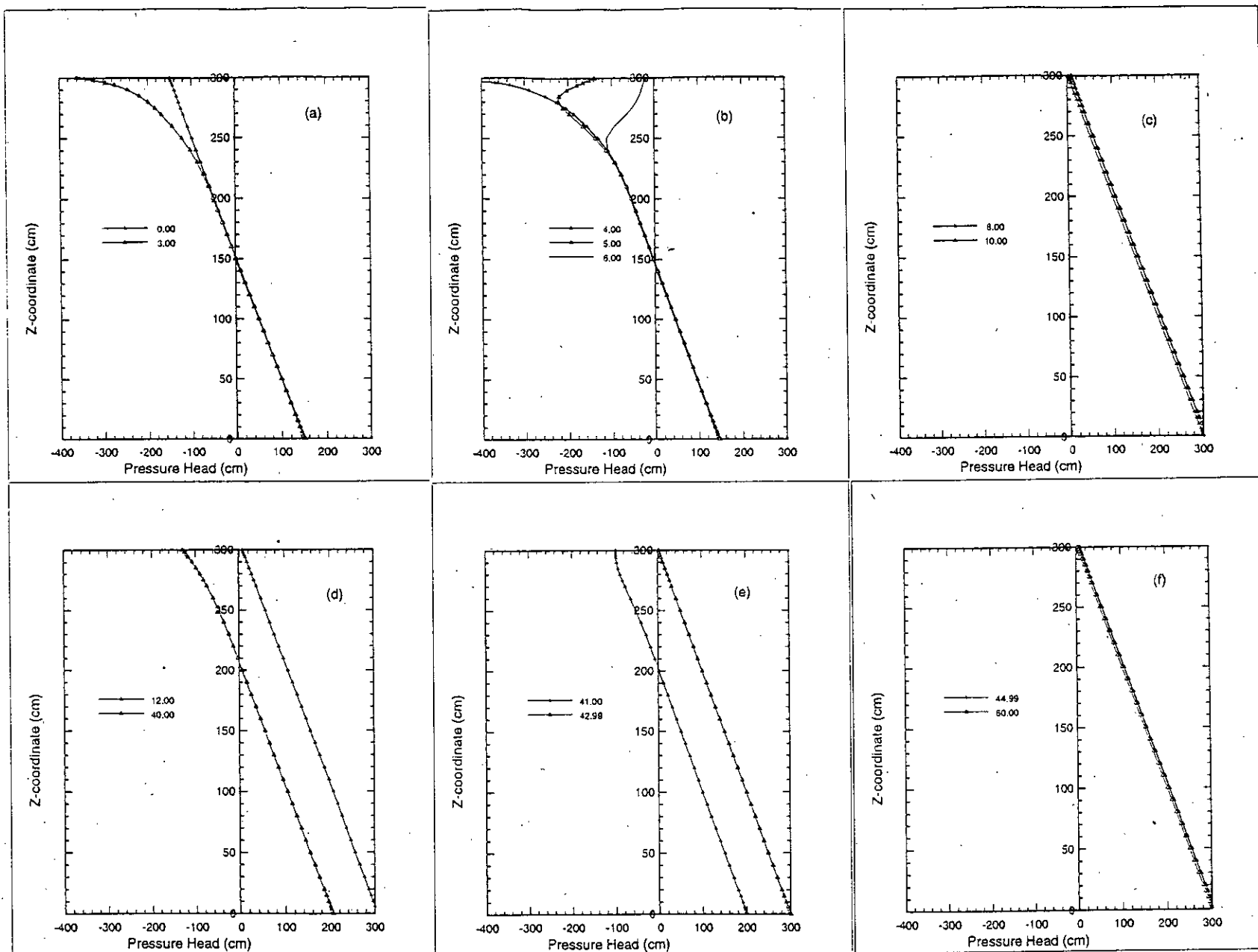
Fig. 6.11: (a) to (f) Simulated pressure head profilies in the soil column at the end of different days

slope of the dashed line in Fig. 6.9(a) is again increasing, until new rainfall comes on 41st day. The whole situation then repeated with water remaining on the soil surface till the end of the simulation period. No evaporation from the soil surface takes place during the periods of ponding (instead, the potential evaporation occurred from the water layer on the soil surface but this is not comprised in Fig.6.9(a)). Transpiration is totally suppressed during the periods when the soil profile is saturated (the dashed line of actual cumulative transpiration in Fig. 6.9(b) is horizontal). Most plants would be heavily damaged by anaerobiosis during the surface ponding.Therefore, as soon as the soil profile becomes aerated again (on about 34th day), transpiration recovers with almost potential intensity, until the new ponding at 41st day.

In Figs. 6.10(a) to 6.10(f), the vertical moisture content profiles for different simulation times are presented. The events described above can be equally well followed from the moisture content profiles. The soil heterogeneity (the soil profile is composed of three layers) is most explicitly expressed in the heights 200-210 cm (measured from the profile bottom) where the saturated moisture content is changing. It is the property of the model that a boundary between two different soil materials is not abrupt but occupies a strip of finite width (10 cm in our case) in which the soil properties are changing in a linear manner . Figs. 6.11(a) to 6.11(f) allow us to follow the time development of pressure heads and of the groundwater table (indicated by the zero pressure head). The groundwater table is falling slightly during the initial dry period (due to both bottom drainage and transpiration) but the main part of water for evaporation and transpiration is extracted from the upper, unsaturated part of the profile. When the rain begins, water content is replenished from above (on 6th day, Fig. 6.11(b), we have yet no sensible influence of infiltration upon the groundwater table which is at 150 cm from base). In the Fig. 6.11(b), pressure head development in the upper part and in the root zone is seen at 4th, 5th and 6th days ; the curves turn right gradually showing pressure closing towards the saturation (pressure head =0) and at the end of 6th day the surface is still unsaturated. After that day the water table begins to rise and total zone at 8th day becomes saturated showing groundwater table at the surface. During the dry spell the water table fall day by day. Fig.6.11(d) shows that at day 12, there is some water on the soil surface but at day 40 (end of the dry spell), the water table falls to a value near 210 cm. In the last two boxes of the same page, the effect of

second rainfall events on the pressure head profile are presented which show again the water table rise and some ponding on the surface upto the end of simulation.

From the above discussion, it may be concluded that, the model has behaved in the desired manner under the postulated hydrometeorological conditions. The saturated-unsaturated integrated simulation of the rainfall events, infiltration, redistribution ,ponding and groundwater table rise occurred correctly. These results are also compared with those from a two-dimensional groundwater flow model by Simunek et al. (1992). The precipitation and evaporation data used is on daily basis. So during starting of a new day, there is an abrupt change in the model input and output. But in order to have convergence, the internal time step values are less enough upto maximum value of 0.5 day. So it will be more suitable if the input data can be adjusted to the internal time step values which are variable depending on the converging behavior and iterations required in the previous time step.

6.4 Problems Associated with River Bank

This section deals with problems where flow domain is bounded by river in one side. The important phenomena frequently occur in such situation is seepage from the adjacent groundwater body through the river bank exposed to the atmosphere. Two cases are handled here ; one considers constant river water level and other is subjected to variable water level resembling real river hydrograph.

6.4.1 Transient Drainage From a Domain

This example is chosen to verify the performance of the algorithm in modeling transient flow situation involving seepage-face boundary. The problem was presented by Huyakorn et al. (1986) to test their model. So a comparison of the results with respect to the present algorithm is presented here.

Geometry of the flow region and initial and boundary conditions used in the simulation are presented in the Fig. 6.12(a). The flow system is assumed to be initially in

79
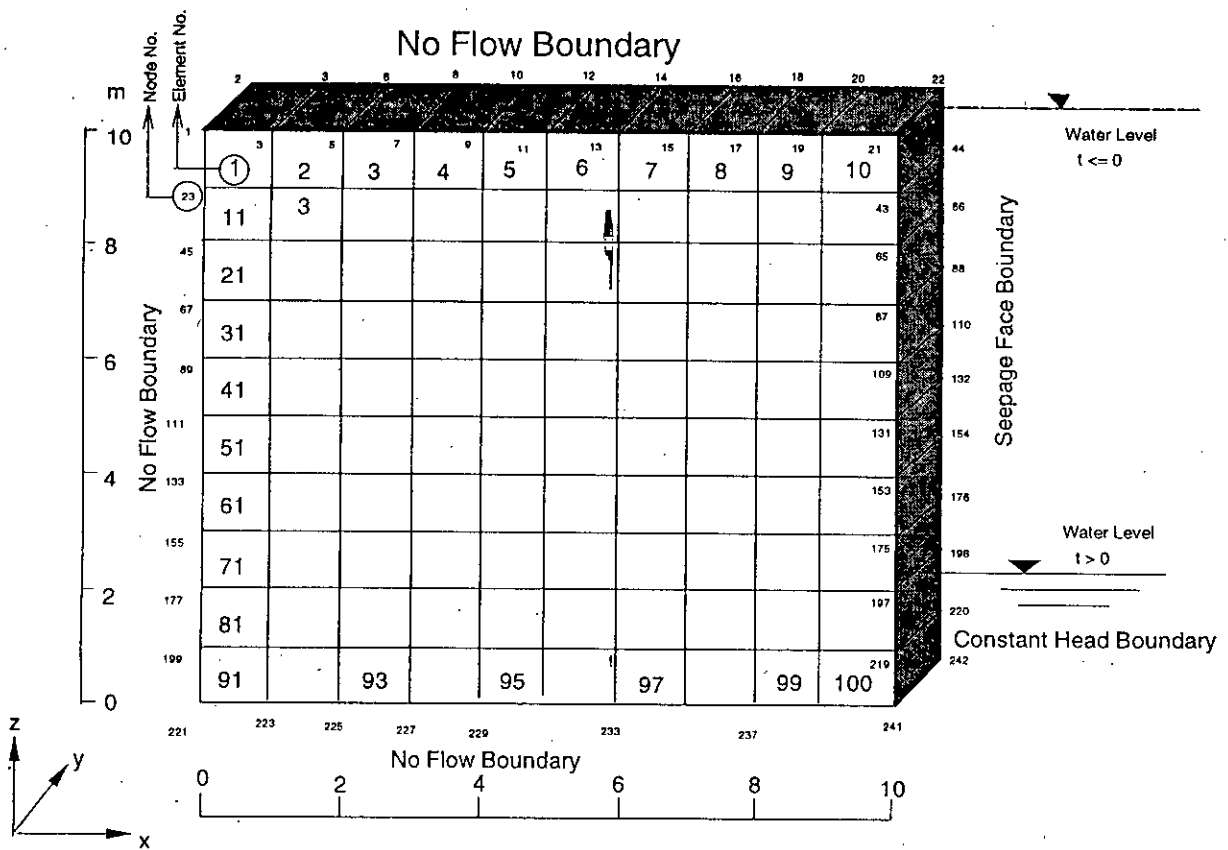
Fig.6.12a: Finite element mesh and boundary conditions of the
flow domain in example 6.4.1
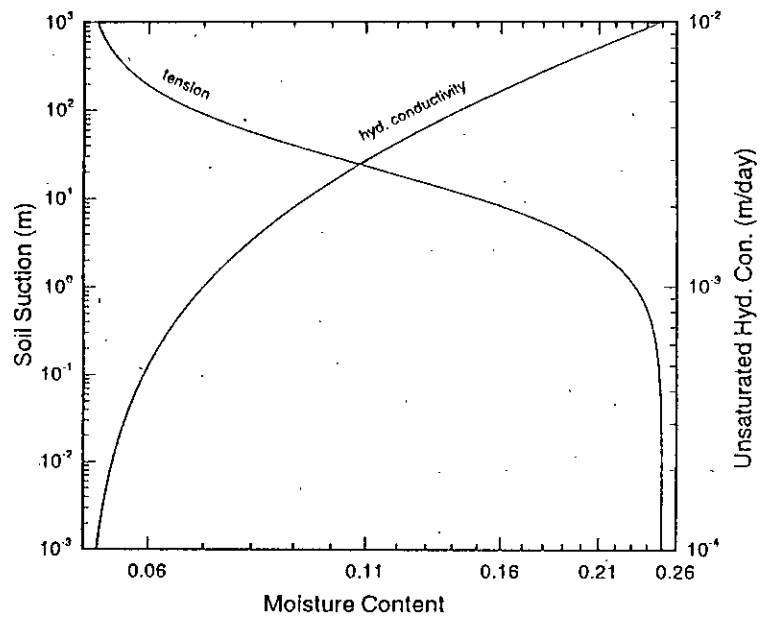
Fig. 6.12(b) : Soil-moisture characteristic curves for example 6.4.1

static equilibrium. The water level at the right face of the block is then lowered suddenly, from 10 m to 2 m and maintained at this level thereafter allowing free drainage of the block.

The water retention of the soil is presented by Eqs. 4.7, using values of A=10m, B=1, porosity, Φ= 0.25, air entry value, ψ_a =0.0 m, residual water saturation, S_{wr} =0.2 . For the relative hydraulic conductivity function, n=1. These are shown graphically in Fig. 6.11(b). The specific storage and saturated hydraulic conductivity of the porous media are 10^{-4} and 0.01 m/day respectively.

From the Fig. 6.12(a), the flow model has **no-flow boundary** on the bottom, top and on the left face. At time t=0^+ , after lowering of the water table, the temporal location of the seepage face is unknown until the problem is solved at a given time. Hence, on the right hand side, the seepage face boundary is transiently determined between the heights 2m and 10 m. Initially the seepage face boundary is identified as Dirichlet boundary condition with pressure head, ψ=0 at all the seepage face nodes. At the subsequent times, seepage face position and associated boundary type is determined iteratively as discussed in Section 5.3.4.2. Below the external water table of 2m, a constant head boundary of h=ψ+z=2.0 m is applied for each simulation time.

The flow domain is discretized by Δx=1m, Δy=1m and Δz=1m. Due to the nature of the flow boundaries and homogeneous as well as isotropic nature of the soil characteristics, it is sufficient to schemetized the model of flow as two-dimensional in x-z plane. This is accomplished by taking unit width in the y-direction. Thus total number of elements in the flow domain is 100 and total number of nodes is 242. It is clear from the nature of the flow lines in such a problem, the water level variation is pronounced near the seepage face. So it is logical to take a finer grid near the seepage face.

Computed profiles of the water table at various times are plotted in Fig. 6.13(a). There is an excellent agreement between the water table position predicted by the present model and other models (published by Huyakorn et al., 1986). A plot of outflow rate through the seepage face nodes versus elapsed time is presented in Fig. 6.13(b). The present results agree fairly well with those predicted by other two models. At first few time steps, there
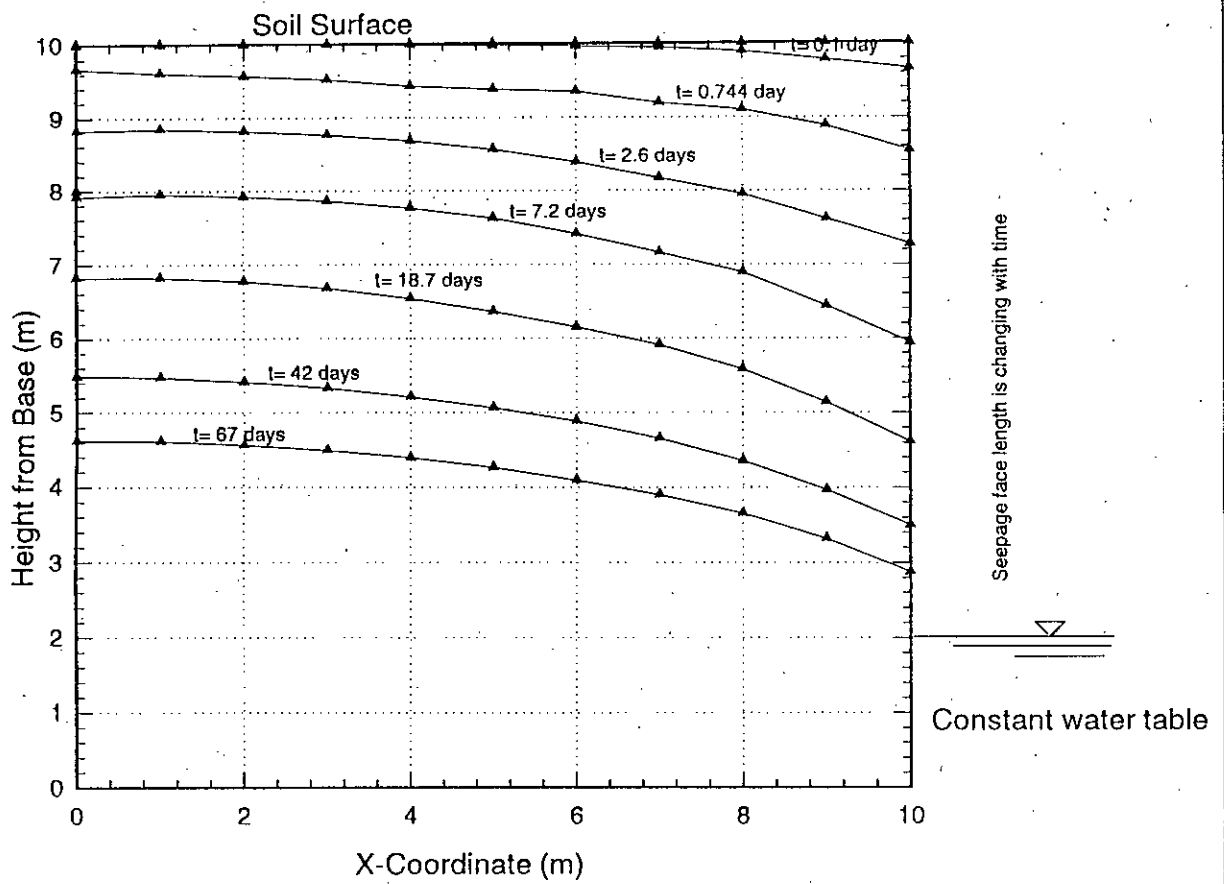
Fig. 6.13a : Computed profiles of water table in xz plane at different time
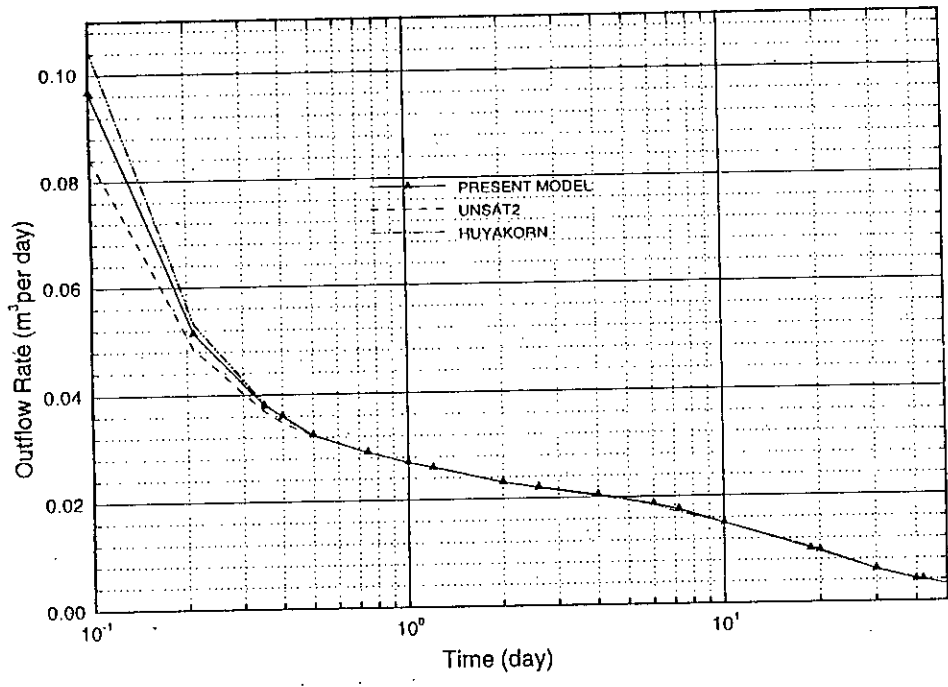
Fig. 6.13(b) : Computed profiles of outflow rate through seepage face by present model and same with other two models (published by Huyakorn et al., 1986)

84

is some deviation of the results from the other models. this may be due to the different schemes used by the models. This inconsistency may be improved converging to closer solutions if in each case at the initial stage of computation smaller time steps are used and the grid spacings are made sufficiently finer especially near the seepage face where pressure head gradient changes rapidly.

6.4.2 Flow Simulation under the Influence of Water Level Fluctuation in River

This example problem is designed to illustrate water movement in a zone of soil adjacent to a river bank, induced by fluctuating water level in the river, with seepage face of variable position above the water level. The soil condition is heterogeneous which is composed of three layers and the size of the flow domain is similar to the previous problem.

The upper atmospheric boundary face of the flow region is defined as a no-flow boundary, to prevent any disturbing influence of atmospheric events. The same boundary condition is postulated also for the off-river face of the flow region (the right edge of the domain). To set the initial condition for the transient problem , the nodal points above water level on the bank face (on the left edge of rectangle) are assigned the seepage-face boundary condition, while the Dirichlet boundary condition of variable pressure head is imposed on the points below water level on the same bank face.

The bottom face of the flow domain is considered as variable drainage flux boundary. Initial groundwater table within the flow region is assumed horizontal and in equilibrium with the water level in the river, 5 m above the bottom surface (Fig. 6.14(a)). Initial pressure head and moisture content values within the flow region are assumed in equilibrium with this groundwater table.

The flow region is discretized into 1242 nodal points and 572 elements (Fig. 6.14(b)). The element dimensions are smaller along the top, bottom and river faces, where large pressure head gradients could be expected. The region is composed of three layers with slightly different hydraulic parameters (Fig. 6.8(a),(b)). The soil parameters are also the

No-Flow Boundary

SOIL 1

SOIL 2

Initial Groundwater Table

SOIL

Seepage Face Boundary

Dirichlet Boundary

No-Flow Boundary

Initial hydrostatic pressure head
in eqilibrium with the river water level

cm

1000

900

800

700

600

500

400

300

200

100

0

z

y

x

FLOW DOMAIN
SIX

Deep Drainage Face

00   200   400   600   800   1000   cm
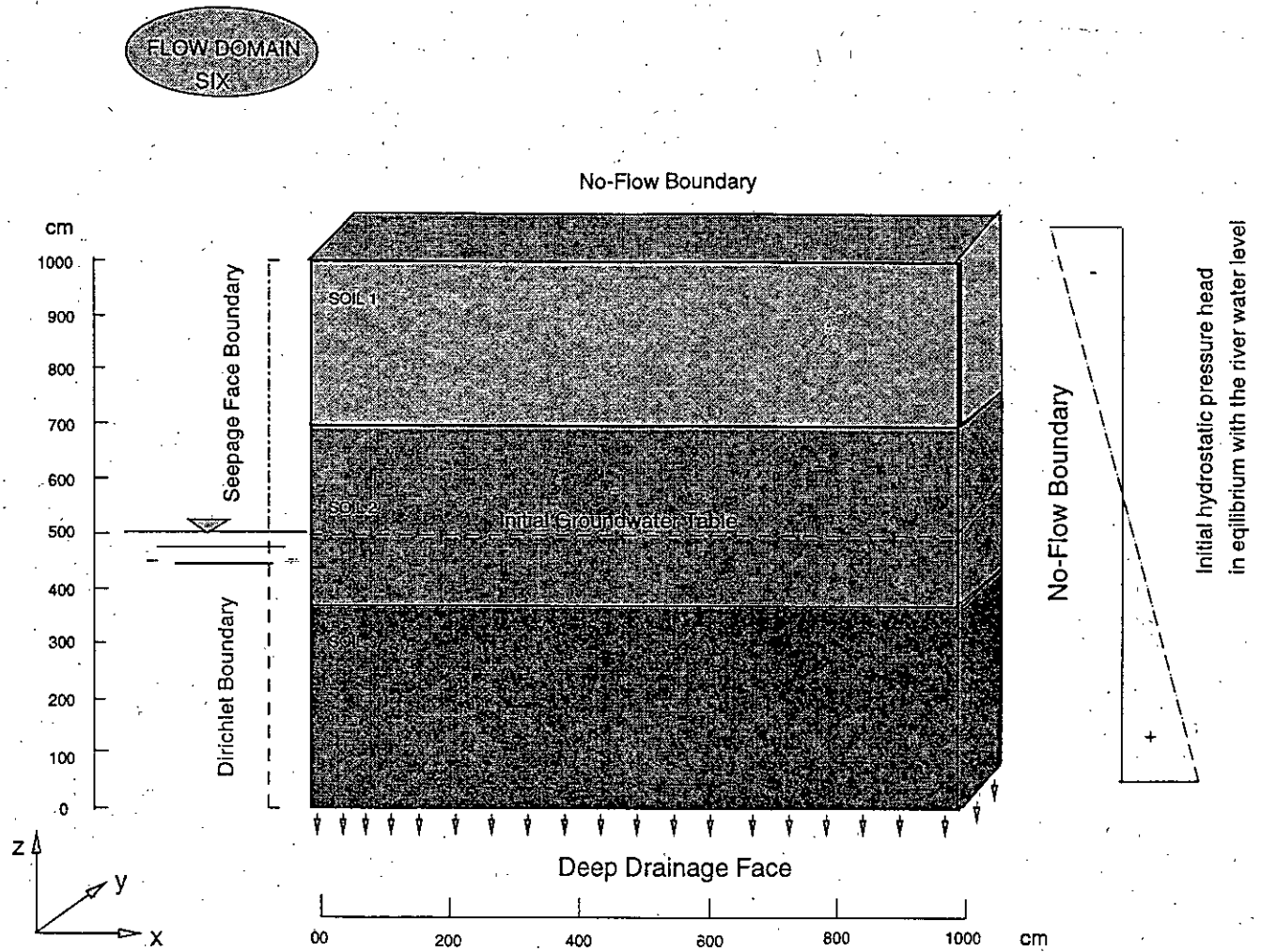
Fig. 6.14(a) : Flow System with Initial and Boundary Conditions for Problem 6.4.2

Atmospheric Face : No atmospheric acivities
is allowed to verify the river influences only.
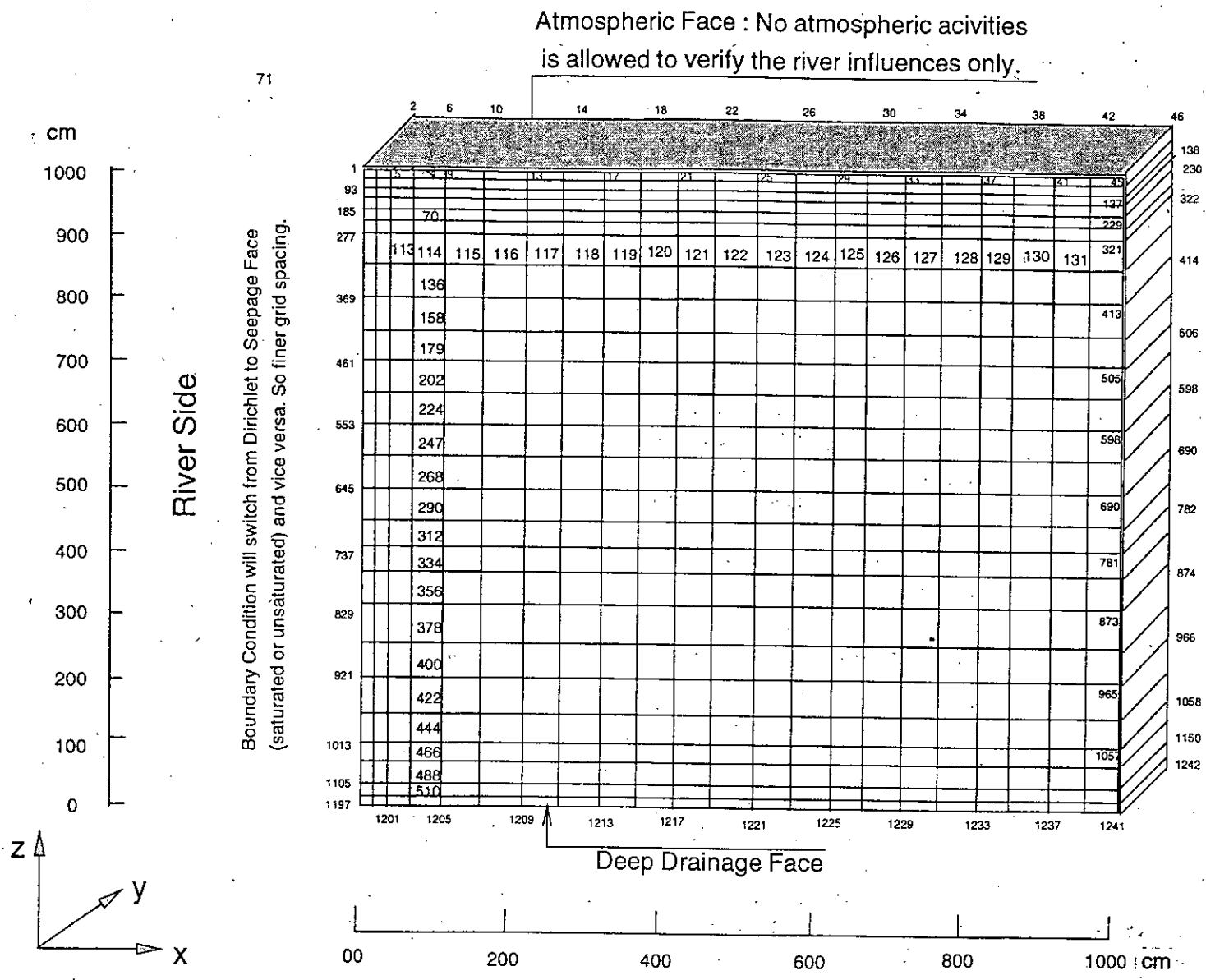
Fig. 6.14(b) : Finite element discretization of the flow domain for Example 6.4.2
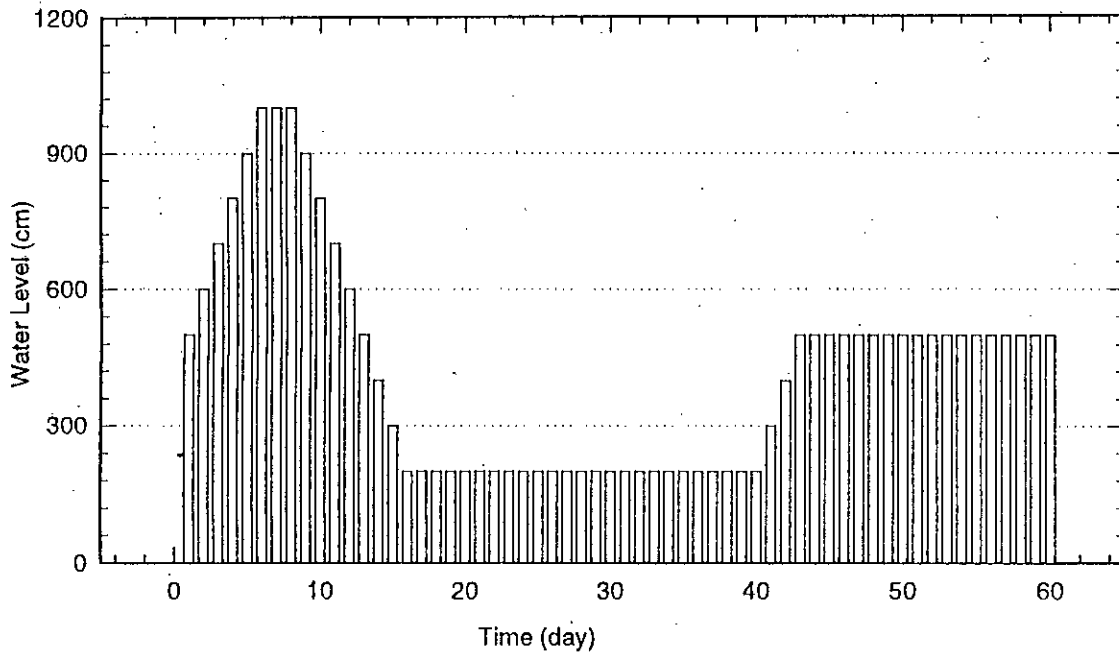
Fig. 6.15 : Hypothetical daily water level fluctuations in the river
for Example 6.4.2

88

same as in Example 6.3 but the thicknesses of individual layers are different from that example.

Water level fluctuations in the hypothetical river left to the flow domain (Fig. 6.15) are adopted to test the functioning of the variable seepage face treatment in the algorithm. An extreme trapezoidal flood wave is supposed to take place during the first 15 days with the peak level 10 m (just at the level of soil surface so that spillage does not occur) held constant during the 6th, 7th and 8th day; after that, water level gradually fall to a minimum value of 2 m in the day 16. This low water level (2 m above bottom) is maintained till the 40th day. Finally, water level again increases gradually to 5 m from 41st to 43rd day and is maintained at the latter level till the end of simulation. Water level is kept constant during each day; the whole daily change of level is assumed to occur suddenly at midnight. Basic soil hydraulic parameters are summarized in the following Table 6.4(a).

Table 6.4(a): Input Hydraulic Parameters

Soil Characteristic Functions : Vogel and Cislerova, 1988 (Eqs. 4.3 to 4.5)

Parameters	1st layer (1000-700 cm)	2nd layer (700-400 cm)	3rd layer (0-400 cm)
$\theta_s = \theta_m = \theta_k$	0.399	0.339	0.339
$\theta_r = \theta_a$	0.0001	0.0001	0.0001
$K_s = K_k$, m/day	0.2975	0.4534	0.5534
α (m^{-1})	1.740	1.390	1.300
n	1.3757	1.6024	1.7024

Results and Discussion :

Results of simulation for some selected typical time instants are presented in detail in the following pages. Results obtained in this simulation, in spite of the schematic nature of the example, can throw some light on the pattern of soil moisture and groundwater movement in river banks during real hydrologic events.

Solid line : flow through the saturated river side   Dashed line : flow through the base of the domain

+ve flow means outward the domain   -ve flow means inward the domain
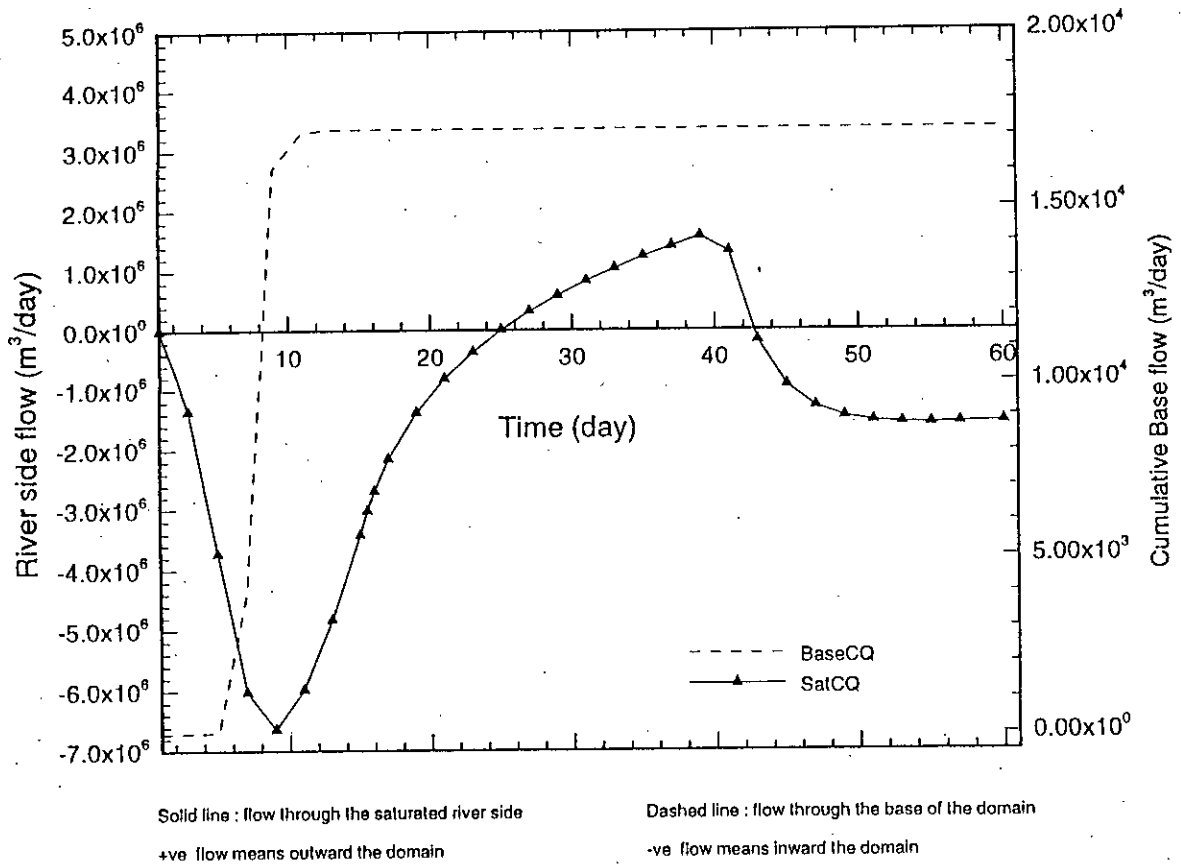
Fig. 6.16 : Cumulative flow through the saturated boundaries of the domain
under the fluctuating river water level

| Simulation Time : day 0.02 | Simulation Time : day 3 | Simulation Time : day 4 |
| River water level : 500 | River water level : 700 (rising) | River water level : 800 (rising) |

| Simulation Time : day 7 | Simulation Time : day 8 | Simulation Time : day 9 |
| River water level : 1000 (Peak value reached) | River water level : 1000 (peak continues) | River water level : 900 (falling) |
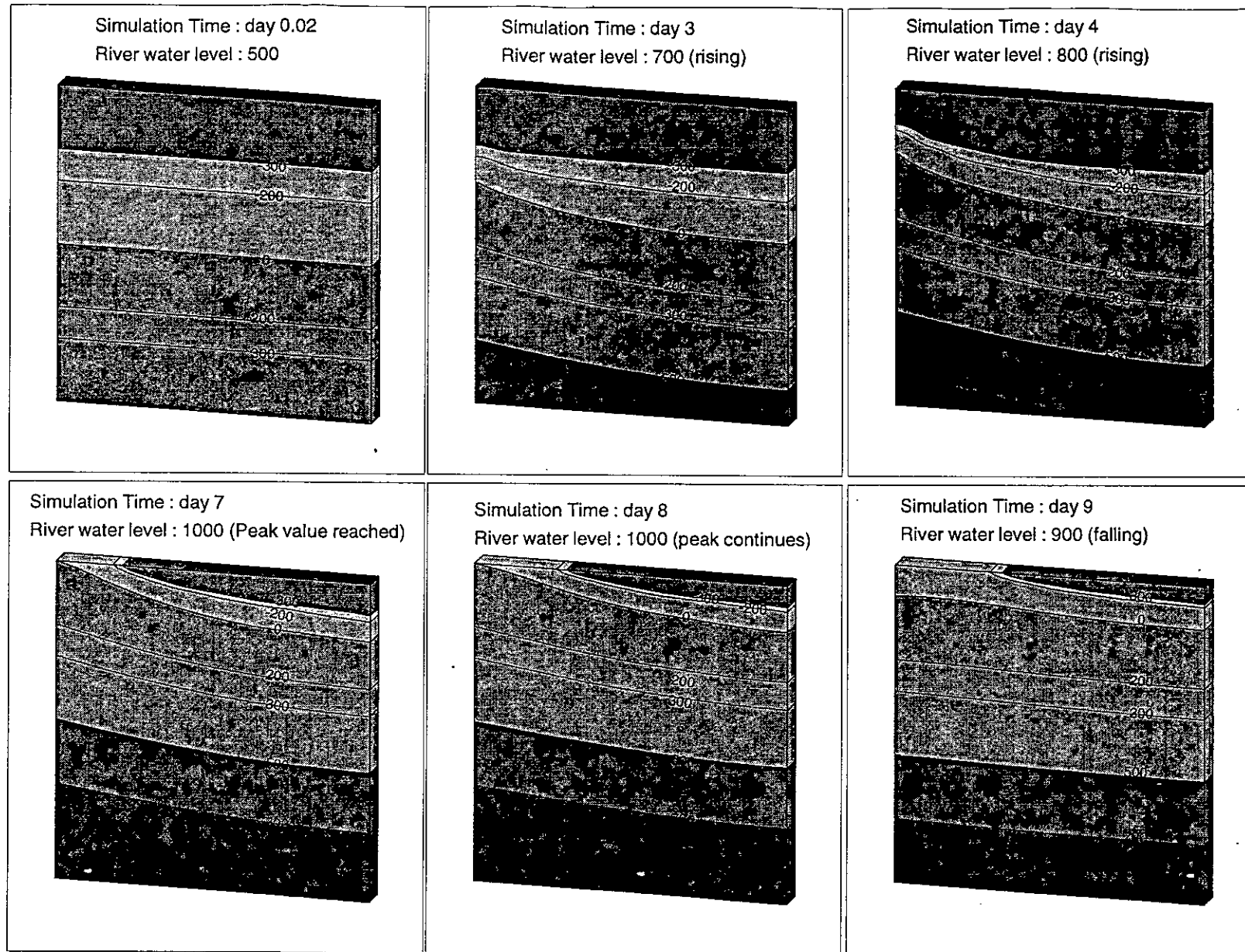
Fig 6.17 : (a) to (f) Contour of the simulated pressure head (in cm) corresponding
to the times at the end of the days indicated.

Simulation Time : day 13
River water level : 500 (falling)

(g)
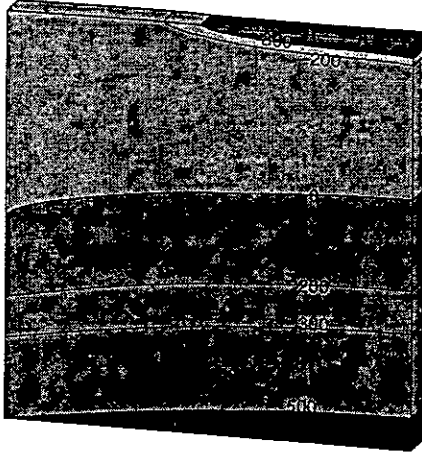
Simulation Time : day 17
River water level : 200 (minimum)
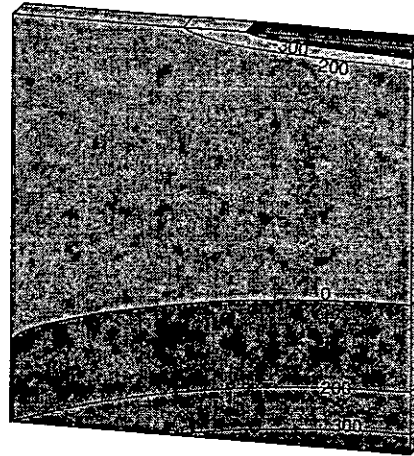
(h)

Simulation Time : day 20
River water level : 200 (minimum cont.)
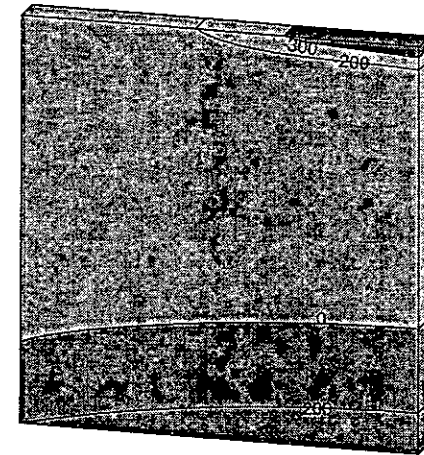
(i)

Simulation Time : day 40
River water level : 200 (last day of min.)
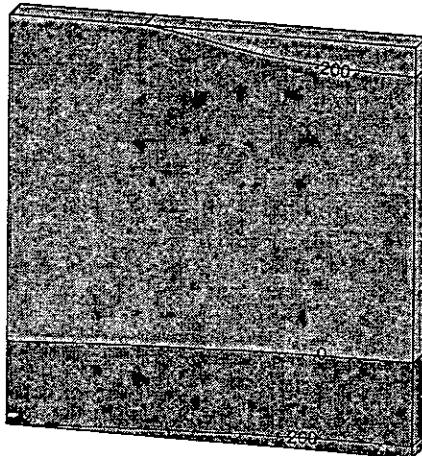
(j)

Simulation Time : day 43
River water level : 500 (peak of 2nd. flood)
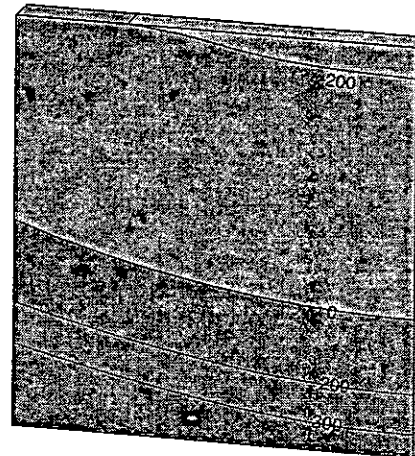
(k)

Simulation Time : day 50
River water level : 500 (constant)
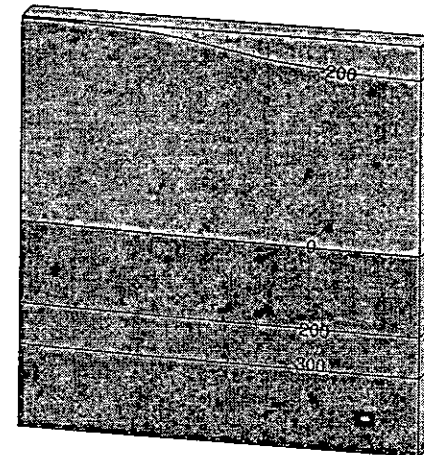
(l)

Fig 6.17 : (g) to (l) Contour of the simulated pressure head (in cm) corresponding
to the times at the end of the days indicated.

Simulation time : day 0.2
River water level : 500 (initial)
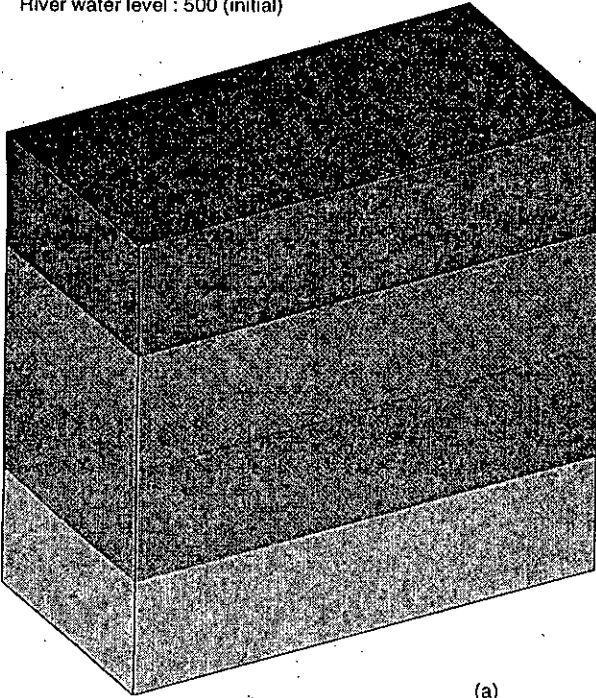
(a)

Simulation time : day 3
River water level : 700 (rising)
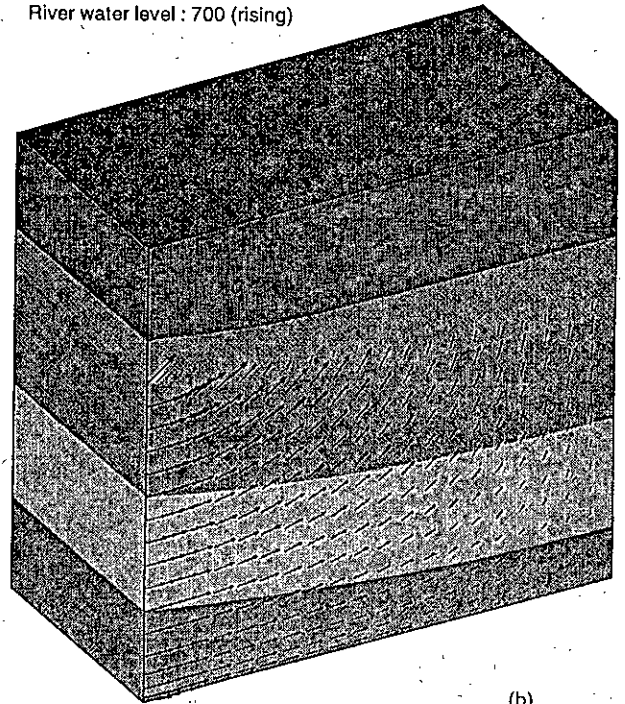
(b)

Simulation time : day 7
River water level : 1000 (maximum)
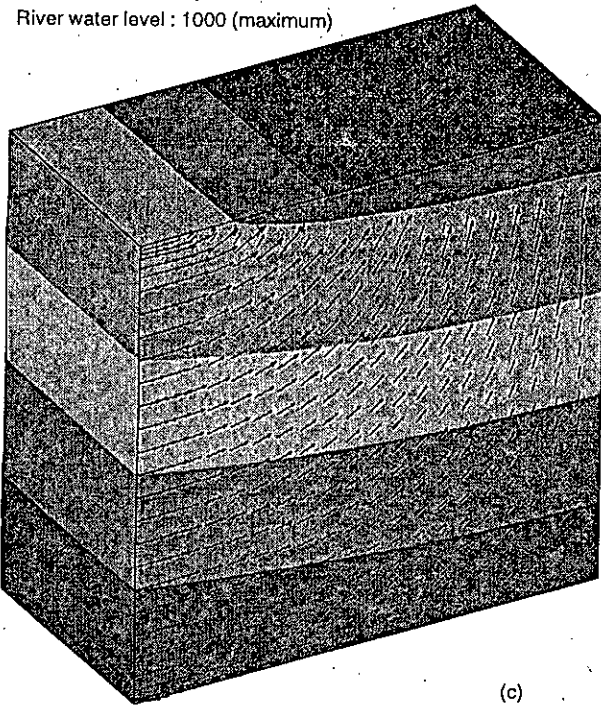
(c)

Simulation time : day 9
River water level : 1000 (recession just start)
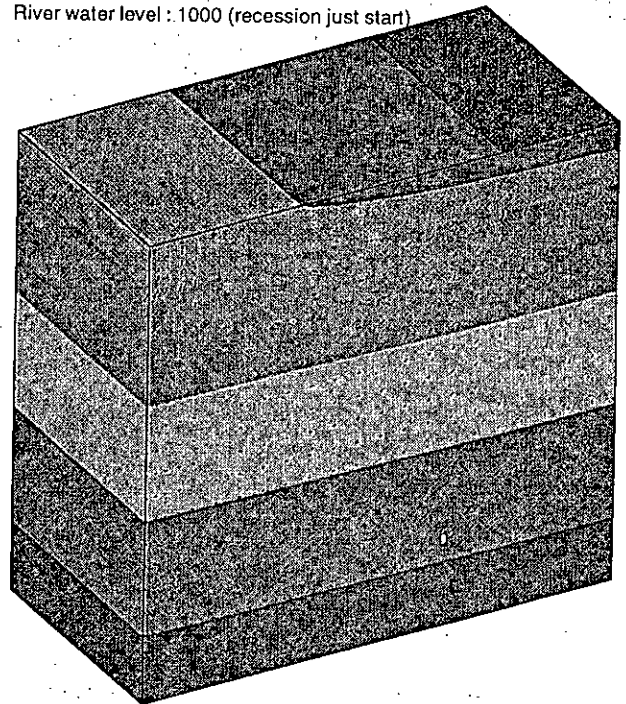
(d)

Fig 6.18 : (a) to (d) Vector plot on a two-dimensional xz-plane at different simulatation time

Simulation time : day 13
River water level : 500 (falling)

(e)
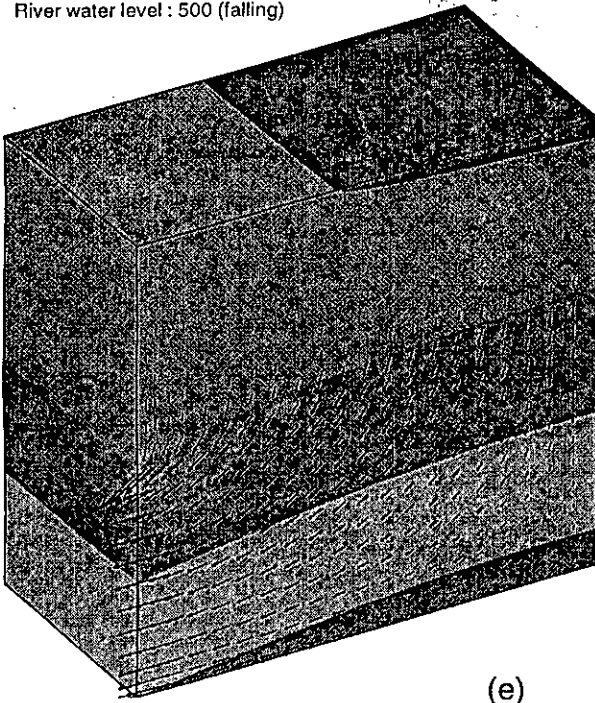
Simulation time : day 16
River water level : 200 (lowest after the flood)
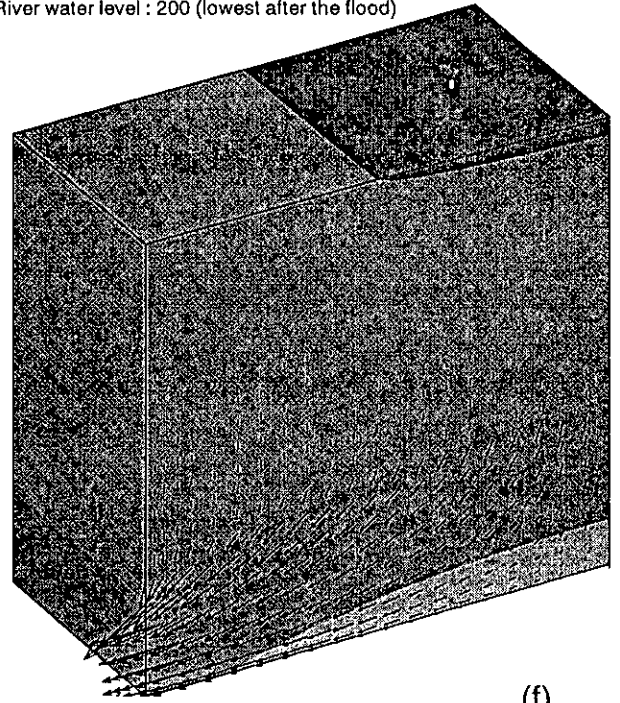
(f)

Simulation time : day 37
River water level : 200 (constant)

(g)
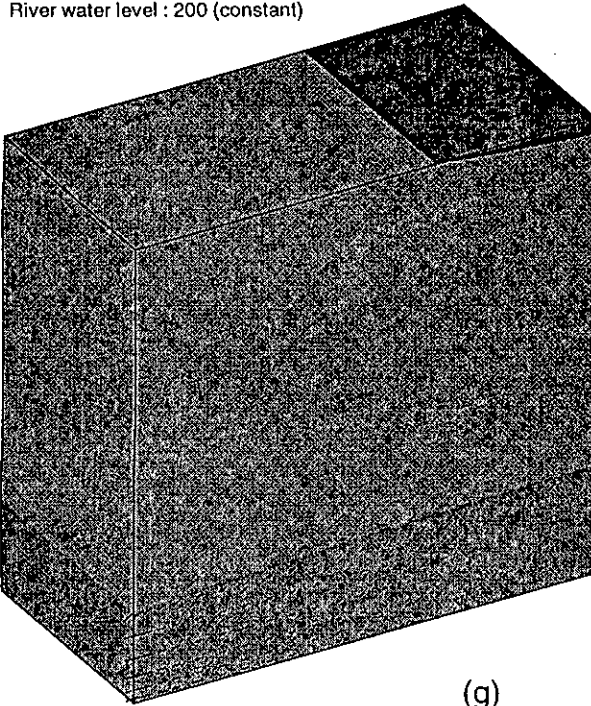
Simulation time : day 43
River water level : 500 (peak of 2nd flood)
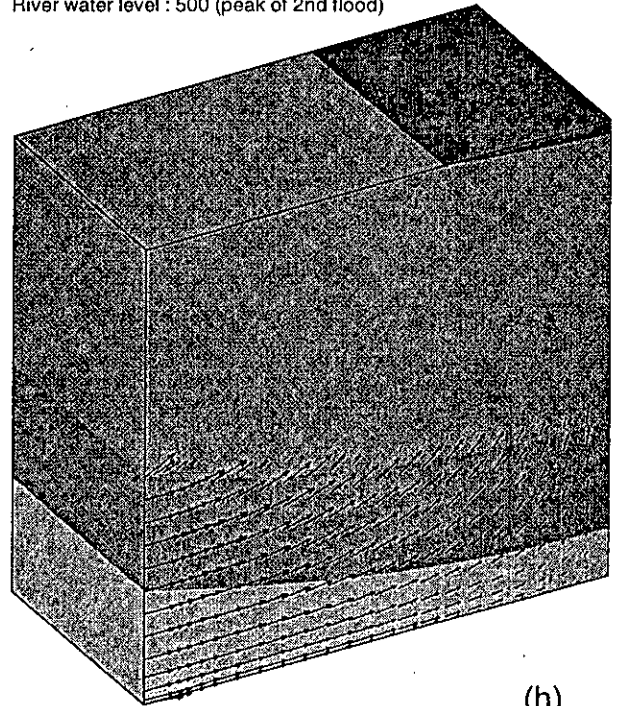
(h)

Fig 6.18 : (e) to (h) Vector plot on a two-dimensional xz-plane at different
simulatation time

94

In Fig. 6.16, the cumulative flows (inward or outward of the domain) are plotted against elapsed time. These show how the flow direction and magnitude vary with time under the influence of river water level fluctuation through the two saturated boundaries of the domain. Upto day 6, the steepening slope of the downward curve of cumulative flow through river side (solid line), shows increasing volume of inward (-ve value) flow to the domain when peak of the flood just reached. After that the curve turns slightly rightward indicating the inward flow decreasing although cumulative volume of water is changing to higher values upto day 9, when peak value is just going to recede. Then the curve directed upward showing outward flow from the domain. Here the cumulative curve shows steep upward trend followed by flatter slope indicating higher values of initial outward flow when drainage starts from almost all the domain. Flattening of the drainage portion of the curve starts at day 16 immediately after minimum water level is reached. Gradually the outward flow leads the curve to the positive side of the axis when cumulative outward flow superceeding cumulative inward flow approximately at day 25. This reducing drainage of the zone under low river water level continues upto day 40. With the second time rise of the water level, the processes described above repeats. The recharge of the domain starts with high value and reduces rapidly to a small amount as the maximum value of 5m is continued to the end of simulation. This fact is revealed by the upward convex curve followed by almost horizontal nature of the curve between day 40 to 60 with a negligible slope at the last segment which caused by the rapid saturation of the previously drained soil with the continued static water level in the river.

The nature of the cumulative base flow curve (dashed line in Fig. 6.16), is controlled by the average pressure head in the domain and the river water level (drainage Eq. 5.6). Just when the river water level is reached maximum to 10 m (day 6), then the base flow starts and increases rapidly during the peak flood period.. This flow reduces rapidly to zero after the two days of the recession starts (day 10). Out of these time durations, in the most of simulation period base flow is zero which is reflected in the horizontal portion of the curve because the pressure head of the domain is always less than the required maximum value (10m).

Figs. 6.17(a) to 6.17(l) present the groundwater pressure head contour; In these one can observe how the groundwater table (a contour of 0 cm pressure head) changes with the river water level, sloping off-river (to the right) in the period of rising river hydrograph and shortly after (2nd to 8th day and 41st to 43rd day), and to the river bank (to the left) in the periods when the hydrograph is falling for several days or constant at a low level (10th to 40th day). On 1st day, we observe an obvious static equilibrium with all contours horizontal. The contours in the saturated zone below groundwater table (labelled 200 to 700 cm) are at all time effectively parallel to the groundwater table at distances corresponding to their nominal values. This means that the vertical gradient of hydraulic head in the saturated zone differs little from the hydrostatic one (validity of the well-known Dupit-Forchheimer assumption of vertical equipotential lines in unconfined aquifers is thus demonstrated again). The contours in the unsaturated zone (marked as -200 to -500 cm) behave in a different manner. They become very near to each other in the period of rising groundwater table (especially after 4th day) and remain this relative position so during the whole simulation period. A thorough observaton may recognize that the contours -200 and -300 cm, being nearest to each other probably at the end of the 8th day (at the top of the flood), apart from each other more and more between 9th and 20th day. In the final period of simulation (40th to 43rd day), unsaturated contours are almost without movement, contour -200 being situated sensibly lower and contour -300 sensibly higher. This behavior of unsaturated contours demonstrates: (a) significant difference in time scale between saturated and unsaturated movement (the unsaturated movement being much slower), (b) the process of wetting continues to take place in the upper and right part of the flow region, even if the rectangle as a whole undergoes intensive drainage, (c) the lower part of the unsaturated zone undergoes drainage which is very slow even if hysteresis of the retention curve is not allowed for ; this rehabilitates the concept of field capacity.

The vectors of magnitude of Darcian flux for different time instants are given in Figs. 6.18(a) to 6.18(h). Having plotted the vector of Darcian flux, we can identify the zones of dangerous seepage pressure concentration which can, under certain conditions, lead to a landslide or a collapse of the river bank. There is obviously no flux in the static situation on 1st day   (Fig.6.18(a)). We can see that high fluxes occur in the period of rising hydrograph, beginning from 3rd day, especially in the vicinity of groundwater table and

slightly above it the vectors are of high magnitude (Fig. 6.18(b) and (c)). This can be explained by the need of unsaturated zone to the saturated before watertable can rise. Much water is needed for the saturation to be accomplished, and this water must be brought to the spot by both horizontal and vertical flux from the river and also the zone around groundwater table has the zone of maximum vertical flux. The intensive fluxes disappear during and just after the top flood when everything in the flow region is either saturated or at least wet enough (Fig.6.18(d)). It takes several days after the beginning of the recession phase before large fluxes appear (Fig.6.18(e)), again in the vicinity of groundwater table beginning from 12th day, later in the whole saturated profile near the river bank 13th to 17th day (Fig.6.18(e) and (f)). This phase of receding hydrogrpah ,from 12th to about 20th day, is most dangerous for stability of the river bank, even if there is no clear evidence for a saturated seepage face of non-negligible size above the river water level.

Flux have almost disappeared after a prolonged period of low water levels (37th day, Fig.6.18(g)) but the zone of high fluxes around groundwater table and, if the groundwater table is low, in the whole saturated part of the river bank, appears again during the new rising limb of the hydrograph (41st to 43rd day ; in Fig.6.18(h) for 43rd day) .

DHAKA CITY STRIP MODELING

6.5 Application of the Model to a Real Hydrogeological Situation (Dhaka City Strip Modeling)

6.5.1 General

A strip of Dhaka city along the bank of the river Burhiganga (Fig. 6.19) has been selected to verify the applicability and performance of the model. Under the specific types of hydrogeological situation along the river bank, continuous high abstractions with natural as well as urban recharges, thereof, the model will be executed with most of it's features. Beneath the selected area, the soil profile consists of about 10 meters of red-brown silty clay known as the Madhupur clay, which overlies brown sands and are fine-grained and silty at the top but becomes progressively coarser with depth. These sands belong to the Dupi Tila Formation, and are the main source of water withdrawn by deep tubewells in the area. The base of the aquifer is at about 120-150 meters below ground and there is no evidence of any other major aquifers in the upper 450 meters of the geological sequence. A vertical cross section through the domain (North-South) is shown in Fig. 6.19 which shows the different layers of the geological sequence.

In the Dhaka city, annual abstraction of groundwater by Dhaka WASA and other private and industrial units has risen continuously since the early 1960s to reach approximately 250 million cubic meters today. Almost 95% of this huge volume of water is drawn from the Dupi Tila Formation. Outside Dhaka city the aquifers are fully recharged each year, with groundwater levels returning their original levels a month or so before the end of the monsoon. But beneath Dhaka city, the situation is fully different ; here water levels in the aquifer have fallen steadily over the last 25 years in response to continually increasing abstraction and reached a maximum of over 20-25 meters in some areas. Near the river Burhiganga the water levels in the aquifers rise steeply towards the surface and water level of the river. But away from the river, the soil profile shows a separation in the water levels in the shallow clays, which shows no overall trend, and the levels in the underlying sands. The water levels in the boreholes indicate that the clays have remained saturated even through the sands at the top of the aquifer have been unsaturated for ten to fifteen years

98
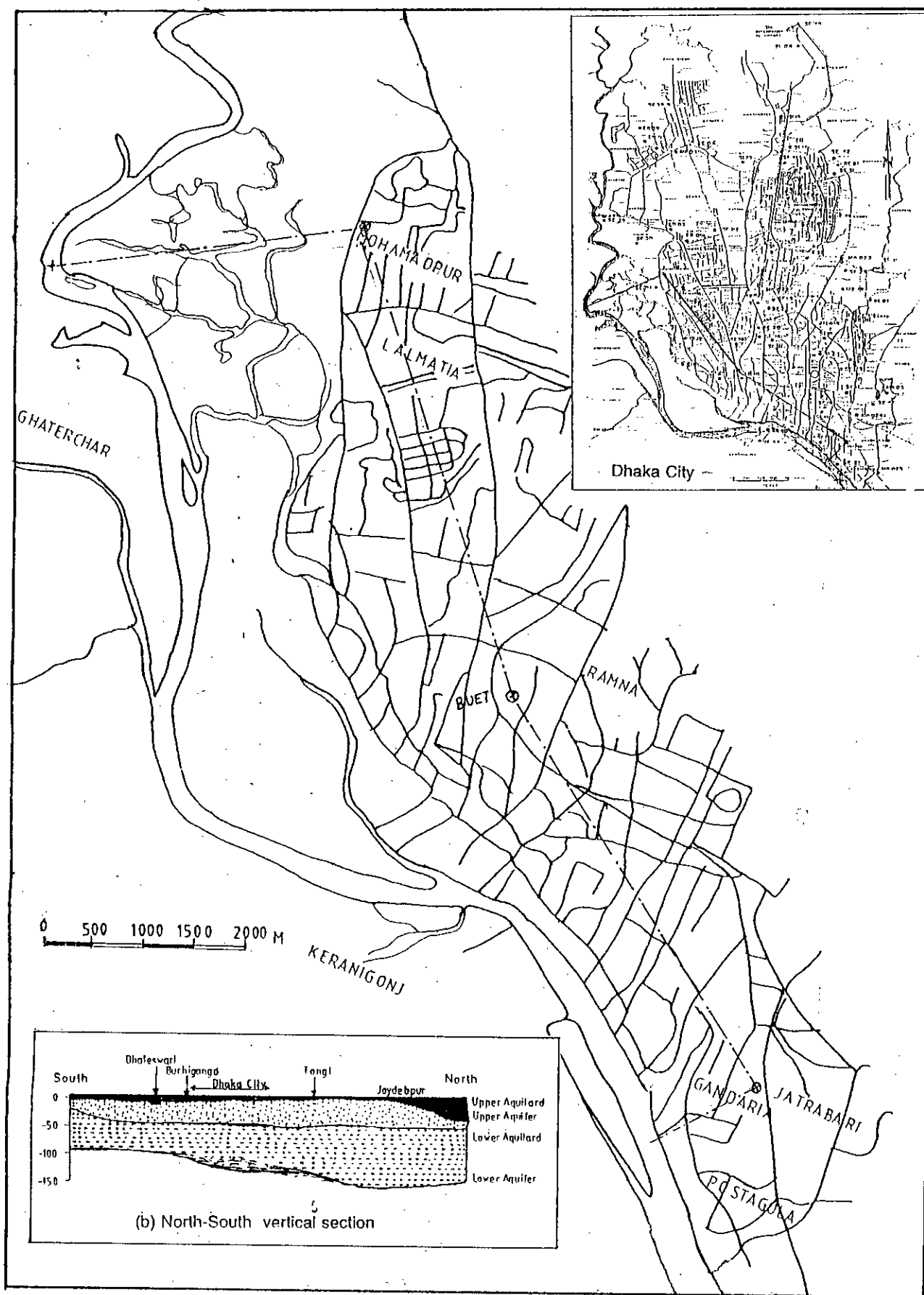
Fig. 6.19 : Dhaka city and the selected strip along Burhiganga river

99

(WASA, 1989). In this context, analysis of groundwater flow with respect to water balance and piezometric head declining trend in the selected area as stated above will be suitable for the model testing purpose as well it will highlight the overall concept of recharge by river and other mechanisms in the Dhaka city as a whole.

6.5.2 Description and Discretization of the Domain

The area selected for application of the model includes old Dhaka along the Burhiganga river bank and extend upstream of the river as shown in Fig. 6.19. The total surface area is approximately 28.4 km². Width of the domain is variable (1 km to 3 km) and length is approximately 9 km in straighline distance. The model flow domain is bounded by the River Burhiganga in the west side and the east or city side of the domain is an artificial boundary derived from the existing known observation piezometer network. The area chosen consists of variable surface elevation as high as 8.0 m PWD level to as low as 2.0 m PWD level.

The vertical extent of the domain includes four layers. The upper aquitard, which is composed of low permeable clays and silts, overlies the upper aquifer and is present in all of the area modeled. This layer extends from the ground surface to when the percentage of silt and clay is less than 50 percent. Below this is the upper aquifer of fine to medium fine sands and is present in all of the modeled area. Abstraction from this aquifer is by shallow tubewells and deep tubewells. The next layer is the lower aquitard that separate the lower aquifer from the upper aquifer . The lower aquifer is the main aquifer consisting mainly of medium to coarse sands, from which water is abstracted by deep tubewells for both industrial and municipal water supply. These layers of the domain are shown in Fig. 6.20 with established coordinate system. Due to the scale effect, surface undulation (upto 6 m) are not explicit in the figure with respect to the total depth of the soil profile (upto 160 meters).

For the finite element representation of the domain (Fig. 6.21), the surface area is divided into four strips along the longitudinal direction and 10 strips along the transverse direction. Due to abrupt change of the hydraulic properties of the soil layers, the vertical discretization is made fine enough. This also helps in the proper simulation of the near
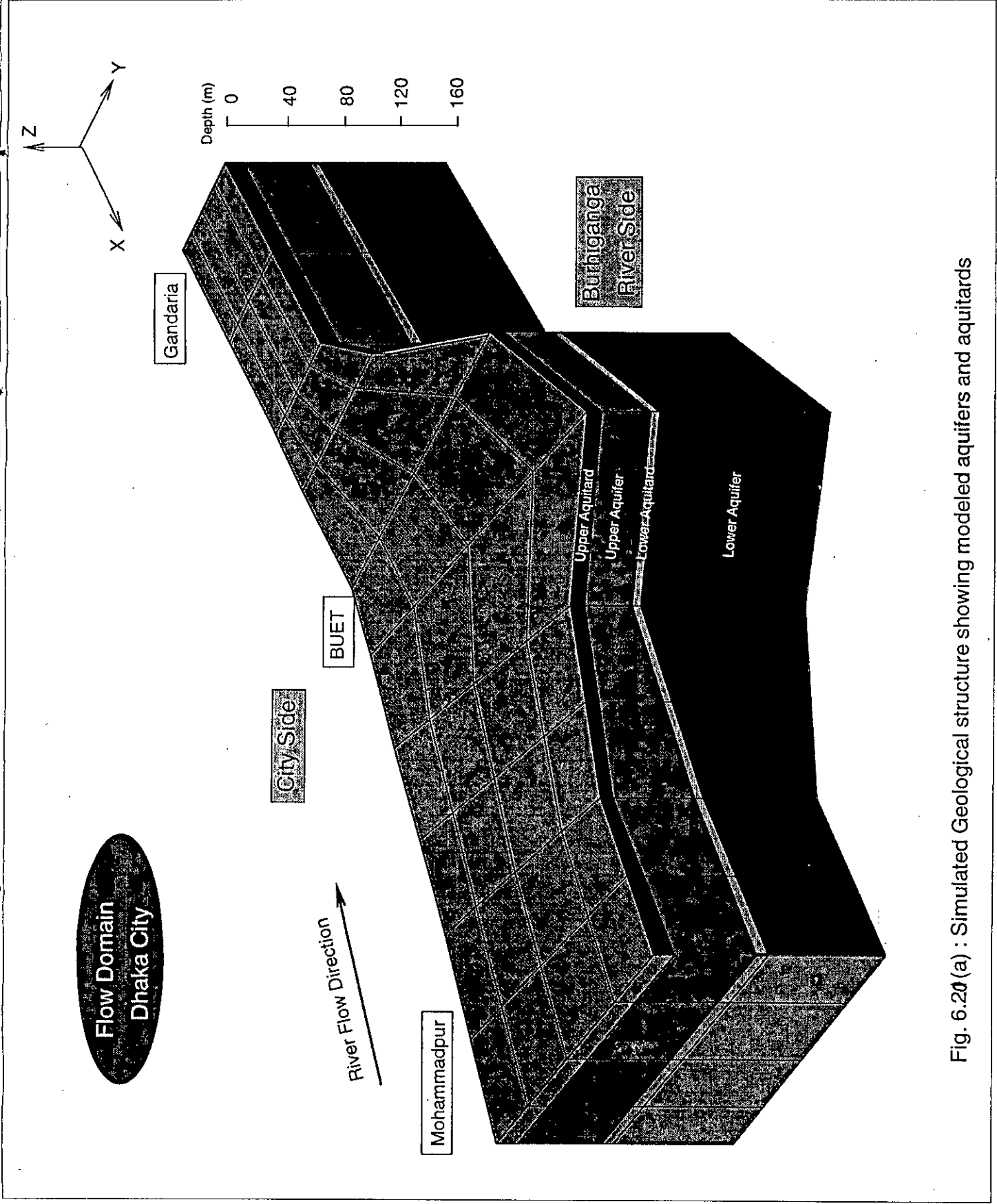
Fig. 6.20(a) : Simulated Geological structure showing modeled aquifers and aquitards
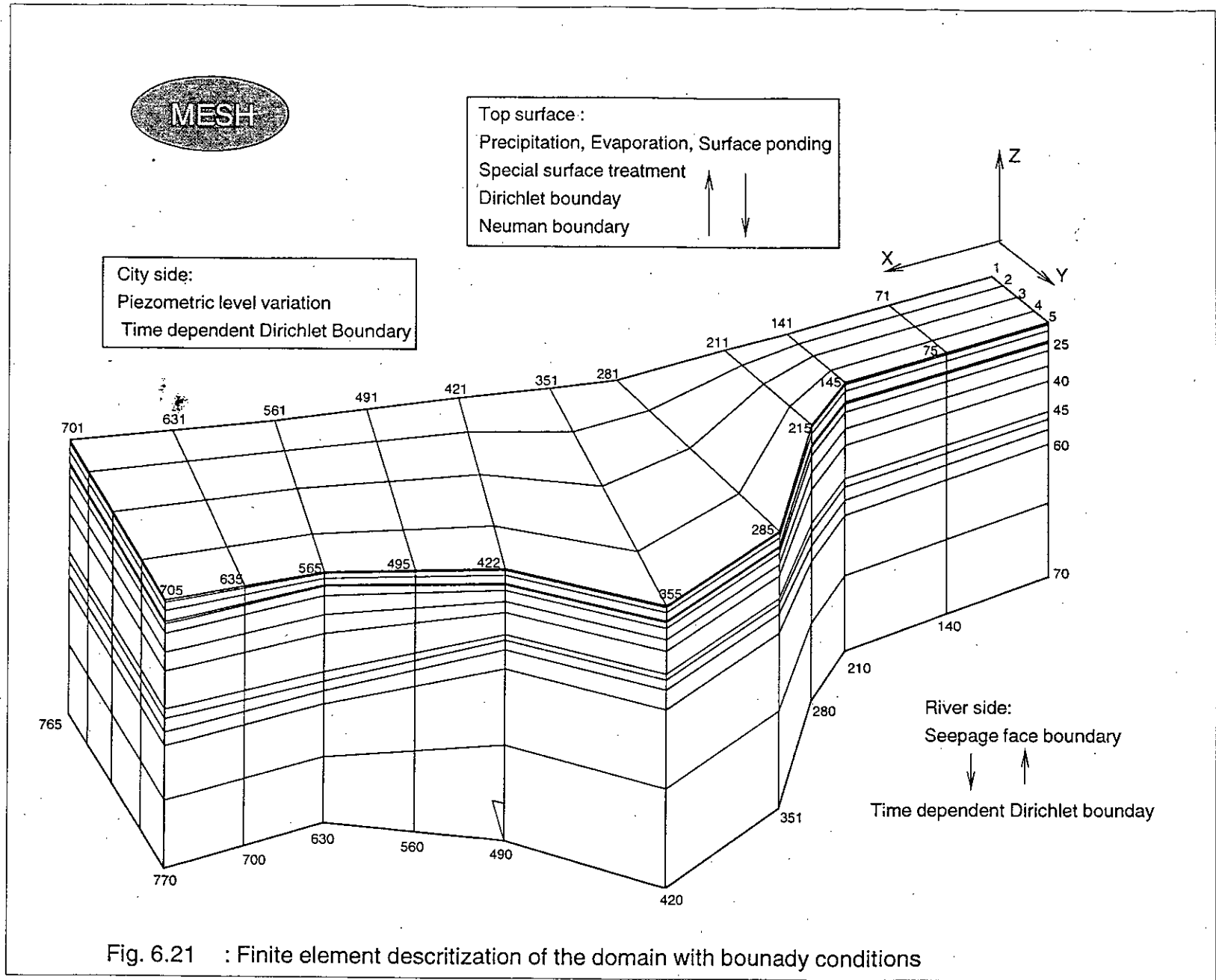
Fig. 6.21 : Finite element descritization of the domain with bounady conditions

surface and atmospheric occurrences. Total number of segments in vertical direction is 13 of varying thickness. The upper aquitard and upper aquifer are discretized into four and five sublayers respectively. The lower aquitard being of smaller thickness simulated as one single layer. The lower aquifer is divided into three sublayers. All these discretizations are performed with MESH program with minimum number of input data of geometry of the aquifer and the generated mesh is shown in Fig. 6.21. The total number of brick elements is 520 and nodes is 770. In the main program, these brick elements are internally subdivided into tetrahedral elements to give rise proper discretization of the domain.

6.5.3 Model Boundaries

The river side of the flow domain (west boundary) is bounded by the vertical plane passing through the axis of the river. In the city side abstraction is enormously higher than the opposite side of the river. So obviously a high gradient towards the city from the opposite side of the river prevails. It is assumed that the river is hydraulically connected with the soil layers below it's bed. Thus a time dependent Dirichlet boundary condition is imposed in this side of the flow domain. This condition prevails upto the river water level along this boundary face. The nodes above river water level are the potential seepage face nodes as discussed and demonstrated in Example 6.4. As the water level vary with time, the extent of this potential seepage face is also changed. In each time level, the river hydrograph input data is adjusted and the actual saturated ($\psi=0$) or unsaturated ($q=0$) seepage face nodes are identified by iteration, as described in Section 5.3.4.

The bottom of the domain rests on an impermeable base. So a no flow boundary ($q=0$) condition is imposed in each node of this face. Problem is faced when attempt is made to select the off-river vertical boundary of the flow domain (city side). There is no distinct natural boundary along this face. So an artificial time dependent Dirichlet boundary condition is imposed based on the observation wells' data and their interpolation values in the intermediate nodes. As long as this simulation for analysis of the model behavior contains calibration for estimating proportionality of the different flow components of the region, this kind of boundary does not create any problem. But when the program is required to run in

predictive mode then this boundary should be replaced by natural boundary away from the existing one.

The upper surface of the domain is the atmospheric boundary as described in Section 5.3.4.1. But here needs some real considerations. The surface of the selected area consists of different elevation with low land (Kamrangir Char, PWD level 2 m) and high land (with PWD level 8 m), there is frequent flooding or submergence in some parts by internal or external flood water. With the construction of the Dhaka flood protection embankment, this situation has changed especially in case of external water flooding or spilling from river. On the contrary, the densely populated old city portion is mostly of paved area which reduces natural replenishment. To simulate the near surface boundary phenomena properly, the paved and unpaved area and the submergence conditions of the different portions of the area should be known properly. But in the present work, the case is simplified by considering that the rainfall is not allowed to flow out of the area by overland flow but this is kept as average surface ponding over the area for certain time if rainfall is of such intensity to make surface ponding. Other boundaries of the model are kept no flow boundaries. The internal boundary nodes are specified explicitly as Neuman boundary under the condition of abstraction nodes of the aquifers and for urban recharge.

6.5.4 Data Preparation and Parameter Fitting

Data required for the present simulation includes :

(a) data defining the geometry of the aquifer system (e.g., average surface elevation, elevation of the base of each simulated layer)

(b) geometry of the model grid network which are generated by the MESH program.

(c) data defining the hydrogeological characteristics of the aquifer system (e.g., saturated hydraulic conductivity, unsaturated characteristic curves and storage coefficients for each layer).

104
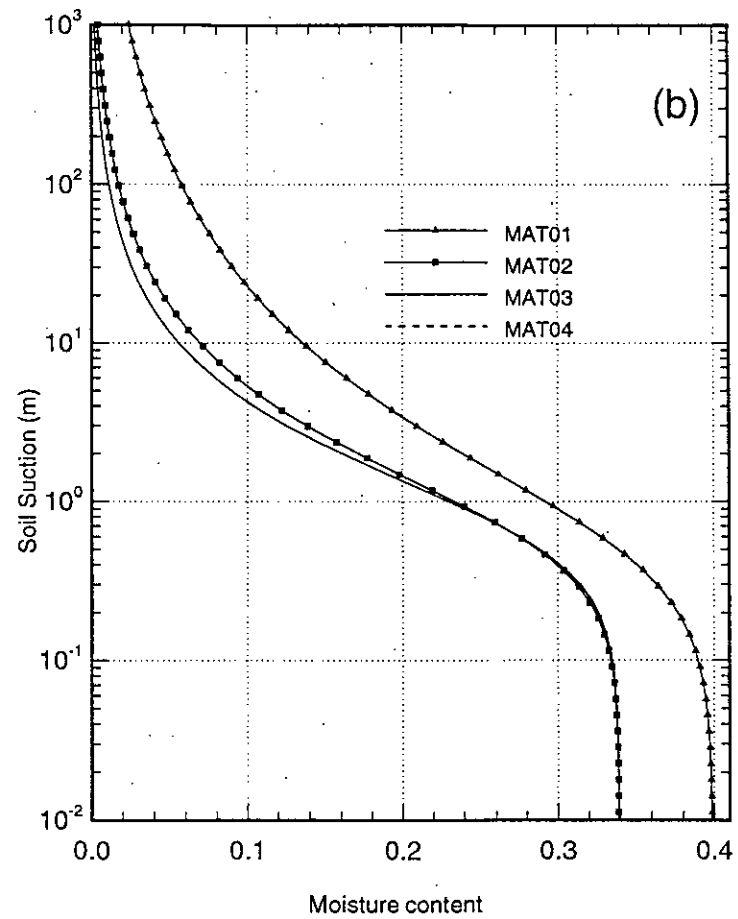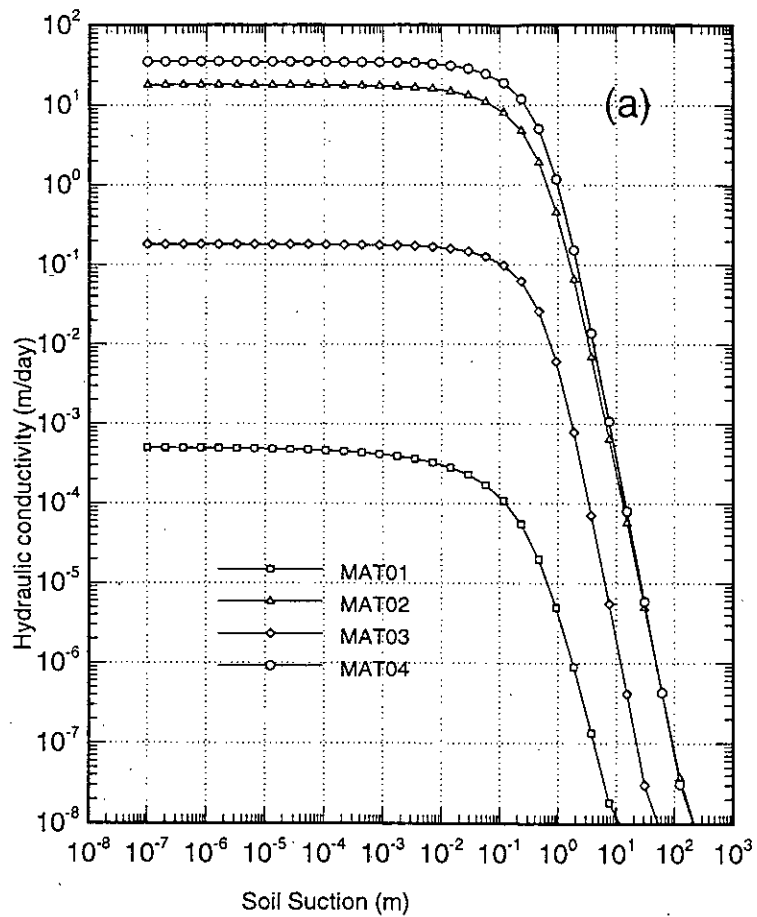
Fig. 6.22 : Plot of soil characteristic functions: (a) Hydraulic conductivity ; (b) Soil moisture retention
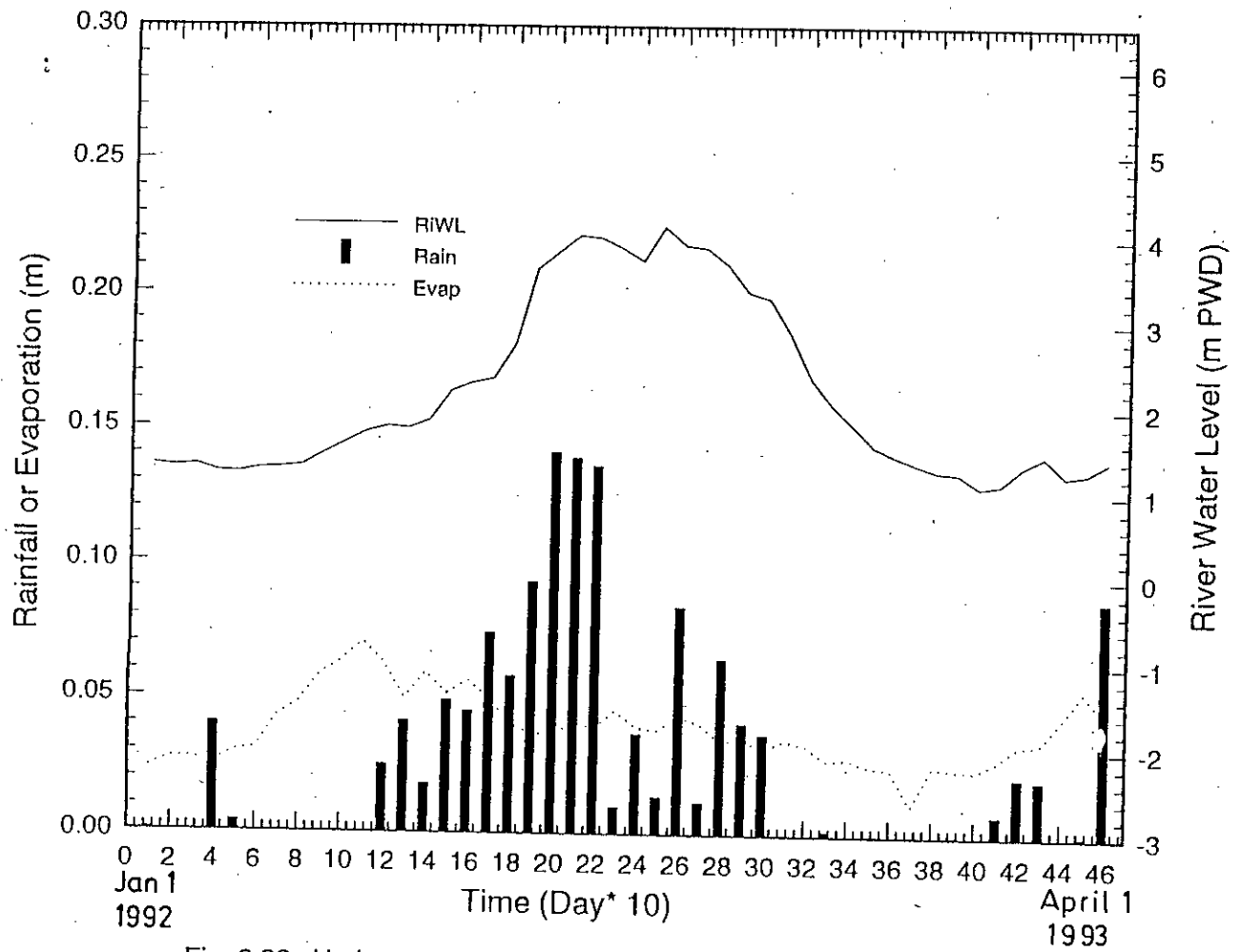
Fig. 6.23 : Hydrometeorological input data for the selected period
(Precipitation, Evaporation and River water level)

(d) data related to the boundary conditions (e.g., for river side river hydrograph ; for off-river side, known piezometric data of the observation wells ; for the atmospheric face, precipitation, evaporation, extent of root zone (if exists) etc. are required).

(e) data related to the aquifer system excitations (e.g., abstraction of water by WASA and private wells, return flow from the municipal water supply).

The hydrogeological data are collected from the Dhaka WASA. They have defined the saturated hydraulic conductivity of different zones of Dhaka region. The hydraulic conductivities of the aquifers are inferred from a correlation between the results of pumping tests and lithological profiles. Storage coefficients are also determined from pumping tests. To take into account the uncertainty related to some of these parameters, wherever possible, data are averaged over conveniently small areas. The vertical permeabilities are derived from the horizontal permeabilities by assigning (K_h/K_v) a single value of anisotropy for each layer. Based on the mean anisotropic ratio evaluated by BGS (1989), ratios of 1.5 and 2.5 for the upper and lower aquifers, respectively, are adopted. But in the present study, for the strip near the river where lateral flow and vertical flows are assumed to be equally dominant ,the anisotropy value is taken to be one.

For the characterization of the unsaturated soil behavior, one of the characteristic functions which are described in Section 4.2, should be used. Here the van Genuchten's equations modified by Vogel and Cislerova (1988) is selected. The parameters related with this are θ_r ,θ_s , θ_a, θ_m ,θ_k, α, n, K_k ,K_S , which are defined in Section 4.2.1. For accurate characterization , a set of field data is required for moisture content, soil water suction and unsaturated hydraulic conductivity. These are then fitted to the relations of Eqs. 4.3 to 4.5. But in the present study, due to some limitations, collection of such type of field data are not possible and a set of arbitrary fitting parameters are taken. A plot of these characteristic functions are shown in Fig. 6.22.

Atmospheric data (mean daily precipitation and evaporation) and river water level data are collected from SWMC. The piezometric and abstraction data for the area are collected from WASA. Table 6.5 shows the annual abstractions of the production wells of Dhaka

WASA under the selected area. Two separate programs have been developed to check these data to feed the program in the specified time interval and specified format. These data are shown in Fig. 6.23.

Table 6.5 : Annual Abstraction of Pumping Wells in the Simulated Area

Well Nr.	Well Name/Location	Abstraction MCM per year
DW1/19	Farashgonj	1.53
DW1/18	Lakhsmibazar(WASA)	0.95
DW2/17	Simpson Road	1.31
DW2/15	Jagannath College	0.715
DW2/16	Mitford Hospital	1.08
DW2/22	Armanitola Math	1.06
DW2/20	S.D. Park	1.23
DW2/13	Abul Hasnat Road	0.98
--------	Islambag	1.00
DW2/2	Dhaka Water Works	1.32
DW2/3	Bakshibazar	0.79
DW2/1	Dhakeshwari(WASA)	1.22
DW2/4	Rahmatullah High School	1.36
DW2/7	Azimpur Nr. 7 (Near OHT)	1.20
------	Rajnarayan Road	0.90
DW2/5	Nawabganj	0.97
DW2/8	Peel Khana Nr. 2	1.08
DW2/6	Ajimpur Nr. 6	0.93
-----	B.D.R	1.00
DW2/10	Hazaribag Nr. 4	1.20
------	Hazaribagh (Lather Tech.)	1.00
DW3/11	Laboratory School	1.40
DW2/11	Hazaribag Nr. 3	1.42
DW3/15	Jhikatola	1.11
DW3/16	Rayer Bazar PWD	1.38
-----	Rayer Bazar	1.00
DW3/17	Dhanmondi Nr. 8	1.52
DW3/21	Rayer Bazar (Sultangonj)	1.37
DW3/7	Lalmatia Nr. 2 (SOHT)	1.91
DW3/6	Lalmatia Nr. 4	1.33
DW3/5	Nazrul Islam Rd. Md. Pur	1.69

(---) well nos. are not known

Other private wells in the area :

BUET   :   3 wells @ 750 m^3/day

Hazaribag :   Total 6000-12000 m^3/day

6.5.5 Calibration of the Model

After the numerical setup, to simulate a physical system, calibration or identification of a model is the most important phase in which the various model parameters are determined. Uncertainties arise through a lack of data, imprecision of data and the extrapolation of data defined on the local scale to the larger scale of the model. Through the calibration process, adjustments may be made to the model parameters in order to create a closer agreement between the model's response and a known real flow system. But an important note here is that, this inverse problem of calibration does not yield an unique solution and different set of parameters may result same kind of responses depending on the method used. Also to reduce the noise introduced in the model because of the various assumptions which underlie the passage from the real system to the model one to an acceptable limit , it is generally recommended that the model should be constructed to simulate the considered aquifer as close as possible and to use as much data as is available for its calibration.

Although there exists sophisticated probabilistic or optimistic calibration procedure, the frequently used method are performed by the traditional trial-and-error processes of deterministic model calibration. A detail calibration may be done from historic data by steady state and transient state flow under consideration. Due to the fact that the stable pressure head distribution in three-dimensional region is not easy to represent in the model from the limited number of field data, the steady state calibration can be used to set up stable initial condition for the transient simulation.

In the present study due to lack of time and data, no rigorous calibration method followed. Inside the selected area there is only one observation well at Lalbag. The piezometric levels observed in this well has been used for calibration. Due to the lack of sufficient observation data in the zone, more importance is given to the sensitivity analysis of the calibrated parameters and the related responses.

During the calibration, first step is to determine which parameters most strongly control the drawdown pattern in the area. From the existing piezometry and hydrogeological conditions, it is revealed that drawdown in the main aquifer increases towards the center of the city and at a lower value near the river. Water table is still higher in the other side of the Burhiganga river which mostly penetrate partially in the upper aquitard. Also the piezometric level fluctuation near the river has similarity with the river water level fluctuation and this diminishes rapidly away from the river towards the city. The conclusion may be drawn that the river Burhiganga is hydraulically connected to the underlying aquifer system and the lateral flow towards the city is also fed by the high water level of the off-city side of the river. This lateral flow is controlled by the aquifer horizontal hydraulic conductivity. Other way of aquifer recharge is by the direct vertical transfer of water through the surface from the precipitation and subsequent ponding in lower areas . But this vertical transfer of the water is mostly controlled by the hydraulic conductivity of the upper aquitard. So the hydraulic conductivities of the upper aquitard and aquifers constitute major calibration parameters. Another important point is that most part of the upper aquitard beneath the area is saturated throughout the year with water table in the dugwell showing few meters below surface although piezometric levels in the aquifer fall below the base of the aquitard. The saturation of the soil in the upper aquitard is mainly due to the return flow from the urban water used (both domestic and industrial). This causes a continuous leakage of water from the upper layer. Correct assessment of this urban recharge is tough which is generally for the different cities in the world in the range of 10 percent to 40 percent of the total volume of water used. So urban recharge is taken one of the important calibration parameters. Other calibration parameters that may control the drawdown of the piezometric levels of the aquifers under the existing heavy pumpings are the storage coefficients of the aquifers. These are also considered within their confidence range. From data analysis, the acceptable range of values for the main calibration parameters are shown in Table 6.6 .

Calibration parameters	Confidence Range
Hyd. conductivity of upper aquitard	0.0001 to 0.005 m/day
Hyd. conductivity of upper aquifer	9.0 to 18.0 m/day
Hyd. conductivity of lower aquitard	0.05 to 0.01 m/day
Hyd. conductivity of main aquifer	25.0 to 35.0 m/day
Urban Recharge	10% to 40%
Storage coefficient of upper aquifer	0.0001 to 0.0004
Storage coefficient of the main aquifer	0.0003 to 0.0008

Calibration Results:

With a set of values of parameters the program has run repetitively in the trial-and-error approach. A period of time from 1st January, 1992 to 1st April, 1993 is selected for the calibration run. The purpose is to simulate a year round flow pattern (from January to December or April to March) of the zone. Initially a time step value of 10 days with a total 46 time steps are selected to run the program. In each run, the simulated piezometric level variation of the observation well position is plotted to check the observed values for the time period. A total of twelve model runs are made before the simulated piezometry matched the observed piezometry. Due to the lack of availability of observed data, as stated earlier, it is not possible to check the piezometric head contours of the total area. After a matching set of parameters has been found on the 10 day basis run, the same parameter values are used to run the model with daily data having a total of 460 time steps. Now the solution converges rapidly than the previous case. This is due to the fact that the input data (for precipitation, evaporation) on 10 day basis are of high value and enters in the calculation as a high impact which is largely reduced on the daily basis data. Finally, the outputs from 10 day basis and

CALIBRATION RUN
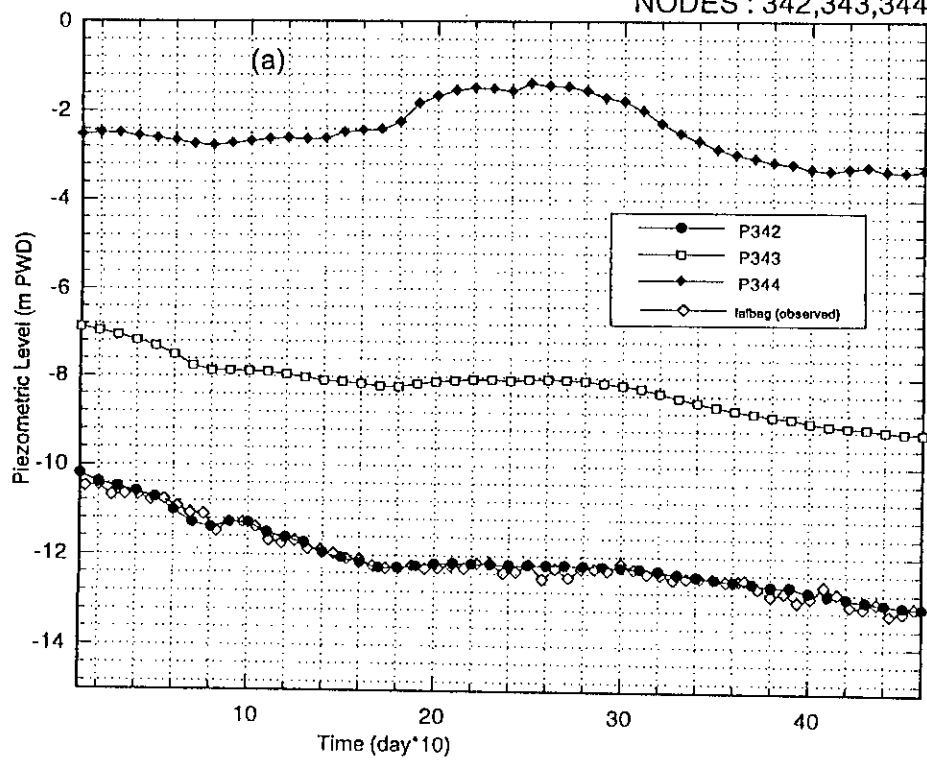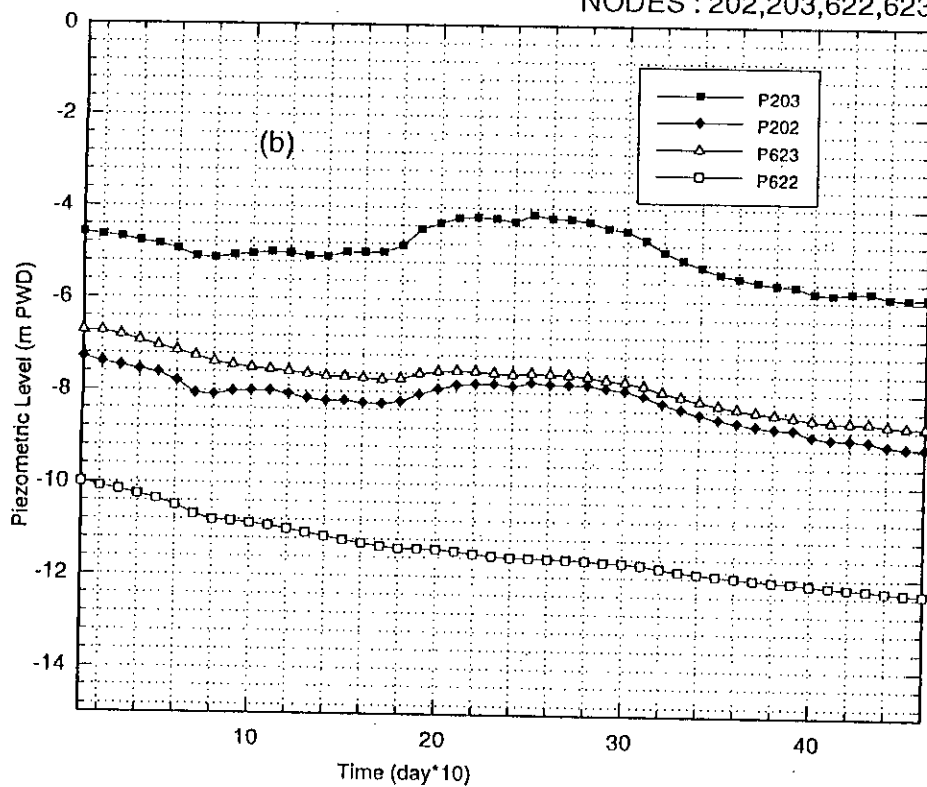
Fig 6.24 :(a) Simulated piezometric head with observed values at Lalbag
(b) Piezometric head profiles at other selected nodes

daily basis simulation are checked against observed piezometry and found no significant difference between the results of daily basis and 10 day basis simulations. To save time the subsequent runs are performed on 10 day basis data. The parameters selected from the final calibration run are shown in Table 6.7.

Table 6.7 : Calibrated Values of the Parameters

Parameters	Calibrated Values
Hyd. conductivity of upper aquitard	0.0005 m/day
Hyd. conductivity of upper aquifer	15.0 m/day
Hyd. conductivity of lower aquitard	0.02 m/day
Hyd. conductivity of main aquifer	27.0 m/day
Urban Recharge	30%
Storage coefficient of upper aquifer	0.0003
Storage coefficient of the main aquifer	0.0006

In Fig. 6.24(a) the piezometric head near BUET and Lalbag areas (node nos. 342,343,344) are presented. In the initial few time steps the results show some deviation. This is mainly because of some discrepancy in initial condition setting in the internal nodes due to lack of sufficient observation wells in the simulated area. Subsequently after few time steps, this inconsistency diminishes rapidly to have a balanced condition of pressure head distribution in the domain. In Fig. 6.24(b) simulated piezometry of some other locations are shown. From these (Figs. 6.24), it is clear that in a certain x (the established coordinate system for simulation, Fig.6.21) , if we go towards the river (e.g., from node 342 to 343 to 344 etc.), the piezometric levels are at higher levels showing higher gradients towards the city. At the nodes near the river (e.g., node 202,203 etc.) the piezometric levels fall and rise

113

almost with the river water level but this tendency reduces rapidly away from the river (e.g. node 622, 342 etc). This supports the fact that the river effect on the annual piezometric level fluctuation is upto approximately 3 km away from the river (the node 342 is approximately 2.5 km from the river). From the shapes of the curves it is seen that the declining trend with time of the piezometers away from the river are rapid with maximum piezometric level fall in the most remote nodes at a value between 0.8 and 1.2m.

After fulfilling the calibration requirement the water balance of the domain is shown in Table 6.8 for time period March, 1992 to next year end of February 1993.

Table 6.8 : Different Components of Flow Balance

Components	Volume (m³)
Abstraction	41.62×10^6
Top surface (Atmospheric face)	$*4.06 \times 10^6$(cumulative outward)
	2.47×10^6 (cumulative inward)
Difference of flow between river side and city side (net inward)	25.55×10^6
Return flow from water supply	12.84×10^6
Storage reduction in upper aquifer	5.20×10^6
Seepage face	0.60×10^6

* value indicates loss of water from the surface when no ponding of water on the surface exists
i.e., evaporation loss from ponding water instantaneously after heavy precipitation is excluded.

From the above water balance, it is seen that the abstraction of water is mainly compensated in the domain by the boundary flow from the riverside which is reflected in the third item in the Table 6.8. But it should be clear here that this volume of water is not only contributed from the river itself but from the high water table of the surrounding area (from

the other side of the river) also. The volume of water entered to the soil domain from the direct precipitation is only 5.92 percent of the abstraction volume but later from sensitivity analysis it is found that this volume does not instantaneously contribute to the aquifer storage and consequently this has less direct effect on the piezometric head decline of the zone. Most part of the precipitation gets evaporated and lost by surface runoff due to the low hydraulic conductivity of the upper aquifer. Another important reason for less direct contribution from rainwater is that the maximum part of the upper layer below surface remains in saturated condition by urban leakage throughout the simulation time so that downward hydraulic gradient becomes very small.

The storage reduction volume shown in the table are of the total moisture volume both in the saturated and unsaturated zone. The storage volume of upper layer vary with the surface or atmospheric events, i.e., evaporation and precipitation and also by river water level. But the storage of the main aquifer does not change with time indicating full saturation at all the simulation time. It is the upper aquifer which is subjected to storage change with the lowering of the piezometric level. In the time period mentioned, the storage volume reduced is given in the table. This volume is 1.79 percent of the initial storage volume of the upper aquifer and 0.53 percent of the initial storage of the total domain. When compared to the abstraction volume of the area, this reduction is 12.46 percent of the total abstraction volume.

6.5.6 Sensitivity Analysis

After the calibration of the model, sensitivity analysis of the parameters are performed by the simple perturbation method. The purpose is to define the poorly calibrated parameters to their realistic confidence limit and analyze the variation or sensitivity of the output to the variation of the parameters. It helps to identify the most important parameter or parameters which have relatively greater effect on the behavior of the simulated hydrogeological system. In the sensitivity analysis the model is run sequentially by perturbing one parameter setting

its value to the highest or lowest value while the other parameters in the same run are kept constant. Then the simulated piezometric head profiles are compared with those of the calibrated output. A total of 13 sensitivity runs are carried out and the ranges of the parameter tested is shown in Table 6.9.

Table 6.9: Sensitivity Runs and Perturbed Parameter Values

Run No.	Parameters	Lower Value	Upper Value
SR01 and SR02	Hydraulic Conductivity of Upper aquitard	.0001 m/day	.001 m/day
SR03 and SR04	Hydraulic conductivities of upper and lower aquifers	Upper aquifer: 10 m/day Lower aquifer: 20 m/day	18 m/day 35 m/day
SR05 and SR06	Storage coefficient of upper aquifer	0.0003	0.05
SR07 and SR08	Storage coefficient of lower aquifer	0.0003	0.0008
SR09 and SR10	Return flow	10%	40%
SER11	Precipitation is made zero throughout the simulation period		
SER12	River water level is reduced by 1.5 m throughout the simulation period		
SER13	River water level is kept constant at low level (1.2 m PWD) throughout		

Sensitivity Analysis Results:

The piezometric head profiles from different sensitivity runs are plotted in Figs. 6.25(a) to 6.25(e) for some selected nodes. In these figures, each box contains simulated piezometric head profiles of two nodes; the upper one is nearer the river than the lower curve. Same nodes are used for each parameter with same scale of the axes so that from the

116

Fig 6.25(a): Simulated Piezometric Head showing sensitivity of upper aquitard
hydraulic conductivity at different nodes

Fig. 6.25(b) : Simulated Piezomtric head showing sensitivity of
hydraulic conductivities of aquifers

Sensitivity Analysis : Run-SR05 & SR06

Parameter : Storage Coefficient (Upper Aquifer)

GANDARIA/J.COLLEGE (Node : 202,203)

Note :

$S_y = 0.0003$
(-..- lines)
$S_y = 0.05$
(--- lines)
$S_y = 0.003$
(symbols ; calibrated)
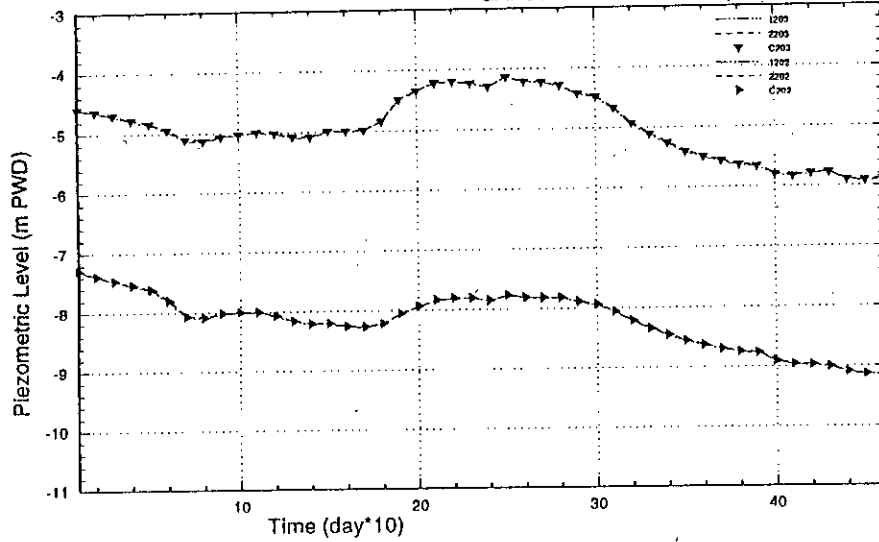
BUET/LALBAG (Node : 342,343)
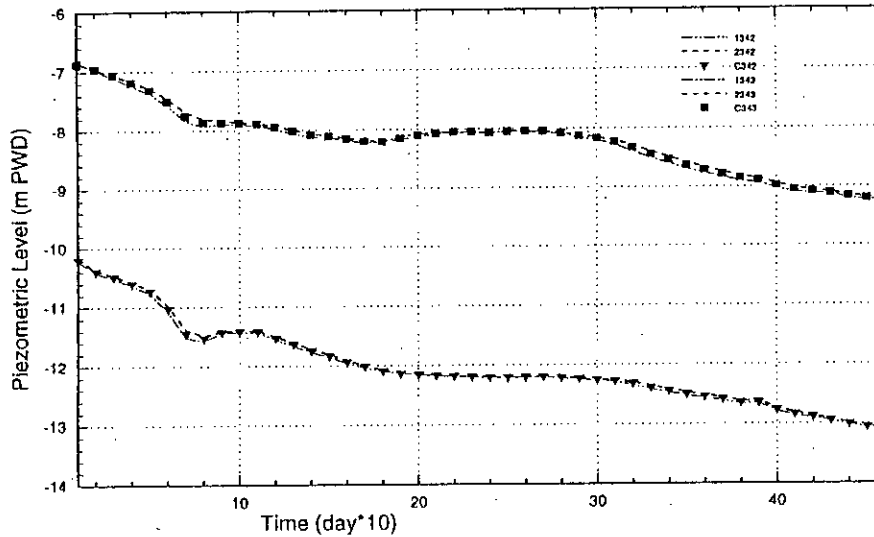
$S_y = 0.0003$
(-..- lines)
$S_s = 0.05$
(--- lines)
$S_y = 0.003$
(symbols ; calibrated)

HAZARIBAG/M.PUR (Node : 622,623)
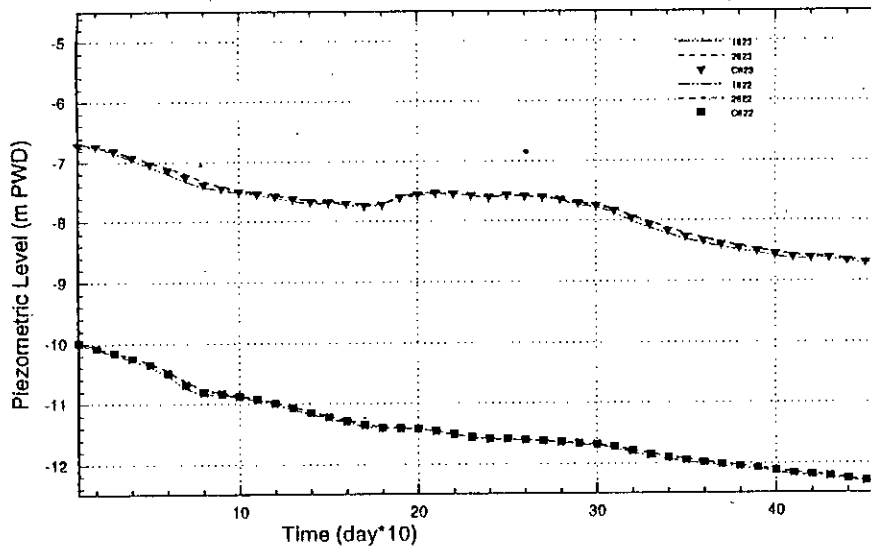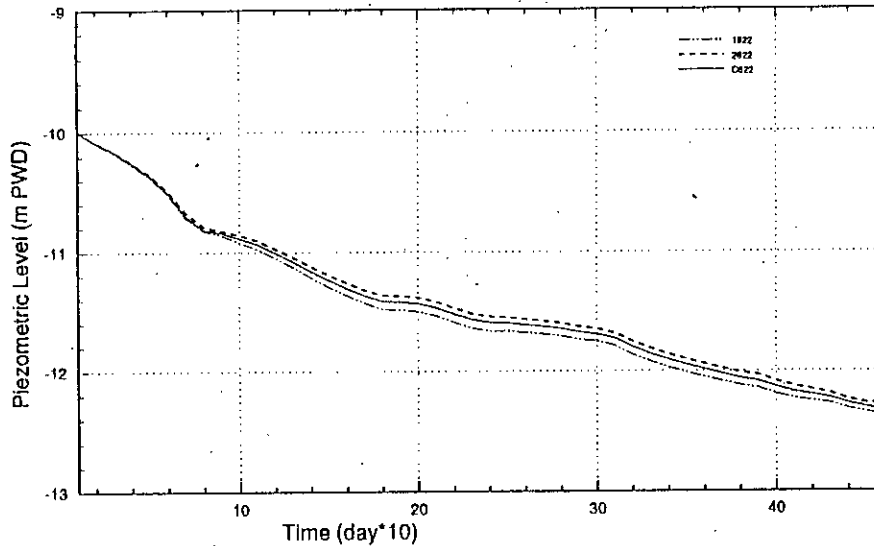
$S_y = 0.0003$
(-..- lines)
$S_s = 0.05$
(--- lines)
$S_y = 0.003$
(symbols ; calibrated)

Fig 6.25(c): Simulated Piezometric Head showing sensitivity of Storage Coefficient

Fig.6.25(d): Simulated Piezometric Head showing sensitivity of storage coefficient

Fig 6.25(e): Simulated Piezometric Head showing sensitivity of urban recharge
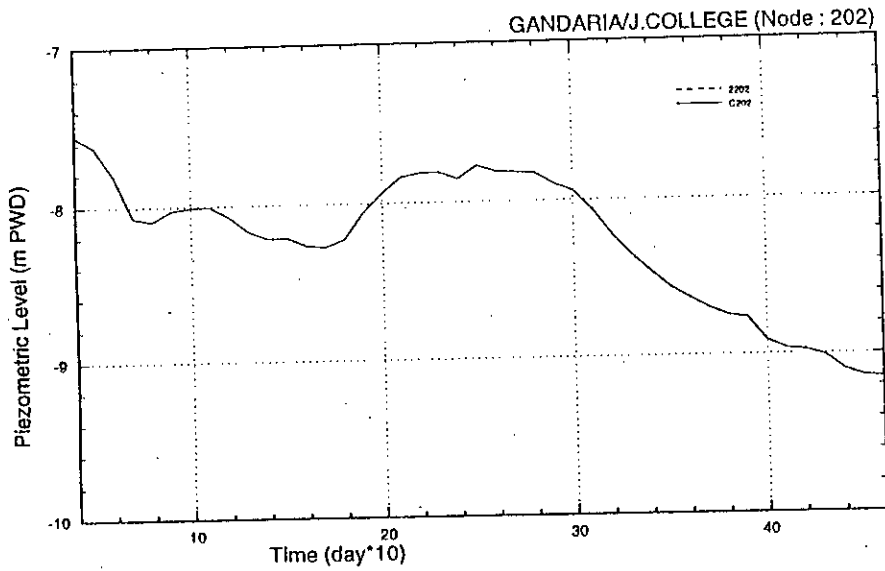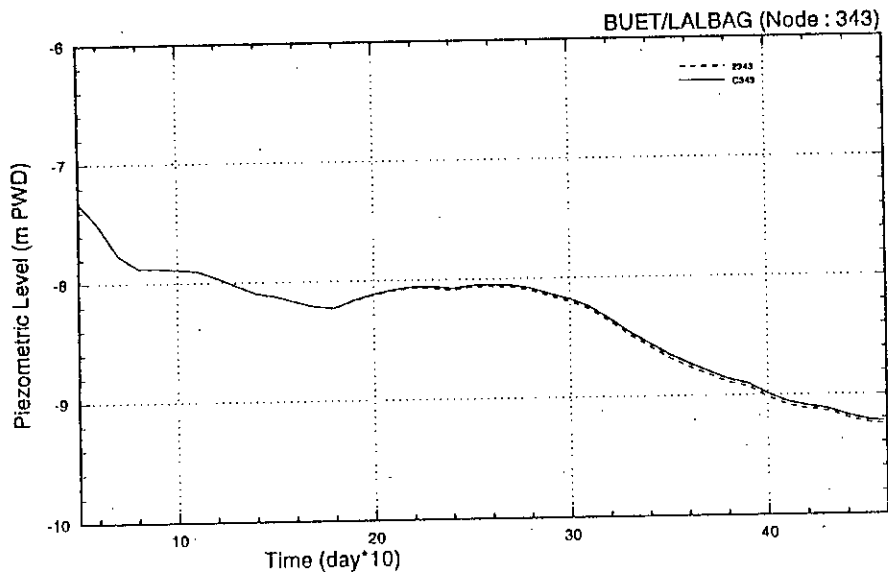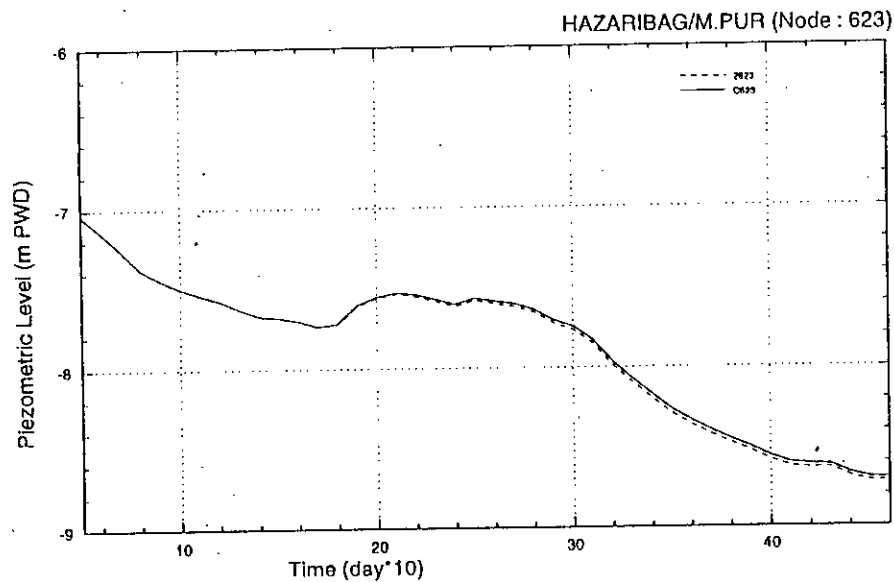
Fig. 6.26 : Simulated Piezometric Head with and without precipitation showing
negligible effect of the rainfall in the piezometric head declining pattern in the area
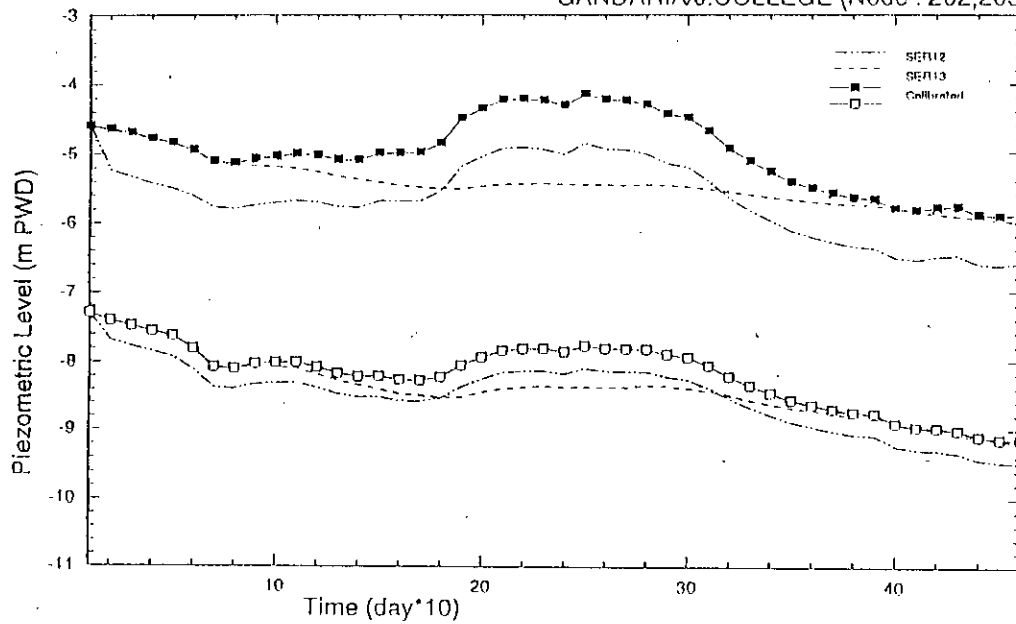
GANDARIA/J.COLLEGE (Node : 202,203)

Note:

SER12 showing water level reduction 1.5 m throughout the simulation time (- .-)

SER13 showing a constant water level of 1.2 m in the river excluding the monsoon rise in river (---)

Symbols : Calibrated

BUET/LALBAG (Node : 342,343)
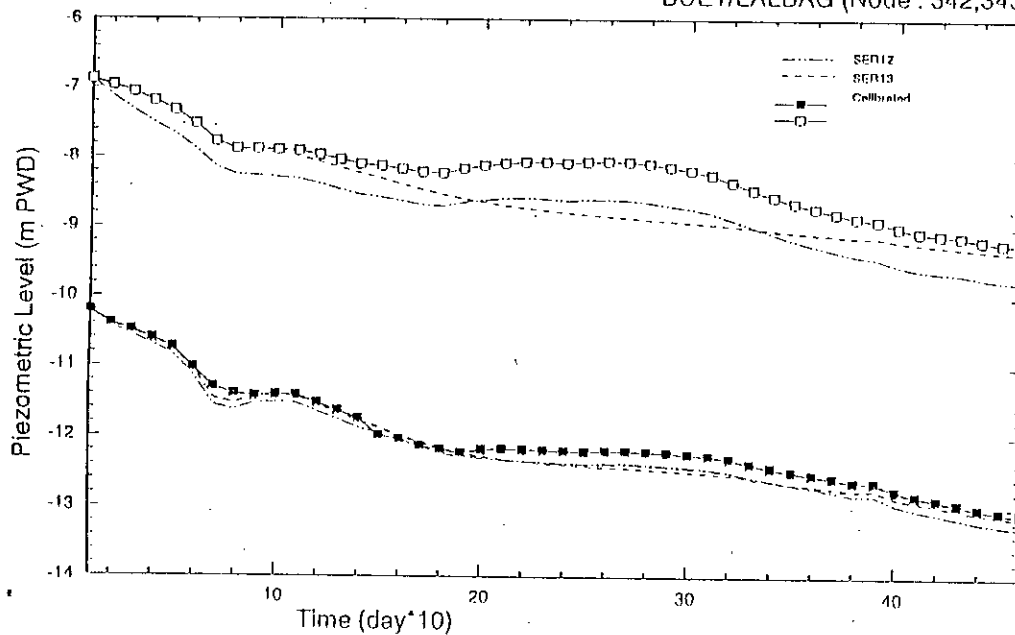
Fig. 6.27(a) : Simulated piezometric head values with different water level conditions in the river

RUNS : SER12 & SER13
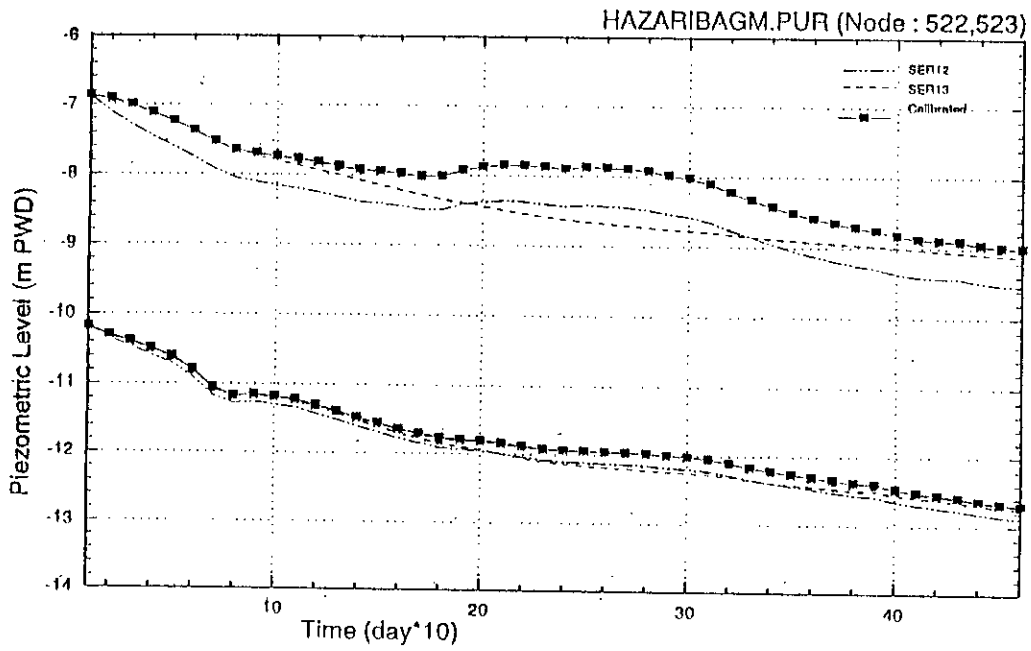
Note:
SER12 showing water level reduction 1.5 m throughout the simulation time
SER13 showing a constant water level of 1.2 m in the river excluding the monsoon rise in river
In the boxes upper three plots are for node 553 or 623 and lower three for node 552 or 622
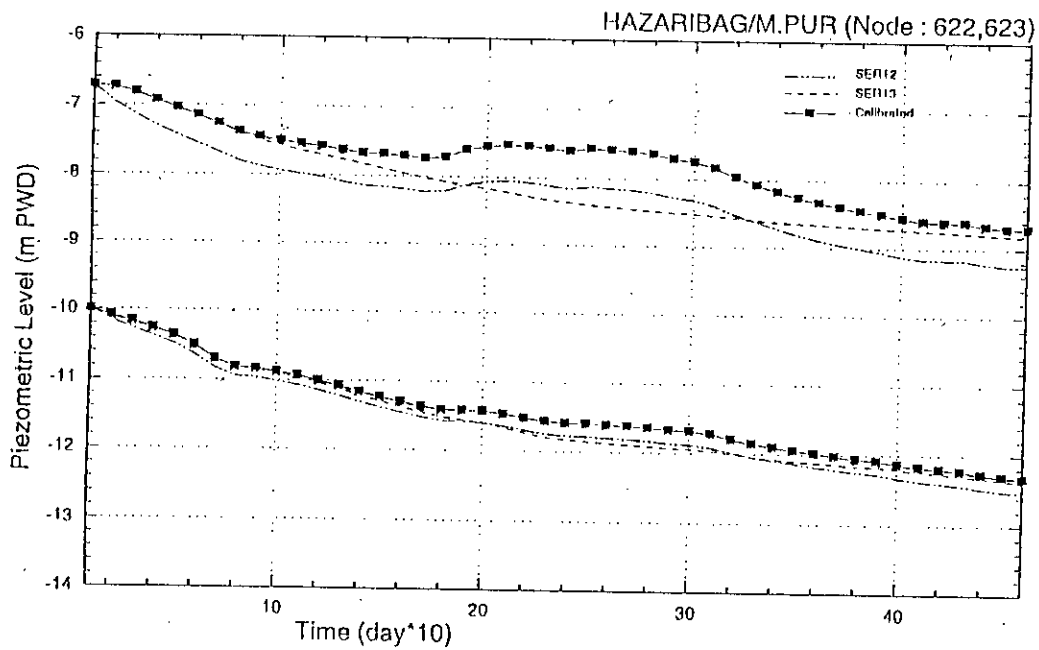
Fig. 6.27(b) : Simulated piezometric head values with different water level conditions
in the river

visual inspection one can immediately identify deviations of the curves from the calibrated plots and compare with one another.

In Fig. 6.25(a), the hydraulic conductivity sensitivity of the upper aquitard is shown. The upper value is 0.001 m/day which is higher than the calibrated value and the lower value is 20 percent of the calibrated value. But the curves show that the piezometric levels are more sensitive in the upper value. This is due to the fact that at higher value of hydraulic conductivity, water from the upper aquitard easily transfers to the upper aquifer and contribute to the piezometric level resulting into lower drawdown. But in the lower value of this parameter, water movement is retarded. The problem with the upper range is that if this high value is allowed, the upper aquitard dry out quickly and continuation of saturation is not possible in this case. The curves of the nodes 202 and 203 show lesser effect than the other distant nodes. This is mainly because these nodes are nearer the river than the other nodes so that the piezometric level near the river are mostly controlled by the river water level.

Similarly Fig. 6.25(b) shows the variation of upper and lower aquifers' hydraulic conductivities on the piezometric levels. Here it is observed that nearer the river the effect is lower (node 202, 203) and the upper and lower hydraulic conductivity curves are nearly parallel to the calibrated curves showing less effect on the storage. But at the nodes which are at relatively larger distance from the river (nodes 342, 343, 622, 623) and where abstraction rate is high, the effect is clear enough with continuously increasing drawdown and subsequent separation from the calibrated curves. Thus an additional piezometric head change of 0.2-0.4 m at the end of simulation period are observed in the specified range of aquifer hydraulic conductivities. This reveals the fact that the hydraulic conductivities of the aquifers have significant effect on the ultimate lowering of piezometric levels.

The variation of storage coefficient for upper aquifer have different type of effect on the piezometric level as shown in Fig. 6.25(c). In the simulated domain, the upper aquifer has different water level position and moisture condition at different locations. At nodes where high abstraction rate exists and relatively at longer distance from the river, the upper part of the aquifer is unsaturated (piezometric level upto -14 m PWD as per data base). So

water level lowering in these locations occur with subsequent drainage of the upper part. But near the river, due to high water level at the river (1.2 to 5.0 m PWD), most of the upper aquifer remain saturated throughout the simulation time. In this situation, for sensitivity analysis the high value of storage coefficient is fixed at a value which is in between the range of values of storage coefficient and specific yield. The low value is at a normal minimum confined storage coefficient value of 0.0003 with an intermediate value 0.003. From the curves it is seen that at the lower range, the simulated piezometric head shows a little variation from the calibration values in all locations of the domain. But at the high value, the plotting shows significant deviation from calibrated profiles and drawdowns are reduced by 0.3 to 0.7 m at the end of simulation. It indicates that to maintain piezometric level at their observed values, the storage coefficient should be as close as possible to the lower range. This phenomena expresses that unsaturation of the domain in the upper aquifer is only at the remote nodes and near the river it remains saturated from the river water flow.

The simulated piezometric levels are less sensitive to the storage coefficient of lower aquifer (Fig. 6.25d). Here as usual, less value of S_s shows high drawdown and higher value less drawdown but variation is very small. Due to the high value of hydraulic conductivity , water readily flows from the river side to the main aquifer keeping it fully saturated at all time and at all nodes. So this less sensitive nature against the high hydraulic conductivity is expected.

The sensitivity of urban recharge is shown in Fig. 6.25(e). For the city area where domestic and industrial water supply exists, this is an important contribution to the storage but correct quantification of this is tough. In the present simulation whole area is not contributed from urban recharge uniformly due to variation of abstraction volume at different locations. The nodes in the low lying area near the river, this kind of return flow is not applied at all. Within the confidence range 10 percent and 40 percent, the curves show expected response, i.e., high decline at low return flow and vice versa. But when applying high return flow percentage, an important phenomena is that rejection of water by the soil with outward flux at the surface nodes of the respective locations are obvious. This water contributes to the evaporation loss also. This phenomena reduces the return flow contribution to the aquifer and is observed at some nodes at the present simulation. Due to time

constraint, this rejection pattern and quantity is not analyzed here in detail which might be helpful for the proper estimation of this highly uncertain and important parameter.

Direct contribution from the precipitation to the groundwater body in the simulated domain is less which is shown by the water balance. In the sensitivity analysis, program run SER11 is done with the precipitation value equal to zero at every simulation time level. The output piezometric profiles are shown in Fig. 6.26 and shows that the curves with no rainfall are very close to the calibrated curves. A little additional declining is observed from the mid of the simulation period upto the end of simulation.

From the simulated curves of Figs. 6.24 and 6.25, it is observed that in almost all the curves, there is a rapid fall at the initial period of simulation and then at the mid period of the simulation (at monsoon) the declining rate is reduced or rising is observed followed by rapid fall at the end of the period. The purpose of the extra run SER13 is to identify the effect of monsoon rise of the water level in the river ; whether the stated pattern of piezometric head is maintained to some extent by other source such as high precipitation rate at the same period and the additional declining of piezometric levels that might occur without such monsoon rise in the river. So in this run a constant water level (1.2 m PWD) in the river, a value almost equal to the initial value at the starting of simulation, is applied throughout the simulation time. The resulting piezometric levels show that the rising pattern at the monsoon is almost disappeared but no high additional drawdown is observed without such river water level rise. At the end of simulation, piezometric levels fall less than 0.10 m near the river (nodes 203,343,523 etc.) are observed but away from the river the values are further reduced. This again indicates less effect of river water level to the piezometric head decline at remote locations (node 342,622 etc.). Thus it is proved that stated particular nature of the simulated curves is controlled only by the river water level and not by the high precipitation of the same period. The results of extra runs SER12 and SER13 are presented in Figs. 6.27(a),(b).

In run SER12 the condition setting and output are somewhat different from SER13. Here the river water level is reduced by 1.5 m from the existing values at all simulation times including the monsoon rise. Here the curves has declined from their calibrated

positions to a significant amount showing increasing fall of piezometric head with time. Again the effect is higher near the river and reduced by the monsoon water level rise in the river. The maximum amount of piezometric head decline is 0.6 m near the river and 0.25 m at other remote nodes are observed. So it may be stated here that low level in the river in a year without rise in monsoon are not causing large drawdown in the piezometric head of the simulated area but if river water level is reduced throughout the year (say, by pumping of water from the river for any other purpose) then the effect is more detrimental for the aquifer systems.

CONCLUSIONS AND RECOMMENDATIONS

CHAPTER SEVEN

CONCLUSIONS AND RECOMMENDATIONS
FOR FURTHER STUDIES

7.1 Conclusions

Using Galerkin type finite element method a three-dimensional model has been developed for variably saturated groundwater flow simulation. To check the model behavior and accuracy of the algorithm under different auxiliary conditions six hypothetical problems are used. Finally a real hydrogeological situation of Dhaka city along the east bank of the river Burhiganga has been analyzed. Conclusions from these applications and testing are stated below.

7.1.1 Schematized Problems

Prob. 01 & 02 : Unsaturated flow ; Soil-Moisture Infiltration in a Soil Column under Dirichlet and Neuman Boundary Condition

(a) Simulated pressure head and moisture content profiles shows smooth nature and excellent agreement with published results (Philip's analytical solution and Solution by Paniconi et al., 1991)

(b) Vertical flux profiles are examined as consistent nature but a little disturbances at the front in Dirichlet boundary condition is observed.

(c) No severe fluctuation and convergence difficulties encountered in three-dimensional solution approach which are reported by some researchers in one-dimensional solution.

Prob. 03 : Fully Saturated Steady Flow with Known Surface Flux in a Confined Aquifer

(a) The solution converges in few iterations in steady state mode.

(b) Simulated results of pressure head (averaged over depth) profile along the flow direction are perfectly close to the analytical solution.

Prob. 04 : Flow under Variable Atmospheric Influences

(a) High precipitation after initial and prolonged dry condition produced ponding on the surface with rapid infiltration in initial stage but very slow infiltration after that due to near hydrostatic pressure head distribution.

(b) This saturation process is mostly controlled by the unsaturated soil characteristic functions and hence shows the importance of proper parameterization of the unsaturated soil properties of the upper layer of the soil.

(c) The time interval of the input data (1 day) and the time steps of the computation are (always less than 0.5 day) different because in handling saturated-unsaturated flow very small time steps are required for convergence. an adjustment in the time step of the program and input data may be useful to reduce abrupt changes in the input values (e.g.,high precipitation after long dry spell) and thereby in the model responses.

Prob. 05 : Transient Drainage from a Domain with Seepage Face

(a) Sudden lowering of water level in adjacent surface water body resulted formation of seepage face.

(b) Simulated transient position of the water table and seepage face by iteration method show high gradient near seepage face.

(c) At the beginning few time steps of simulation, the drainage volumes through the seepage face computed by different models show some variation.

(d) Near the seepage face finer discretization, i.e., smaller nodal spacing is required to take care of high pressure head gradient.

Prob. 06 : Drainage-Replenishment due to Fluctuating Water Level in River

(a) High Darcian fluxes occur in the periods of rising river hydrograph, especially in the vicinity of groundwater table and slightly above it.

(b) The intensive fluxes disappear when all parts of the flow region are either saturated or at least wet enough during a prolonged high flood or constant water level.

(c) The phase of receding hydrograph is most dangerous for the stability of the river bank which are recognized from large velocity vectors.

(d) The pressure head contours in the saturated zone below the groundwater table are at all times effectively parallel to the groundwater table.

(e) The behavior of the unsaturated contours indicate a difference in time scale between saturated and unsaturated movement with unsaturated movements being much slower.

7.1.2 Dhaka City Strip Modeling

(a) The program converges within a satisfactory maximum iteration at each time level for both 10-day and daily basis input data.

(b) After a long dry spell when a high precipitation enters as input in the computation, then this works as a high impact which is encountered in the program by automatic time step

reduction. This time consuming process improves sufficiently in daily basis run due to lower magnitudes of stated input data.

(c) The simulated piezometric profiles near the river show pronounced rise and fall with the river water level but this trend diminishes rapidly at locations approximately 2.5 km away from the river.

(d) In one year cycle (March to next year end of March), the piezometric levels don't return to their original position in the remote areas from river and a maximum of 0.8 to 1.2 m of unrecoverable piezometric head decline is observed in areas of high abstractions.

(e) Main component of recharge is by the flow from the river side boundary (approximately 60 percent). Urban recharge contribute to the aquifer as near as 30 percent of the abstraction volume.

(f) Among the four simulated layers, the upper aquifer shows ultimate storage reduction estimating above 1 percent of the initial storage of the layer.

(g) Direct effect of rainfall through infiltration has negligible effect on the piezometric head profiles of the area.

(h) In the sensitivity study, hydraulic conductivities of the aquifers are identified as important parameters. Hydraulic conductivity of upper aquitard and urban recharge control the declining trend of the piezometry of the area.

(i) Without the monsoon rise of the river water level, the additional drawdown is very small but if the water level is reduced throughout the year to a certain value, the effect on the aquifer may be hazardous.

(j) Imposed high percentage of urban recharge causes rejection by the upper aquitard at some locations and rise of water level at surface nodes leads to the conclusion of the necessity for detail analysis of this parameter for correct assessment.

7.2 Recommendations for further Studies

7.2.1 Improvement of the Algorithm

Present model can be improved into a more user-friendly and competitive one by modifications through new subroutines and supporting programs which are summarized as follows :

(a)   To facilitate data generation for three-dimensional domain, which is identified as relatively tedious job in three-dimensional case, existing mesh generator can be modified so that it can easily discretize irregular domain from a less number of input geological structure data with an easy means of editing this data by visual interaction and some sophisticated interpolation technique may be incorporated to allocate hydrogeological data to each node properly. In this connection GIS softwares and macro language may be regarded as important tools.

(b) To increase the efficiency and speed of the algorithm the existing solver can be changed by the optimization type conjugate gradient solver which will be very suitable for regional scale simulation. Another modification and change in the main code can be done by changing the   elements type used and a provision for combination of multiple type of elements to define irregular boundary properly and for a more efficient model.

(c) Present model can be coupled with a two-dimensional surface runoff model which will take into account the runoff water from the heavy precipitation and thus the model may be transformed to a more physically based model.

(d) A hydrodynamic river flow model can be coupled with the present one to simulate riverine area in an integrated approach.

(e) Effect of hysterisis and plant growth with time is not considered in the model. So further modification may be referred to these points.

7.2.2 Dhaka City Detail Modeling

With respect to the Dhaka city detail modeling, the suggestions are :

(a) A complete database of the area should be developed for soil layers of the different locations or geotechnical subareas, their hydrogeological characteristics and the piezometric levels of the observation wells.

(b) For proper quantification of vertical leakage contribution from surface total paved and unpaved areas, the water level conditions in the lakes, and unsaturated soil characteristics of the upper two layers should be examined and defined correctly from field investigation and data analysis.

(c) To estimate urban recharge component properly, the soil saturation condition along depth upto the base of the upper aquitard should be examined in sufficient number of locations and then a detail sensitivity study of the parameter could be done by considering the rejection pattern at different percentage of this imposed volume.

(d) To know correctly the river leakage to the aquifer system only, a number of observation wells should be established in both sides of the river.

REFERENCES

Abrahams, A.D. (Ed.), (1986). Hillslope Processes. Allen and Unwin, Boston.

Abriola, L.M. (1986). "Finite element solution for unsatuarted flow equation using hierarchic basis functions." Proc. of the Sixth International Conference on Finite Elements on Water Resources, Lisboa, Portugal, pp 125-133, Springer-Verlag, New York, 1986.

Allen, M.B., and Murphy, C.L. (1986). "A finite element collocation method for variably saturated flow in two space dimensions." Water Resour. Res., 22, 1537-1542.

Babu, D.K. (1976). "Infiltration analysis and perturbation methods, 3, Vertical infiltration." Water Resour. Res., 12(5), 1019-1024.

Batu, V. (1979). "Flow net from unsatuarted infiltration from strip source." J. Irrig. Drain. Div. ASCE, 105(IR3), 233-245.

Bear, J. (1979). Hydraulics of Groundwater. McGraw-Hill Inc., New York.

Bruch, J.C., and Zyvoloski, Jr. (1974)."Solution of vertical unsaturated flow of soil water." Soil Sci., 116, 417-422.

Boulton, N.S. (1963). "Analysis of data from nonequilibrium pumping tests allowing for delayed yield from storage." Proc. Inst. Civ. Eng., 26(6693), 469-482.

Boulton, N.S., and Streltsova, T.D. (1976)."The drawdown near an abstraction well of large diameter under non-steady conditions in an unconfined aquifer." J. of Hydrol., 30, 29-46.

Boulton, N.S., and Streltsova, T.D. (1977a)."Unsteady flow to a pumped well in a fissured water-bearing formation." J. of Hydrol.,35, 257-269.

Boulton, N.S., and Streltsova, T.D. (1977b)."Unsteady flow to a pumped well in a two-layered water bearing formation." J. of Hydrol., 35, 245-256.

Boulton, N.S., and Streltsova, T.D. (1978)."Unsteady flow in to pumped well in a fissured aquifer with a free surface level maintained constant." Water Resour. Res., 14(3), 527-532.

Boussinesq, J. (1903-4). "Recherches theoriques sur l'ecoulment des nappes d'eau infiltrees dans le sol et sur debit des sources." C.R.H. Acad. Sci., J. Math. Pures Appl. 10, 5-78 (June 1903),363-394(Jan.,1904),cited after Bear(1972).

Brandt, A., Bresler, E., Diner, N., Ben-Asher, L., Heller, J., and Goldman, D. (1971). "Infiltration from a trickle source: 1. Mathematical models." Soil Sci. Soc. Am. Proc., 35, 675-689.

Broadbridge, P. and White, I. (1988). "Constant rate infiltration : A versatile nonlinear model. 1. Analytical solution. " Water Resource Research, 24, 145-154.

Buckingham, E. (1907). "Studies on the movement of soil moisture." U.S. Dept. Agric Bur. Soil Bull. No. 38, cited after Youngs (1988).

Campbelll, G.S. (1985). Soil physics with basic : transport model for soil-plant systems. Developments in soil science, 14. Elsevier, Amsterdam, 150 p.

Celia, M.A., Bouloutas, E.T., Zarba, R.L. (1990). "A general mass-conservative numerical solution for the unsaturated flow equation." Water Resour. Res., 26(7), 1483-1496.

Childs, E.C. (1945). "The water table, equipotentials and streamlines in drained land III." Soil. Sci., 59, 405-415.

Childs, E.C., and Collis-George, N. (1950). "The permeabilty of porous materials." Proc. Roy. Soc., 201A, 392-405.

Clement, T.P., Wise, W.R., and Molz, F.Z. (1994). "A physically based, two-dimensional, finite difference algorithm for modeling variably saturated flow." J. Hydrol., 161, 71-90.

Clothier, B.E., Knight, J.H., and White, I. (1981). "Burgers' equation : Application to field constant-flux infiltration." Soil Sci., 132, 255-261.

Cooley, R.L. (1971). "A finite difference method for unsteady flow in variably saturated porous media: application to a single pumping well." Water Resour. Res., 7, 1607-1625.

Cooley, R.L. (1983). "Some new procedures for numerical solution of variably saturated flow problems." Water Resour. Res., 19(5), 1271-1285.

Crank, J., and Henry, M.E., (1949). "Diffusion in media with variable properties. II. The effect of a variable diffusion coefficient on the rate of absorption and desorption." Transactions of the Faraday Society, 45, 636-650.

Dane, J.H., and Mathis, F.H. (1981). "An adaptive finite difference scheme for the one-dimensional water flow equation." Soil Sci. Soc. Am. J., 45, 1048-1054.

Darcy, H. (1856). "Les fontaines publiques de la ville de Dijon." Dalmont, Paris, 647 pp., cited after Youngs (1958).

Day, P.R., and Luthin, J.N. (1956). "A numerical solution of the differential equation of flow for a vertical drainage problem." Soil Sci. Soc. Am. Proc., 20, 443-446.

Dennemeyer, R. (1968). Introduction to partial differential equations and boundary value problems. MacGraw-Hill, New York, 376 p.

El-Kadi, A.I., and Ling, G. (1993). "The Courant and Peclet number criteria for the numerical solution of the Richards equation." Water Resour. Res., 29(10), 3485-3494.

Feddes, R.A. (1981). "Water use models for assessing root zone modification." In: Modifying the plant root environment. Am. Soc. of Agron., St. Joseph, Michigan, Monograph 4, pp. 347-390.

Feddes, R.A., Bresler, E., and Neuman, S.P. (1974). "Field test of a modified numerical model for water uptake by root systems." Water Resour. Res., 10(6), 1199-1206.

Feddes, R.A., Kowalik, P.J., Zaradny, H. (1978). "Simulation of field water use and crop yield." PUDOC, Wageningen, The Netherlands, 189 p.

Feedes, R.A., Kabat, P., Van Bakel, P.J.T., Bronswijk, J.J.B., and Halbertsma, J. (1988). "Modeling soil water dynamics in the unsatuarted zone." J. Hydrol., 100, 69-111.

Forchheimer, Ph. (1886). "Ueber die Ergiebigkeit von Brunnen-Anlagen und Sickerschhlitzen." (In German) Z. Archit. Ing.-Verein. Konigreich Hannover, 32, 539-563, cited after Youngs (1988).

Forsythe, G.E., and Wasow, W.R. (1960). Finite difference methods for partial diffential equations. Wiley, New York, 444 pp.

Freeze, R.A. (1969). " The mechanism of natural groundwater recharge and discharge 1. One-dimensional, vertical, unsteady, unsaturated flow above a recharging and discharging groundwater flow system." Water Resour. Res., 5, 153-171.

Freeze,R.A. (1971a). "Three-dimensional, transient, saturated-unsaturated flow in a ground-water basin." Water Resour. Res., 7(2), 347-366.

Freeze, R.A. (1971b). "Influences of the unsaturated flow domain on seepage through earth dams." Water Resour. Res., 7, 921-941.

Frind, E.O., and Verge, M.J. (1978). "Three-dimensional modeling of groundwater flow systems." Water Resour. Res., 14(3), 844-856.

Gardner, W.R. (1958). "Some steady-state solutions of the unsaturated moisture flow equation with application to evaporation from a water table." Soil Sci., 85, 228-232.

Gardner, W.R., and Fireman, M. (1958). "Laboratory studies of evaporation from soil columns in the presence of a water table." Soil Sci., 85, 244-249.

Gupta, S.K., Cole, C.R., and Pinder, G.F. (1984). "A finite element three-dimensional groundwater model for a multiaquifer system." Water Resour. Res., 20(5), 553-563.

Gottardi, G., and Venutelli, M. (1992). "Moving finite element model for one-dimensional infiltration in unsaturated soil." Water Resour. Res., 28(12), 3259-3267.

Gray, W.G., and Hassanizadeh, S.M. (1991). "Paradoxes and realities in unsaturated flow theory." Water Resour. Res., 27(8), 1847-1854.

Gray, W.G., and Hassanizadeh, S.M. (1991). "Unsaturated flow theory including interfacial phenomena." Water Resour. Res., 27(8), 1855-1863.

Green, W.H. and Ampt, G.A. (1911). "Studies in soil physics. I. The flow of air and water through soils." J. Agric. Sci., 4, 1-24.

Gupta, S.K., and Tanji, K.K. (1976)." A three-dimensional finite element solution of flow through multiaquifers in Sutter basin, California." Water Resour. Res., 12(2), 155-162.

Hackbusch, W. (1985). Multigrid methods and applications. Springer Verlag, Berlin.

Haverkamp, R., and Vouclin, M. (1981). "A comparative study of three forms of the Richards equation used for predicting one-dimensional infiltration in unsaturated soil." Soil Sci. Soc. Am. J., 45, 13-20.

Haverkamp, R., Vouclin, M., Touma, J., Weirenga, P.J., and Vachud, G. (1977). "Comparision of numerical simulation models for one-dimensional infiltration." Soil Sci. Soc. Am. J., 41, 285-294.

Hayhoe, H.N. (1978). "Study of the relative efficiency of finite difference and Galerkin techniques for modeling soil-water transfer." Water Resour. Res., 14(1), 97-102.

Healy, R.W. (1990). "Simulation of solute transport invariably saturated porous media with supplemental information on modifications to the USGS computer program VS2D." USGS Water Resour. Invest. Rep., 90-4025.

Hillel, D. (1980). Applications of soil Physics. Academic Press, New York, 385 p.

Huyakorn, P.S., and Pinder, G.F. (1983). Computational methods in subsurface flow. Academic Press, London, 473 p.

Huyakorn, P.S., Thomas, S.D., Thoompson, B.M. (1984). "Techniques for making finite elements competitive in modeling flow in variably saturated porous media." Water Resour. Res., 20, 1099-1115.

Huyakorn, P.S., Springer, E.P., Guvanasen, V., and Wadsworth, T.D. (1986). "A three-dimensional finite element model for simulating water flow in variably saturated porous media." Water Resour. Res., 22(13), 1790-1808.

Istok, J. (1989). "Groundwater modeling by the finite element method." Water Resour. Monograph 13, Am. Geophys. Union, Washington, D.C.

Javadel, I., and Witherspoon, P.A. (1968). "Application to the finite element method to transient flow in porous media." Soc. Pet. Eng. J., 8, 241-252.

Kirkby, M.J. (Ed.) (1978). Hillslope Hydrology. John Wiley, New York.

Kirkland, M.R. (1991). Algorithm for solving Richards' equation for variably satuarated soils. Ph.D. Thesis, Department of Mechanical Engg., New Mexico State University, Las Cruces.

Kirkland, M.R., Hills, R.G., and Weirenga, P.J. (1992). "Algorithm for solving Richards' equation for variably satuarated soils." Water Resour. Res., 28, 2049-2958.

Master Plan Organization (MPO), (1987). National Water Plan Project Phase-II, Simulation Model Report, Vol. III, Groundwater Models, May 1991.

Meinzeir, O.E., (1923). "The occurrence of Groundwater in the United States." USGS Water Supply Paper 489.

Molz, F.J. (1981). "Models of water transport in soil-plant system. A review." Water Resour. Res., 17, 1245-1260.

Molz, F.J., and Remson, I., (1970). "Extraction term models for soil moisture use by transpiring plants." Water Resour. Res., 6(5), 1346-1356.

Morel-Seytoux, H.J. (1973). "Two-phase flows in porous media." Adv. Hydrosci., 9, 119-202.

Mualem, Y. (1976). "A new model predicting the hydraulic conductivity of unsaturated porous media." Water Resour. Res., 12(3), 513-522.

Narasimhan, T.N., and Witherspoon, P.A., and Edwards, A.L. (1978). "Numerical model of saturated-unsaturated flow in deformable porous media, 2. The algorithm." Water Resour. Res., 14, 255-261.

Neuman, S.P. (1972). "Finite element computer programs for flow in saturated-unsaturated porous media." Second Annual Report, Project No. A10-SWC-77, Hydraulic Engineering Lab., Technion, Haifa, Israel, 87 p.

Neuman, S.P. (1973). "Saturated-unsaturated seepage by finite elements." Proc. Am. Soc. Civil Engrs., J. of Hydraul. Div., 99 (HY12), 2233-2250.

Neuman, S.P. (1975). "Analysis of pumping test data from anisotropic unconfined aquifers considering delayed gravity response." Water Resour. Res., 11(2), 329-342.

Neuman, S.P., Feddes, R.A., Bresler, E. (1974). "Finite element simulation of saturated-unsaturated soil considering water uptake by plants." Third Annual Report, Project No. A10-SWC-77, Hydraulic Engineering Lab., Technion, Haifa, Israel, 104 p.

Neuman, S.P., and Witherspoon, P.A. (1970). "Finite element method of analyzing steady seepage with a free surface." Water Resour. Res., 6, 889-897.

Neuman, S.P., and Witherspoon, P.A. (1971). "Analysis of non-steady flow with a free surface using the finite element method." Water Resour. Res., 7, 611-623.

Nimah, M.N., and Hanks, R.J. (1973a). "Model of estimating soil water, plant and atmospheric interrelations. 1. Description and sensitivity." Soil Sci. Soc. Am. Proc., 37, 522-527.

Parlange, J.Y. (1971a). "Theory of water movement in soils. 1. One-dimensional absorption." Soil Sci., 111, 134-137.

Parlange, J.Y. (1971b). "Theory of water movement in soils. 2. One-dimensional infiltration." Soil Sci., 111, 170-174.

Panday, S., Huyakorn, P.S., Therrien, R., and Nichols, R.L. (1993). "Improved three-dimensional finite element techniques for field simulation of variably saturated flow and transport." J. Contaminant Hydrol., 12, 3-33.

Paniconi, C., and Wood, E.F. (1993). "A detail model for simulation of catchment scale subsurface hydrologic process." Water Resour. Res., 29(6), 1601-1620.

Papadopulos, I.S., and Cooper, H.H. (1967). "Drawdown in a well of large diameter." Water Resour. Res., 3(1), 241-244.

Philip, J.R. (1955). "Numerical solution of equations of the diffusion type with diffusivity concentration-dependent." Transaction of the Faraday Soc., No. 391, Vol. 51, Part 7, 885-892.

Philip, J.R. (1957a). "The theory of infiltration. 1. The infiltration equation and its solution." Soil Sci., 83, 345-357.

Philip, J.R. (1957b). "The theory of infiltration. 4. Sorptivity and algebraic infiltration equations." Soil Sci., 84, 257-264.

Philip, J.R. (1960a). "General method of exact solution of the concentration-dependent diffusion." Austral. J. Phys., 13, 1-12.

Philip, J.R. (1960b). "A very general class of exact solutions of the concentration-dependent diffusion." Nature, 185, 233.

Philip, J.R. (1960c). "The function inverfc(theta)." Austral. J. Phys. 13, 13-20.

Philip, J.R. (1969). "The theory of infiltration." In: Ven Te Chow (ed.), Advances in Hydroscience, Vol.5, Academic Press, New York, pp. 215-296.

Philip, J.R. (1986). "Linearized unsteady multidimensional infiltration." Water Resour. Res., 22, 1717-1727.

Philip, J.R. (1989). "Multidimensional steady infiltration to a water table." Water Resour. Res., 25, 109-116.

Philip, J.R. (1991). "Hillslope infiltration: planer slopes." Water Resour. Res., 27(1), 109-117.

Philip, J.R., and Knight, J.H., (1974). "On solving the unsaturated flow equation. 3. New quasi-analytical technique." Soil Sci., 117, 1-13.

Philip, J.R., Knight, J.H., and Waechter, R.T. (1989). "Unsaturated seepage and subterraian holes: Conspectus, and exclusion problem for circular cylindrical cavities." Water Resour. Res. 25, 16-28.

Poiseuille, J.L. (1840). Comte Rendus, Vol. 11, pp 961 and 1041.

Raats, P.A.C., and Gardner, W.R. (1974). "Movement of water in a unsaturated soil near a water table." In : van Schilfgaarde, J. (ed.), Drainage for Agriculture. Agronomy Series No. 17, Am. Soc. of Agron., Madison, Wisconsin, USA, 700 p., pp. 311-357.

Reeves, M., and Duguit, J.O. (1975). "Water movement through saturated-unsaturated porous media, a finite element Gherkin model." Oak Ridge Natl. Lab., Oak Ridge, Calif., ORNL-4927, 232 pp., cited after Gureghian (1981).

Reisenauer, A.E., Key, K.T., Narashimhan, T.N., Nelson, R.W. (1982). "A computer program for variably saturated flow in multidimensional deformable media, U.S. Nucl. REg. Comm., Washington, D.C., cited after Huyakorn, 1991, p.252.

Remson, I., Hornberger, G.M., and Molz, R.D. (1971). Numerical methods in subsurface hydrology. Wiley, New York, 389 p.

Richards, L.A. (1931). "Capillary conduction of liquids through porous mediums." Physics, 1, 318-333.

Rubin, J. (1968). "Theoretical analysis of two-dimensional, transient flow of water in unsaturated and partly saturated soils." Soil Sci. Soc. Am. Proc., 32, 607-615.

Scarborough, J.B. (1966). Numerical mathematical analysis. John Hopkins Press, Baltimore, Md., 600 p.

Simunek, J., Vogel, T., and van Genuchten (1992). The SWMC_2D code for simulating water flow and solute transport in two-dimensional variably saturated media. U.S. Department of Agriculture, Riverside, CA, USA, 169 p.

Smith, R.E., and Parlenge, J.-Y. (1978). "A parameter-efficient hydrologic infiltration model." Water Resour. Res., 14, 533-538.

Stallman, R.W. (1963). "Type curves for the solution of single-boundary problems." In: Shortcuts and special problems in aquifer tests. USGS Water Supply Pap., 1545-C: 45-47.

Taylor, R.L., and Brown, C.B. (1967). "Darcy flow solutions with a free surface." Proc Am. Soc. Civ. Eng., 93 (HY2), 25-33.

Theim, A. (1870). "Die Ergiebigkeit artesischer Bohrlocher, Sahachtbrunnen, und Filtergallerien." J. Gasbaleuchtung Wasserversorgung (Munich), vol. 14.

Theis, C.V. (1935). "The relation between lowering of the piezometric surface and the rate and duration of discharge of a well using groundwater storage." Trans. Am. Geophys. Un., 16th annual meeting, pt. 2, 519-524.

UNDP/BWDB, Water Balance Studies, Bangladesh, April, 1984.

Vandenberg, A. (1977). "Type curves for analysis of pump tests in leaky strip aquifers." J. Hydrol., 33(1/2), 15-26.

Vogel, T. (1987). SWMII - Numerical model of two-dimensional flow in a variably saturated porous media. Dept. of Hydraulics and Catchment Hydrology, Agric. Univ., Wageningen, The Netherlends.

Vogel, T., and Cislerova, M. (1988). "On the reliability of unsatuarted hydraulic conductivity calculated from the moisture retention curve." Transport in Porous Media, 3, 1-15.

Walton, W.C. (1979). "Progress in analytical groundwater modeling." J. of Hydrol., 43, 149-159.

Wang, H.F., and Anderson, M.P. (1982). Introduction to groundwater modeling. Finite difference and finite element methods. Freeman, New York, 237 p.

Warrick, A.W., and Amoozegar-Fard, A. (1979). "Infiltration and drainage calculations using spatially scaled hydraulic properties." Water Resour. Res., 15(5), 1116-1120.

WASA, Dhaka region Groundwater and Subsidence Project, Draft final report, Feb. 1991.

Whistler, F.D., and Watson, K.K. (1968). "One-dimensional gravity drainage of uniform columns of porous materials." J. of Hydrol., 6, 277-296.

White, I., Smiles, D.E., and Perroux, K.M. (1979). "Absorption of water by soil: The constant-flux boundary condition." Soil Sci. Soc. Am. J., 43, 659-664.

Witherspoon, P.A., Javandel, I., Neuman, S.P., and Freeze, R.A. (1967). Interpretation of aquifer gas storage conditions from water pumping tests. Am. Gas Assoc., New York, N.Y., 273 pp.

Wooding, R.A. (1968). "Steady infiltration from a shallow circular pond." Water Resour. Res., 4, 1259-1273.

Youngs, E.G. (1957). "Moisture profiles during vertical infiltration." Soil Sci., 84, 283-290.

Youngs, E.G., and Poulovassilis, A. (1976). "The different forms of moisture profile development during the redistribution of soil water after infiltration." Water Resour. Res., 12, 1007-1012.

Yu, X.F., and Singh, V.P. (1994). "Modeling 3d groundwater flow by modified finite element method." Journal of Irrigation and Drainage Engg., 120(5), 892-909.

Zienkiewicz, O.C. (1977). The finite element method. 3rd ed., McGraw-Hill, London.

Zienkiewicz, O.C., Meyer, P., and Cheung, Y.K. (1966). "Solution of anisotropic seepage problems by finite elements." Proc. Am. Soc. Civ. Eng., 92 (EM1), 111-120.

APPENDIX A

SIMPLIFIED FLOW CHART

```
                    ( START )
                        │
                        ▼
            ┌──────────────────────────────┐
            │ OPEN INPUT AND OUTPUT FILES   │
            └──────────────────────────────┘
                        │
                        ▼
          /────────────────────────────────────────\
         /              READ Data                     \
        /      Material characteristic parameters      \
       / Time increament, expansion and reduction factor/
      /────────────────────────────────────────────────/
                        │
                        ▼
     /─────────────────────────────────────────────────/
    / Read node numbers array and boundary conditions  /
   /──────────────────────────────────────────────────/
                        │
                        ▼
        /─────────────────────────────────────/
       / Read element connectivity matrix     /
      /──────────────────────────────────────/
                        │
                        ▼
            ┌──────────────────────────────┐
            │  Creat table for parameters   │
            │  Calculate K,C,θ for each node│
            └──────────────────────────────┘
                        │
                        ▼
       /────────────────────────────────────────/
      / Read· River water level, Precipitation  /
     /          Evaporation data               /
    /─────────────────────────────────────────/
                        │
                        ▼
        ┌──────────────────────────────────────────┐
        │ Set initial time dependent boundary condition│
        └──────────────────────────────────────────┘
                        │
                        ▼
          /──────────────────────────────────/
         / Read parameters for Sink term     /
        /───────────────────────────────────/
                        │
                        ▼
                       ⎧ A ⎫
                       ⎩   ⎭
```

144

```
                    ┌───┐
                    │ A │
                    └─┬─┘
                      │
          No        ╱─┴─╲
 ┌──────────────── ╱  Is  ╲
 │                 ╲there seepage╱
 │                  ╲ face ? ╱
 │                   ╲──┬──╱
 │                      │ Yes
 │             ┌────────┴─────────────┐
 │            ╱ Read initial seepage face nodes and ╱
 │           ╱  adjust with river water level      ╱
 │          └────────┬──────────────┘
 │                   │
 └───────────────────┤
                     │
            ┌────────┴──────────────┐
           ╱ Print nodal pressure head and moisture ╱
          ╱  content for initial time              ╱
         └─────────┬──────────────┘
```

```
 ┌──────────────────────────────────────────────┐
 │                                                │
┌┴┐                                               │
│C│   ┌────────────────────────────────────┐      │
└─┘   │ Calculate K,C,θ for each node corresponding │  │
      │ to new pressure head                       │  │
      └────────────────┬───────────────────┘      │
                       │                            │
      ┌────────────────┴───────────────────┐      │
      │ Calculate element matrix and vector elements │  │
      │ and assemble them to form global matrix equation │ │
      └────────────────┬───────────────────┘      │
                       │                            │
      ┌────────────────┴───────────────────┐      │
      │ Modify boundary conditions in seepage face and │ │
      │ face exposed to the atmosphere depending on │   │
      │ new pressure head and flux computed        │  │
      └────────────────┬───────────────────┘      │
                       │                            │
      ┌────────────────┴───────────────────┐      │
      │ Modify the global matrix equation for imposed │ │
      │ Dirichlet boundary condition and solve     │  │
      └────────────────┬───────────────────┘      │
                       │                            │
                     ╱─┴─╲           No             │
                    ╱ Is the ╲ ───────────────────────┘
                    ╲convergence criteria╱
                     ╲ fulfilled ? ╱
                      ╲──┬──╱
                         │ Yes
      ┌──────────────────┴───────────────┐
      │ Calculate nodal fluxes with computed │
      │ pressure head values               │
      └──────────────────┬───────────────┘
                         │
                       ┌─┴─┐
                       │ B │
                       └───┘
```

145

146